PRESSURE LOSSES AND HEAT TRANSFER FOR THE FLOW OF MIXTURES OF IMMISCIBLE LIQUIDS IN CIRCULAR TUBES

by

JEROME WOODRUFF FINNIGAN

A THESIS

submitted to

OREGON STATE COLLEGE

in partial fulfillment of
the requirements for the
degree of

DOCTOR OF PHILOSOPHY

June 1958

APPROVED:

Redacted for privacy

Professor of Chemical Engineering

In Charge of Major

Redacted for privacy

Head of Department of Chemical Engineering

Redacted for privacy

Chairman of School Graduate Committee

Redacted for privacy

Dean of Graduate School

Date thesis is presented May 14, 1958

Typed by Rose Amos

ACKNOWLEDGMENTS

The writer is priviledged to make the following acknowledgments:

To the National Science Foundation for financial support in the form of a research grant.

To Dr. James G. Knudsen, the writer's major professor, for suggesting the overall problem and the method of determining heat transfer coefficients, for obtaining the research grant, and for his helpful guidance during the course of the work.

To Mr. Robert C. Mang, machinist in the Chemical Engineering Department, both for his machine work and for his many constructive suggestions regarding fabrication of the equipment.

To Mr. F. D. Stevenson, graduate student in the Chemical Engineering Department, for making several physical property measurements of interest in this investigation.

Finally to my wife Nancy, who played the dual role of mother and father to our children, and to whom this thesis is dedicated.

TABLE OF CONTENTS

TABLE OF CONTENTS (continued)

LIST OF FIGURES

LIST OF FIGURES (continued)

LIST OF TABLES

PRESSURE LOSSES AND HEAT TRANSFER FOR THE FLOW OF MIXTURES OF IMMISCIBLE LIQUIDS IN CIRCULAR TUBES

CHAPTER 1

INTRODUCTION

The flow behavior of two-phase fluids has become increasingly important to the process industries in recent years. Modern developments in fluidized catalytic chemical reactors and the resurgence of interest in liquid-liquid extraction brought about by the nuclear energy program may be cited as well known examples.

There are several possible phase combinations in such systems. The fluid may consist of liquid-vapor, liquid-liquid, liquid-solid, or vapor-solid mixtures. Extensions of these catagories involving, for example, several solid phases suspended in a liquid are also conceivable. All of the above system types are of interest in current technology.

Through the use of a two-phase mixture it may be possible to obtain a combination of desirable properties not readily attainable with a single phase. In heat transfer applications the latent heat of vaporization may be utilized by permitting a portion of a liquid cooling medium to be vaporized. Such systems offer considerable promise in high specific power output devices such as nuclear reactors.

Pipe-line contactors, in which mixtures of two immiscible liquids flow cocurrently through a pipe, are of interest in the petroleum industry. In the design of such equipment an estimate of frictional pressure losses is required in order to determine pumping power requirements. Heat transfer characteristics may also be important, particularly if a chemical reaction is involved. In addition, it is necessary to be able to measure flow rates accurately and economically, so the flow behavior of mixtures in conventional metering devices is of interest.

Considerable effort has been devoted to the study of liquid-vapor, liquid-solid and vapor-solid systems. However, little attention has been given to the flow and heat transfer characteristics of mixtures of immiscible liquids. It was considered desirable to undertake an extensive investigation of such mixtures to obtain fundamental engineering information and perhaps useful design relationships.

A flow system was designed and built to permit measurement of friction factors, film heat transfer coefficients, and orifice meter coefficients for mixtures of immiscible liquids flowing in circular conduits. This thesis presents the results of the initial phase of this investigation.

CHAPTER 2

LITERATURE SURVEY AND THEORETICAL DISCUSSION

Review of Previous Work on Two-Phase Flow

Taken as a whole, the literature on flow and heat transfer properties of two-phase fluids is quite extensive. The literature concerning vapor-solid, vapor-liquid, and liquid-solid systems will be reviewed briefly. No attempt at completeness has been made, the aim being merely to indicate the scope of the work. Following this, liquid-liquid systems will be considered.

The flow of gases containing solid particles is important in the operation of fluidized catalytic chemical reactors and in pneumatic conveying of granular solids. Hariu and Molstad [27, p. 1160] studied the flow of closely sized sand particles in air and found that the overall pressure drop could be considered as the sum of a pressure drop due to carrier gas alone plus a solids pressure drop. Farbar [16, p. 1184-1191] investigated the isothermal flow characteristics of air-solids mixtures in horizontal and vertical pipes. Heat transfer in fluidized beds has been studied by Levenspiel and Walton [43, p. 1-13] and by Mickley and Fairbanks [51, p. 374-384].

Vapor-liquid mixtures, flowing in pipes, have received considerable attention in recent years. Heat transfer and pressure drop characteristics of air-liquid systems have been investigated by Alves [1, p. 449-456], Chenoweth and Martin [9, p. 151-155], Fried [18, p. 47-51], Lockhart and Martinelli [44, p. 39-48], and Reid [63, p. 321-324]. Hoopes [32, p. 268-275] and others have studied steam-water mixtures.

Suspensions or slurries of solid particles in liquids have been treated by Alves [2, p. 107-109], Binder and Busher [5, p. 101-105], Bonilla, et al [6, p. 127-135], Happel [26, p. 1181-1186], Orr and Dalla Valle [60, p. 29-45], and Salamone and Newman [71, p. 283-288]. Many of these systems have been found to be non-Newtonian in character, that is, the viscosity of a given mixture depended on the flow rate as well as on the temperature. In one paper known to the writer [84, p. 1-14] a three-phase system, consisting of air and a non-Newtonian suspension of clay in water, has been studied.

In the engineering research on liquid-liquid systems, emphasis has been placed on studies of agitation in tanks, mass and heat transfer between the two liquid phases, and measurement of droplet sizes and interfacial areas. All of these considerations are important in the industrial operation of liquid extraction equipment.

Miller and Mann [53, p. 709-745] and Olney and Carlson [59, p. 473-480] have studied the agitation of immiscible liquids in tanks, while the interfacial area produced by this type of mixing has been investigated by Rodger, Trice, and Rushton [68, p. 515-520], Trice and Rodger [79, p. 205-210], and Vermeulen, Williams, and Langlois [81, p. 85-94].

The mechanisms of phase dispersion in liquid-liquid systems and the settling and coalescence of unstable emulsions have been treated in papers by Hinze [31, p. 289-295] and by Meissner and Chertow [47, p. 856-859], respectively.

The flow of an immiscible oil-water system through a porous medium such as sand is of importance in the recovery of crude oil from the earth. Idealized mathematical treatments of this problem have been presented by Kidder [38, p. 866-869] and by Meyer and Garder [50, p. 1400-1406]. Several authors have discussed the flow of immiscible liquids through packed extraction towers [78, p. 305-308; 11, vol. 2, p. 412-413].

Keulegan [37, p. 487-500] has treated the problem of stratified flow of a light liquid over a body of heavier liquid with which it is miscible. At low velocities an interface may be formed at which there is a sharp density discontinuity, and thus the system behaves as an immiscible one.

Richardson [66, p. 369] and others have studied the laminar flow of stabilized emulsions in capillary tubes in connection with viscosity determinations. Very extensive treatments of all aspects of stabilized emulsion technology have been given by Clayton [10] and Becher [4].

The only investigations known to the writer which involve turbulent flow of immiscible liquids in pipes are those of Grover [25], Roy and Rushton [70], and Clay [4, p. 218]. Grover's work was concerned with heat transfer between the liquid phases in concurrent flow, while the other two papers dealt with the influence of turbulent pipe flow on droplet size distribution in liquid dispersions.

In most engineering analyses of fluid flow and convection heat transfer problems, the fluid properties of importance are the density, viscosity, specific heat, and thermal conductivity. These properties, together with the geometry of the system under consideration, determine the flow and heat transfer behavior in a given application. It is evident that when two phases are considered the number of variables is greatly increased since, in general, the properties of each of the phases would be expected to influence the situation.

There are two methods of approach which have been used in the treatment of two-phase systems. In much of the work on vapor-solid [27, p. 1160] and vapor-liquid

[44] systems the two phases have been considered as separate and distinct flow streams. On the other hand, slurries are generally considered as single fluid streams with considerable effort devoted to determining suitable means of combining the properties of the individual phases to yield "effective" values for the mixture [5, p. 105; 71, p. 285-286].

The latter method appears to be the more suitable one for dealing with liquid-liquid dispersions and it will be used in this paper. The methods of obtaining effective property values for dispersions will be discussed in detail in Chapter 6. At this point it seems appropriate to consider briefly the conventional methods of calculation and data correlation for flow and heat transfer in single-phase fluid systems.

Fluid Friction in Smooth Tubes

Consider the steady flow of a liquid between two points in a conduit, the direction of flow being taken from point 1 to point 2. Two of the most powerful tools used in analyzing flow problems are the general energy equation and the continuity equation. The first of these is a statement of the law of conservation of energy while the continuity equation expresses the conservation of mass. If the flow is approximately isothermal and if the fluid may be considered incompressible, as is the case

for most liquids, the energy equation may be written as follows for a unit mass of flowing fluid:

$$(1) \qquad \frac{P_2-P_1}{\rho} + \frac{V_2^2-V_1^2}{2\alpha g_c} + \frac{g(Z_2-Z_1)}{g_c} = -\bar{w} - \overline{lw}.$$

In this equation the symbols have the following meanings:

P_1 is the pressure at point 1 in $\frac{lb_f}{ft^2}$, and similarly for P_2 at point 2,

ρ is the density of the liquid in $\frac{lb_m}{ft^3}$,

V is the average linear velocity in $\frac{ft}{sec}$,

g is the acceleration due to gravity in $\frac{ft}{sec^2}$,

$g_c = 32.174 \frac{(lb_m)\ (ft)}{(lb_f)(sec^2)}$, a conversion constant introduced because of the common engineering practice of using the pound as a unit both of force (lb_f) and of mass (lb_m),

Z is the elevation above an arbitrary datum plane in ft,

$\bar{w}$ is the work done by the fluid in passing between points 1 and 2 in $\frac{(ft)(lb_f)}{lb_m}$ (in the case of a pump in the system, work would be done by the pump on the fluid and $\bar{w}$ would be negative by convention),

$\overline{lw}$ is "lost work", i.e. energy that could have done work but was dissipated in irreversibilities (friction)

in the flowing fluid, in $\frac{(ft)(lb_f)}{lb_m}$.

When a fluid flows in a conduit, a frictional drag arises in the region of the solid boundaries producing a velocity distribution across any section perpendicular to the flow direction. The average linear velocity (V) used in the kinetic energy term of equation (1) is conveniently defined as the ratio of the volumetric flow rate to the cross-sectional area of the conduit. The factor, α, in the kinetic energy term is a correction factor to account for the fact that the velocity distribution varies with the type of flow. For flow in a circular conduit, it can be shown that α is equal to 1/2 for laminar flow and approximately equal to 1 for turbulent flow [11, vol. 1, p. 42, 46].

Inspection of equation (1) reveals that each term has units of $\frac{(ft)(lb_f)}{lb_m}$, i.e. energy per unit mass of flowing fluid. It should also be noted that when $\bar{w}$ and $\overline{lw}$ are both zero, equation (1) becomes the familiar Bernoulli equation. The units given above are not, of course, the only ones that could be used. They are in wide use in engineering work however, and will be applied consistently throughout this report.

For one-dimensional flow in the x-direction, the

continuity equation may be written

$$\frac{d(\rho AV)}{dx} = 0, \tag{2}$$

where A is the cross-sectional area of the flow channel. For a conduit with uniform cross-section, and since ρ is constant, equation (2) reduces to $V_1 = V_2$. If, in addition, no work is done on or by the fluid between points 1 and 2, the energy equation becomes

$$\frac{\Delta P}{\rho} + \frac{g\,\Delta Z}{g_c} = -\overline{Iw} \tag{3}$$

where P_2-P_1 and Z_2-Z_1 have been replaced by ΔP and ΔZ respectively. To review the restrictions which have been placed on the general energy balance, equation (3) is applicable to the steady isothermal flow of a liquid in a uniform conduit containing no work-devices such as pumps or turbines. It has also been tacitly assumed that electrical, magnetic, and chemical effects are negligible, an assumption which is good for most pipe flow problems.

A large amount of experimental work in circular tubes has shown that the type of flow which will occur in a given system may be characterized by a dimensionless ratio known as the Reynolds number, named in honor of Osborne Reynolds. This quantity is defined as $Re = \frac{DV\rho}{\mu}$ where D is the inside diameter of the tube in which the fluid is flowing and μ is the dynamic viscosity of the fluid. For Reynolds numbers below about 2100 the flow is laminar, i.e.

the individual fluid particles all flow parallel to the walls of the tube in smooth layers or lamina. As the Reynolds number is increased above a value of about 2100 local eddies begin to develop and the flow pattern becomes chaotic. This type of flow is called turbulent. Actually, the transition from laminar to turbulent flow is not abrupt but occurs over a range of Reynolds numbers from about 2100 to 3000. This range is known as the critical region. In most process applications turbulent flow is by far the more important type and it will be emphasized here.

A large number of experimental determinations of the turbulent resistance which a flowing fluid encounters have led to the conclusion that this resistance is proportional to the fluid density and to the square of the average velocity and that it is only slightly affected by the fluid viscosity. This relationship is known as the quadratic resistance law and may be expressed as follows [39, p. 118]:

$$F = \frac{f \rho V^2 A'}{2g_c} \tag{4}$$

where F is the resisting force at the wall of the conduit, A' is the surface area of the wall at which F acts, and f is a proportionality factor known as the Fanning friction factor.

For a circular tube of inside diameter D and length L, A' is equal to πDL. The energy required to overcome

the frictional force in moving the fluid through the tube a distance δL would be $F\,\delta L$. This energy would push out of the tube a volume of fluid of $\frac{\pi D^2 \delta L}{4}$ or a mass of $\frac{\rho \pi D^2 \delta L}{4}$. Therefore, the energy required to overcome friction (or dissipated as friction losses) per unit mass of flowing fluid is

$$\overline{lw} = \frac{4F\,\delta L}{\rho \pi D^2\,\delta L} = \frac{2fLV^2}{Dg_c} . \tag{5}$$

If this expression for $\overline{lw}$ is substituted in the energy equation (3) we obtain

$$\frac{\Delta P}{\rho} + \frac{g\,\Delta Z}{g_c} = \frac{-2fLV^2}{Dg_c} , \tag{6}$$

or

$$\Delta P + \frac{\rho g\,\Delta Z}{g_c} = \frac{-2fL\,\rho V^2}{Dg_c} . \tag{6a}$$

For the case of a horizontal pipe ($\Delta Z=0$), this becomes the familiar Fanning equation,

$$-\Delta P_f = \frac{2fL\,\rho V^2}{Dg_c} \tag{7}$$

where $-\Delta P_f$ is the pressure change due to frictional effects alone. Thus the total pressure difference between points 1 and 2 may be written as

$$\Delta P = \Delta P_f - \frac{\rho g\,\Delta Z}{g_c} . \tag{8}$$

It is evident from the above discussion that the problem of calculating the frictional pressure loss for a liquid in turbulent flow in a pipe involves principally the determination of the friction factor. Various relationships for evaluating this quantity will now be discussed.

It has been found experimentally that the friction factor f depends only on the Reynolds number for flow in smooth tubes with a length-to-diameter ratio $\left(\frac{L}{D}\right)$ exceeding about 50 [8, p. 138]. A smooth tube is defined as one without appreciable surface roughness. This condition is well satisfied by commercially available tubing of glass, copper and brass, for example. If the surface roughness is appreciable, as is the case with some commercial pipe, an additional variable known as the relative roughness is involved in the determination of the friction factor. This case will not be treated here since the experimental work described in this paper was done in a smooth brass tube.

The theoretical studies of turbulent flow in smooth tubes by Prandtl [62, p. 105-114] and von Kármán [36, p. 58-76] have given rise to an equation of the following form:

$$\frac{1}{\sqrt{f}} = B \log (Re \sqrt{f}) + E \tag{9}$$

where B and E are constants. This equation has also been

derived in an independent manner by Millikan [54, p. 386-392]. Nikuradse [57, p. 30-31] conducted experiments on the flow of water in smooth tubes for a range of Reynolds numbers from 4000 to 3,200,000. Using his own results as well as the earlier extensive data of Stanton and Pannell [74, p. 217-224], Nikuradse found equation (9) valid over the entire range of Reynolds numbers investigated. Inserting his values of the constants B and E, equation (9) becomes

$$\frac{1}{\sqrt{f}} = 4.0 \log (Re \sqrt{f}) - 0.40. \tag{10}$$

The constants determined by von Kármán were based on an analysis of velocity distribution and differed only slightly from those given by Nikuradse. Equation (10) has been widely used in determining friction factors and convenient charts of Reynolds number versus friction factor, based on this equation, have been presented by Moody [55, p. 672] and others.

A number of empirical expressions relating friction factor and Reynolds number have also been developed. In 1913 Blasius analyzed the data then available and proposed the following relationship [39, p. 122]:

$$f = 0.079 \ (Re)^{-0.25}. \tag{11}$$

This equation is applicable for Reynolds numbers from 3000 to 100,000 but is not accurate beyond this range. Later,

Drew, Koo and McAdams [13, p. 61] analyzed over 1300 experimental points and recommended

$$f = 0.00140 + 0.125\ (Re)^{-0.32}. \tag{12}$$

This equation reproduced the experimental data within ± 5 per cent for Reynolds numbers from 3000 to 3,000,000. Another empirical relationship, due to Miller [52, p. 253] is

$$\frac{1}{\sqrt{2f}} = 2.54 \log (Re) - 2.17. \tag{13}$$

The results of using all of the above equations to calculate friction factors are compared at several values of the Reynolds number in Table 1, taken largely from Knudsen and Katz [39, p. 123].

Table 1

Comparison of Friction Factors
Calculated from Various Equations
[Taken largely from reference 39, p. 123]

Reynolds Number	Nikuradse eq. 10	Blasius eq. 11	Drew et al. eq. 12	Miller eq. 13
3,000	0.0109	0.0107	0.0110	0.0113
10,000	0.00772	0.00790	0.00797	0.00783
100,000	0.00448	0.00444	0.00454	0.00451
1,000,000	0.00291	0.00250	0.00290	0.00293
10,000,000	0.00204	0.00140	0.00212	0.00205

It will be noted that all of the equations agree closely up to a Reynolds number of 100,000. The deviation of the Blasius equation for Reynolds numbers larger than 100,000 is evident. In the present work the experimental results were compared with equation (10) because of its basis in theory and its wide use in engineering.

The above discussion has been confined to the important case of turbulent flow in smooth tubes. For the case of laminar flow in circular pipes, it is shown in textbooks on fluid mechanics [39, p. 118] that a particularly simple relationship exists between the Reynolds number and the friction factor. This relationship is

$$f = \frac{16}{Re} \quad , \quad \text{for } Re < 2100. \tag{14}$$

Flow Measurement with Orifice Meter

Whenever a fluid in steady flow in a conduit encounters a constriction the velocity, and thus the kinetic energy, increases in accordance with the continuity equation. This increase in velocity occurs at the expense of the pressure and thus there is a pressure drop across the constriction. The flow rate may be obtained in terms of this pressure difference by application of the energy and continuity equations. There are a number of types of flow meters based on this principle [82, p. 51-70]. The

simplest of these devices is the orifice meter which consists of a plate containing a hole of smaller diameter than the tube in which it is placed. Two pressure taps are provided, one on the upstream side and one on the downstream side of the orifice plate, and the pressure drop across the orifice is measured by means of a manometer.

Figure 1 shows a sketch of an orifice plate installed in a circular pipeline. The contraction of a stream flowing through an orifice is quite pronounced as indicated by the curved lines in the sketch. The point of minimum cross-sectional area occurs a short distance downstream from the orifice and is known as the vena contracta. This is indicated as point 2 in Figure 1.

As in the previous section, the general energy equation for steady, isothermal, incompressible flow with no work done between points 1 and 2 may be written as

$$\frac{\Delta P}{\rho} + \frac{V_2^2}{2\alpha_2 g_c} - \frac{V_1^2}{2\alpha_1 g_c} + \frac{g\,\Delta Z}{g_c} = -\overline{Iw}. \tag{15}$$

In this case the cross-sectional areas of the flow stream are not the same at points 1 and 2 and the continuity equation gives

$$V_1 = \frac{A_2}{A_1} V_2 , \tag{16}$$

where A_1 is the cross-sectional area of the conduit and A_2 is the cross-sectional area of the vena contracta.

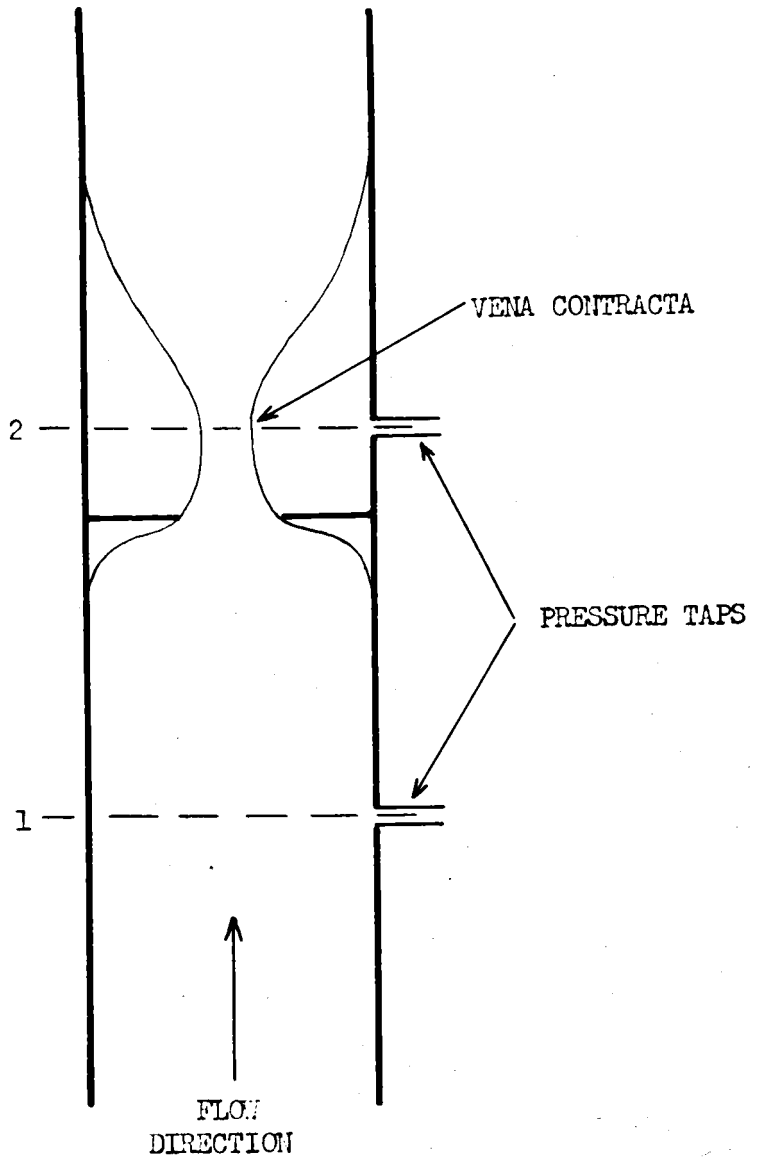

FIGURE 1
ORIFICE PLATE IN A CIRCULAR PIPELINE

Substituting (16) in (15) and solving for V_2 we obtain

$$(17) \qquad V_2 = \left[\frac{2\alpha_2 g_c \left(- \frac{g\,\Delta Z}{g_c} - \frac{\Delta P}{\rho} - \overline{Iw} \right)}{1 - \frac{\alpha_2}{\alpha_1} \left(\frac{A_2}{A_1} \right)^2} \right]^{\frac{1}{2}} .$$

Multiplying by ρA_2 gives the mass rate of flow W, in $\frac{lb_m}{sec}$,

$$(18) \qquad W = A_2 \left[\frac{2\alpha_2 g_c \rho \left(- \frac{\rho g\,\Delta Z}{g_c} - \Delta P - \rho \overline{Iw} \right)}{1 - \frac{\alpha_2}{\alpha_1} \left(\frac{A_2}{A_1} \right)^2} \right]^{\frac{1}{2}} .$$

Expressing the friction losses as a fraction of the pressure difference,

$$- \Delta P - \frac{\rho g\,\Delta Z}{g_c} - \rho \overline{Iw} = C^2 \left(- \Delta P - \frac{\rho g\,\Delta Z}{g_c} \right),$$

we may write

$$(19) \qquad W = CA_2 \left[\frac{2\alpha_2 g_c \rho \left(- \Delta P - \frac{\rho g\,\Delta Z}{g_c} \right)}{1 - \frac{\alpha_2}{\alpha_1} \left(\frac{A_2}{A_1} \right)^2} \right]^{\frac{1}{2}} .$$

The area of the vena contracta A_2 is difficult to measure. It may be conveniently expressed as a fraction of the area of the orifice opening A_0 by defining a coefficient of contraction as

$$C_0 = \frac{A_2}{A_0} . \tag{20}$$

Thus

$$W = CC_0A_0\left[\frac{2\alpha_2 g_c\rho\left(-\Delta P - \frac{\rho g\,\Delta Z}{g_c}\right)}{1 - \frac{\alpha_2}{\alpha_1} C_0^2 \left(\frac{A_0}{A_1}\right)^2}\right]^{\frac{1}{2}} . \tag{21}$$

For the circular conduit the cross-sectional area ratio may be expressed in terms of the diameters. Making this substitution and defining a coefficient of discharge C_D to combine the effects of C, C_0, α_1 and α_2, we obtain

$$W = C_DA_0\left[\frac{2g_c\rho\left(-\Delta P - \frac{\rho g\,\Delta Z}{g_c}\right)}{1 - \left(\frac{D_0}{D_1}\right)^4}\right]^{\frac{1}{2}} \tag{22}$$

where

$$C_D = C\,\frac{A_2}{A_0}\left[\frac{\alpha_2\left[1 - \left(\frac{A_0}{A_1}\right)^2\right]}{1 - \frac{\alpha_2}{\alpha_1}\left(\frac{A_2}{A_1}\right)^2}\right]^{\frac{1}{2}} . \tag{23}$$

It is evident from consideration of equation (23) that the coefficient of discharge is a rather complex function of the Reynolds number and the ratio of orifice diameter to pipe diameter, and is not readily calculable. Convenient plots of discharge coefficient versus Reynolds

number with the diameter ratio as a parameter are available in the literature [8, p. 158]. These curves, determined experimentally, show a marked dependence on both Reynolds number and diameter ratio for low values of the Reynolds number. However, for Reynolds numbers through the orifice greater than 30,000 all of the curves converge to a constant value of the discharge coefficient. This value is approximately 0.61 and is conveniently used in estimating the orifice size required for a given metering problem.

In order to confidently use the curves described above for evaluating the discharge coefficient it is necessary that the orifice meter be fabricated and installed according to certain specifications [64, p. 236-243]. These deal principally with the thickness of the orifice plate, the sharpness of its edges, and the placement of the pressure taps in the pipeline. In practice an orifice meter is usually calibrated experimentally after installation. After the discharge coefficient has been determined, a simple measurement of the pressure drop across the orifice plate suffices to give the mass flow rate for a fluid of density ρ .

The principal disadvantage of the orifice meter is its large permanent pressure loss. For example, in the case of an orifice-to-pipe diameter ratio of 0.5, the permanent pressure loss amounts to approximately 75 per

cent of the measured pressure difference across the orifice plate [8, p. 161]. In spite of this disadvantage the orifice meter is widely used in industrial flow measurements because of its reliability and its simplicity and economy of fabrication.

Many other types of flow measurement devices are available. These are described in standard engineering texts [64, p. 186-337; 61, p. 396-412] and will not be considered here.

Forced Convection Heat Transfer

Heat transfer between a solid surface and a fluid flowing past this surface is a common method of heating and cooling of fluids. Convection involves the transfer of heat by a mixing motion of different parts of the fluid. The motion of the fluid may be entirely due to density differences resulting from temperature differences. In this case the process is known as natural convection. In forced convection the motion is produced by mechanical means, as in pumping a fluid through a conduit. Forced convection is by far the more important case in process applications.

For heat transfer from the surface of a solid at a temperature t_s to a fluid at a temperature t, Newton's law of cooling is usually written

$$(24) \qquad q = hA'(t_s - t) \quad \text{or} \quad h = \frac{q}{A'(t_s - t)}$$

where q is the heat transfer rate in $\frac{Btu}{hr}$,

A' is the area of the solid-fluid interface across which the heat transfer takes place in ft^2,

t_s and t are temperatures in ^oF, and

h is the film coefficient of heat transfer in $\frac{Btu}{(hr)(ft^2)(^oF)}$.

This equation is deceptively simple and, as pointed out by McAdams [46, p. 5], it serves merely to define the heat transfer coefficient.

It is now recognized that the film coefficient depends both on the fluid properties and on the flow variables in a complicated way. Much of the effort in the study of heat transfer by convection has been devoted to methods of predicting film coefficients.

Because of the large number of variables involved in the determination of heat transfer coefficients, mathematical analysis of convection problems is difficult and in many cases prohibitive. It has been customary to apply the principles of dimensional analysis to determine convenient dimensionless quantities which may be used in correlating experimental data.

Consider the case of forced convection heat transfer without phase change involving a liquid flowing in a

circular tube. The following factors are generally considered to be involved in the determination of the film coefficient [46, p. 129].

the density of the fluid, ρ , in $\frac{lb_m}{ft^3}$,

the dynamic viscosity, μ , in $\frac{lb_m}{(sec)(ft)}$,

the thermal conductivity of the fluid, k, in $\frac{Btu}{(hr)(ft)(°F)}$,

the specific heat of the fluid, c_p, in $\frac{Btu}{(lb_m)(°F)}$,

the length of the tube, L, in ft,

the diameter of the tube, D, in ft,

the average velocity, V, in $\frac{ft}{sec}$.

We may therefore write

$$\psi(\mu, k, D, V, \rho, c_p, h, L) = 0 \tag{25}$$

where ψ represents a function of undetermined form. Using mass, length, time and temperature as fundamental dimensions, and noting that eight variables are involved in equation (25), the Buckingham pi theorem states that these variables may be combined into four dimensionless products. Designating these dimensionless products as π_1, π_2, π_3, π_4, it is possible to write

$$\psi'(\pi_1, \pi_2, \pi_3, \pi_4) = 0. \tag{26}$$

If we choose to combine the viscosity, thermal conductivity, diameter, and velocity with each of the other variables in turn, the results are:

$$\pi_1 = \frac{DV\rho}{\mu},$$

$$\pi_2 = \frac{\mu c_p}{k},$$

$$\pi_3 = \frac{hD}{k}, \quad \text{and}$$

$$\pi_4 = \frac{L}{D}.$$

The first of these dimensionless groups is the Reynolds number (Re) as defined previously. The second group is known as the Prandtl number (Pr) and the third group is called the Nusselt number (Nu).

Dimensional analysis is incapable of providing the form of the function in equation (26) so experimental work is required to carry the analysis further. It has been found that the data may be satisfactorily correlated by expressing the Nusselt number as the product of the other three groups, each raised to an appropriate power:

$$\text{Nu} = a(\text{Re})^b(\text{Pr})^c\left(\frac{L}{D}\right)^d \tag{27}$$

where a, b, c, and d are constants. For the units used here it should be noted that a conversion factor is required in the Prandtl number in order to bring the time units into agreement.

It has been found that for highly turbulent flow (Re > 10,000) and for length-to-diameter ratios greater than 60, the exponent on the $\left(\frac{L}{D}\right)$ term in equation (27) is negligible. One of the well known forms of equation (27) is the Dittus-Boelter equation [46, p. 219],

$$Nu = 0.023(Re)^{0.8}(Pr)^{0.4}. \tag{28}$$

In this equation all of the fluid properties are evaluated at the bulk temperature of the fluid stream. Equation (28) is very useful for cases of moderate temperature differences between the wall of the conduit and the flowing fluid. However, the fluid temperature actually varies across the stream and several relationships have been proposed which consider the effect of this temperature variation in an empirical manner. One of the most convenient of these is the equation due to Sieder and Tate [73, p. 1433],

$$Nu = 0.023(Re)^{0.8}(Pr)^{\frac{1}{3}}\left(\frac{\mu}{\mu_s}\right)^{0.14} \tag{29}$$

where μ_s in the viscosity ratio is evaluated at the surface temperature of the conduit, and the rest of the properties are evaluated at the bulk fluid temperature.

Methods for evaluating film coefficients in laminar flow and for the transition region between laminar and turbulent flow are also available in the literature [39, p. 181-183] but will not be considered here.

CHAPTER 3

EXPERIMENTAL EQUIPMENT

General Description

An apparatus has been designed and constructed to permit an investigation of the flow and heat transfer properties of mixtures of immiscible liquids. Figure 2 is a schematic flow diagram showing the essential features of the piping system. A stainless steel supply tank was provided in which the liquid mixtures could be prepared. The liquids were pumped to a vertical test section where the pressure drop and heat transfer measurements were made. A bypass was provided at the pump outlet so that the flow rate through the test section could be controlled by diverting a portion of the fluid back to the supply tank. In addition an orifice plate was installed in the pipeline between the pump and the test section. From the test section the fluid was conducted through the return line back to the supply tank thus completing the circuit. By means of a short flexible hose at the end of the return line the liquid could be diverted to a weighing tank for measurement of the mass flow rate. The important individual components of the system will now be described in detail.

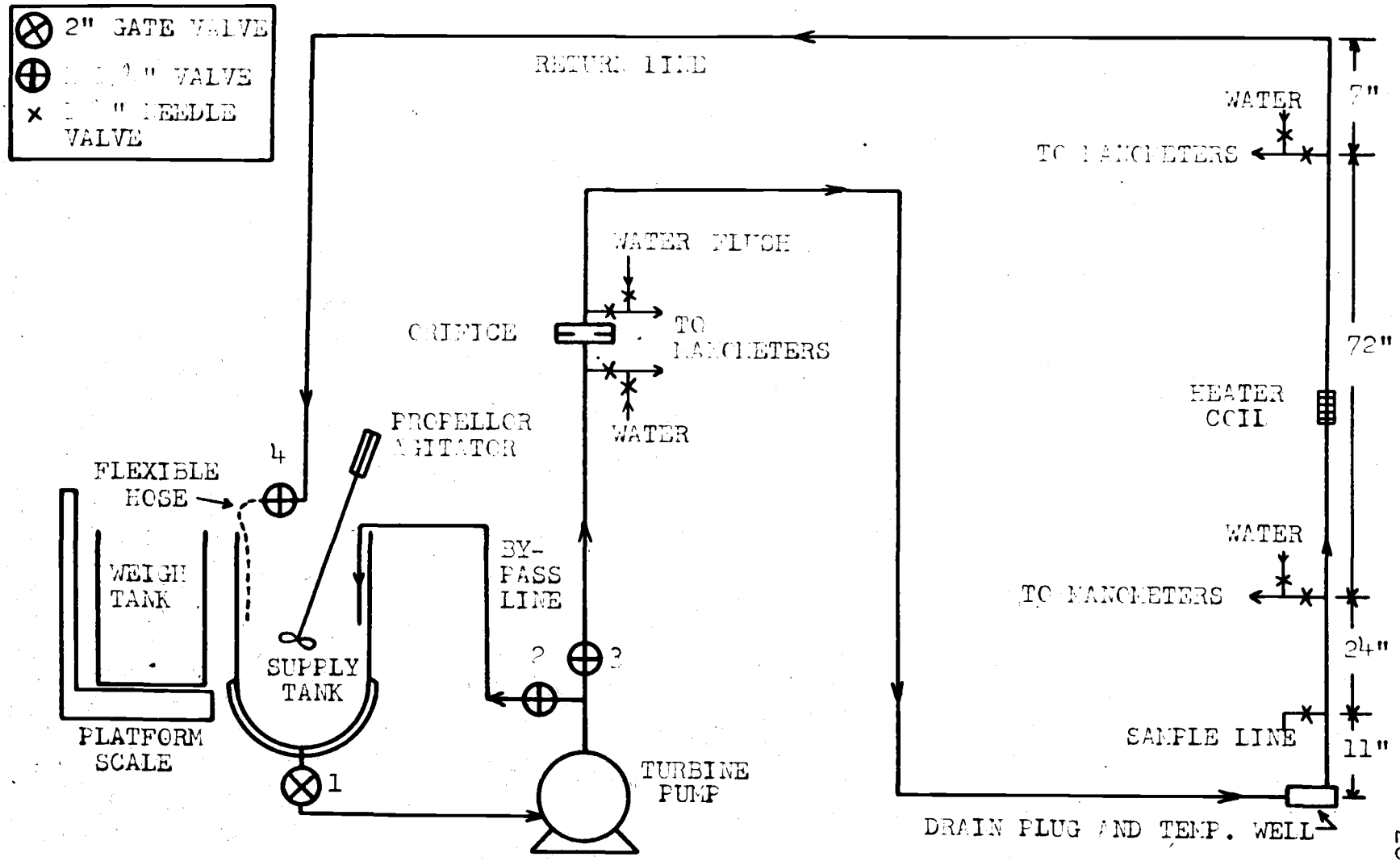

FIGURE 2
SCHEMATIC FLOW DIAGRAM

Supply Tank and Pump

The stainless steel supply tank was cylindrical in shape with a hemispherical bottom and had a total capacity of 80 gallons. The hemispherical portion had a volume of approximately 35 gallons and was jacketed to provide a means of heating or cooling the contents of the tank. In the present work cooling water was circulated through the jacket to keep the tank temperature somewhat below ambient. During operation it was found possible to keep the tank temperature uniform and as low as about 60°F. This greatly reduced the problem of the odor of the petroleum solvent which was used as one of the liquids, and also prevented appreciable loss of solvent or water by evaporation. The temperature of the mixture in the supply tank was measured with a calibrated mercury-in-glass thermometer.

A propellor-type agitator with a variable speed drive was mounted on the edge of the tank. Part of the mixing action was provided by this agitator and part by circulating the liquids through the system with the pump. A perforated plate placed over the outlet opening at the bottom of the tank assisted in preventing vortex formation during operation of the agitator. Figure 3 is an inside view of the supply tank showing the relative locations of the agitator, return line and bypass line.

FIGURE 3
INSIDE VIEW OF SUPPLY TANK

The pump used was a Fairbanks-Morse "Westco" turbine pump driven by a three horsepower electric motor. The pump was made of bronze with mechanical seals and was well suited to service with organic solvents. This type of pump delivers a steady flow, but requires a bypass line for flow control since excessive pressure is built up in the casing if the discharge line is closed. A brief summary of pump characteristics, as supplied by the manufacturer, is given in Table 2.

Table 2

Turbine Pump Characteristics
(supplied by manufacturer)

Material - Bronze
Model Number - BR615
Speed - 1750 rpm

Delivered flow, gpm	Total head, feet of water at 80°F
10	420
20	250
30	110
40	10

In the present system the maximum achievable water flow rate was approximately 30 gallons per minute. A gauge was installed in the line immediately beyond the pump to indicate the pump discharge pressure. In order to assure a positive pressure at all points in the system, the discharge pressure was kept at a minimum value of

about 10 psig by partially closing the valve at the end of the return line (shown as valve number 4 in Figure 2). This was done to prevent leakage of air into the system during operation. Figure 4 shows the supply tank and the pump as well as a portion of the piping system.

Main Piping System

The entire piping system was fabricated of copper or brass, with the exception of the short length of flexible hose at the end of the return line. The piping between the supply tank and the pump inlet was nominal 2-inch red brass pipe. A 2-inch gate valve was inserted in this line to make it possible to drain the system independently of the tank. This is shown as valve number 1 in Figure 2, where the other gate valves are also numbered for convenience of reference. Downstream from the pump the piping loop was made of nominal 1-1/4-inch brass pipe except for the test section which was of 7/8-inch brass tubing. The flexible hose was a 2-foot length of heavy-wall synthetic rubber tubing designed for gasoline service. Tests on this material showed it to be highly resistant to the petroleum solvent used as one of the liquids in this investigation. All threaded connections were made with the assistance of "Cyl-Seal" high pressure sealant manufactured by the West Chester Chemical Company. This material is a highly inert pipe dope which acts as a

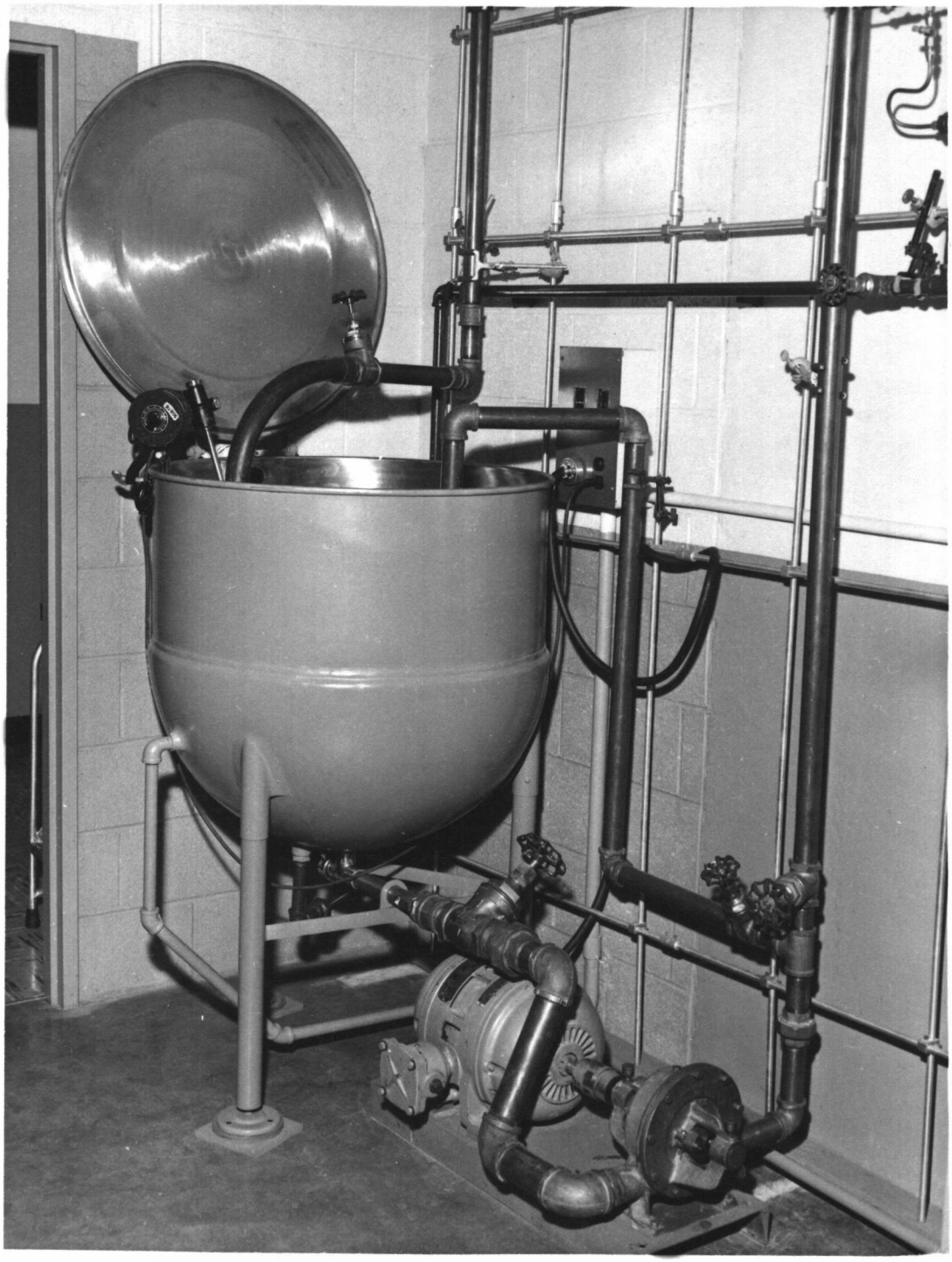

FIGURE 4
SUPPLY TANK AND PUMP

lubricant during assembly of threaded joints and then hardens to prevent leakage.

A considerable effort was made to insure a clean system. As each piping section was assembled it was thoroughly washed with solvent to remove traces of dirt, cutting oil, and sealant. This was done to prevent contamination of the liquids with any material which might have promoted the formation of stable emulsions. Five brass unions were used for ease in assembly and disassembly of the system. A plug was inserted at the low point of the loop to permit draining by gravity. This is indicated at the bottom of Figure 2 just ahead of the vertical test section. The volume of the entire piping loop was approximately 4-1/2 gallons.

A 15-gallon aluminum weighing tank was placed at approximately the same height as the supply tank so the flow stream could be diverted from supply tank to weigh tank by means of the flexible hose. The weigh tank was mounted on a Fairbanks-Morse platform scale with a capacity of 250 pounds and with scale graduations down to 1/16 of a pound. The accuracy of the scale was checked by weighing known volumes of water. It was found that 50 pounds of water could be weighed with an accuracy of $\pm$0.25 per cent. Measurements of the mass flow rate were made by timing the flow of a predetermined weight of fluid (usually 50 pounds) with a stopwatch.

Orifice Meter

A brass orifice plate was mounted between flanges in a vertical section of nominal 1-1/4-inch pipe. The flanges were threaded onto the pipe and were fastened together with four bolts. Gaskets of 1/16-inch thick "Durabla" asbestos paper were used on either side of the orifice plate to create a leak-tight seal. Figure 5 shows the dimensional details of the orifice plate. It was made from 1/16-inch thick brass plate with smooth faces. A hole approximately half the diameter of the pipe was machined in the center of the plate perpendicular to its faces. In addition the downstream face was beveled as indicated in the sketch. Several micrometer measurements were made of the pipe diameter immediately upstream and downstream of the orifice plate. The average pipe diameter was found to be 1.366 ± 0.002 inches. The dimensions given in Figure 5 are within the recommended design specifications for thin-plate or sharp-edged orifices as given by Rhodes [64, p. 237-238].

Piezometer openings were made upstream and downstream of the plate by drilling holes perpendicular to the pipe wall and soldering short lengths of 1/4-inch copper tubing in place. The inside surface was carefully rubbed with emery cloth to assure an opening free from burrs and flush with the inside pipe wall. The upstream piezometer

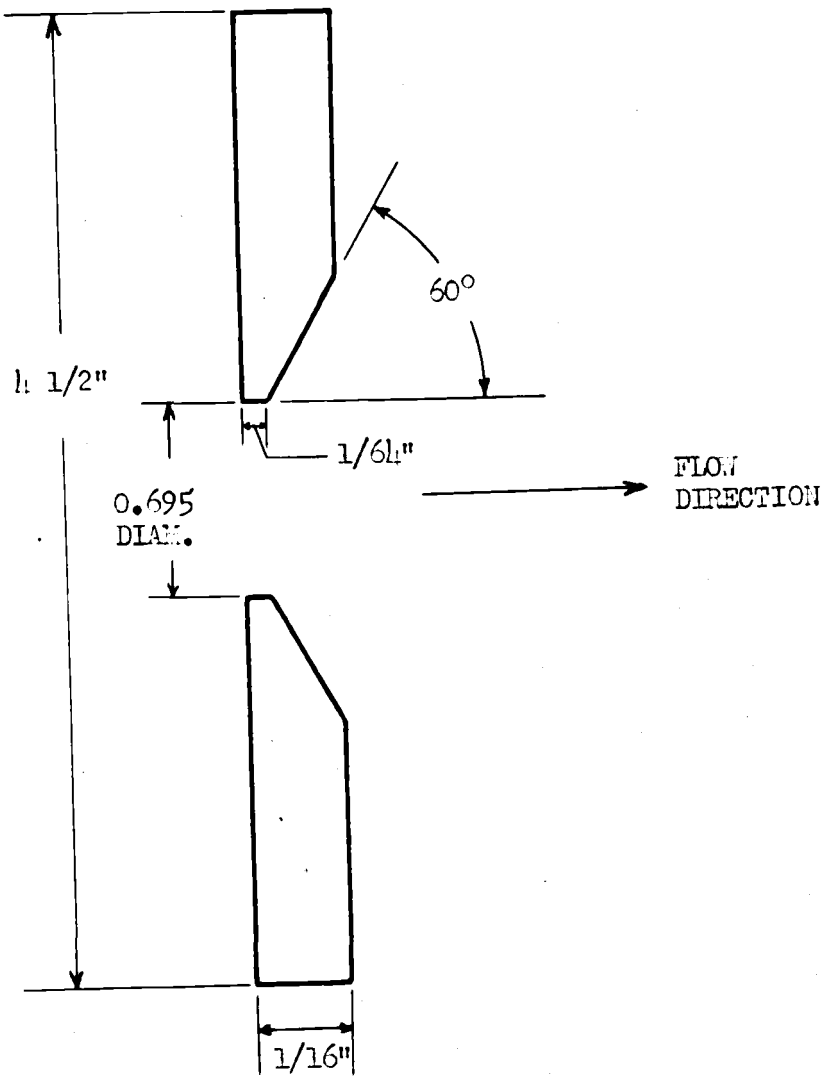

FIGURE 5
DETAIL OF ORIFICE PLATE

tap was located two inches (or about 1-1/2 pipe diameters) from the orifice plate while the downstream tap was placed approximately 2/3 of a pipe diameter from the plate. The location of the downstream tap corresponds closely to the position of the vena contracta for an orifice-to-pipe diameter ratio of 1/2, and these taps are known as vena contracta taps. Since the vena contracta is the position of minimum pressure, the use of taps placed in this way yields the largest obtainable pressure drop readings. Other pressure tap positions in common use are discussed by Perry [61, p. 404-405].

Flow irregularities caused by bends or fittings near an orifice installation can have unpredictable effects on the discharge coefficient. In the present installation the orifice was located in a straight vertical run of pipe about 6 feet long. The plate was separated from any bends or fittings by 45 pipe diameters on the upstream side and by 10 pipe diameters on the downstream side. These distances are considered adequate for stable operation [64, p. 240].

In practice orifice meters are usually calibrated after installation. A very serviceable meter may be constructed without following all of the detailed specifications outlined above. In the present work it was desired to compare the experimentally determined orifice coefficients for two-phase mixtures with the published values

for single-phase fluids as given by Brown [8, p. 158] and others. For this purpose strict attention to the details was required.

Test Section

The vertical test section was made of smooth-wall brass condenser tubing. The outside diameter was 7/8 of an inch and the inside diameter was found by several micrometer measurements at various positions to be 0.7005 ± 0.0005 inches. The section was made vertical to prevent the settling-out of the unstable liquid mixtures along the length of the tube. If the tube had been placed in a horizontal position, the gravitational force favoring settling would have acted in a direction perpendicular to the net flow direction.

Two piezometer taps similar to those described in the preceding section were installed 6 feet apart, thus defining the length of the test section for pressure drop measurements. The overall length of the 7/8-inch brass tube was 9-1/2 feet, leaving 3-1/2 feet for calming sections to eliminate entrance and exit effects. A calming section 35 inches (or 50 diameters) in length preceded the test section and 7 inches (or 10 diameters) were allowed beyond the upper pressure tap (see Figure 2). In addition to the two pressure taps, a third tap was provided two feet below the lower pressure tap. A brass

needle valve allowed access to this tap for sampling to determine the composition of the liquid mixture entering the test section.

In order to measure film heat transfer coefficients a heater coil approximately two inches long was wound on the test section tubing two feet above the lower pressure tap. Six iron-constantan thermocouples were used to measure the tube wall temperature, three directly under the heater coil and three at various distances from the coil. The relative locations of heater coil and thermocouples are indicated in Figure 6. The thermocouples were all made from the same matched spools of number 30 B & S gauge wire supplied by the Leeds and Northrup company. The temperature-voltage characteristics of these thermocouples were found to check closely with the values supplied by the manufacturer [42, p. 6-9]. Slots 1/8-inch wide were milled in the outside tube wall to a depth of about 0.030 of an inch. The thermocouple junctions were soldered to the tube in the positions shown in Figure 6. The leads were run along the slots parallel to the tube for a distance of about one inch or more before being brought out to the measuring instrument. This procedure is recommended in order to reduce the error due to conduction along the wires [46, p. 199].

In addition to those described above, another thermocouple was installed in a temperature well which was

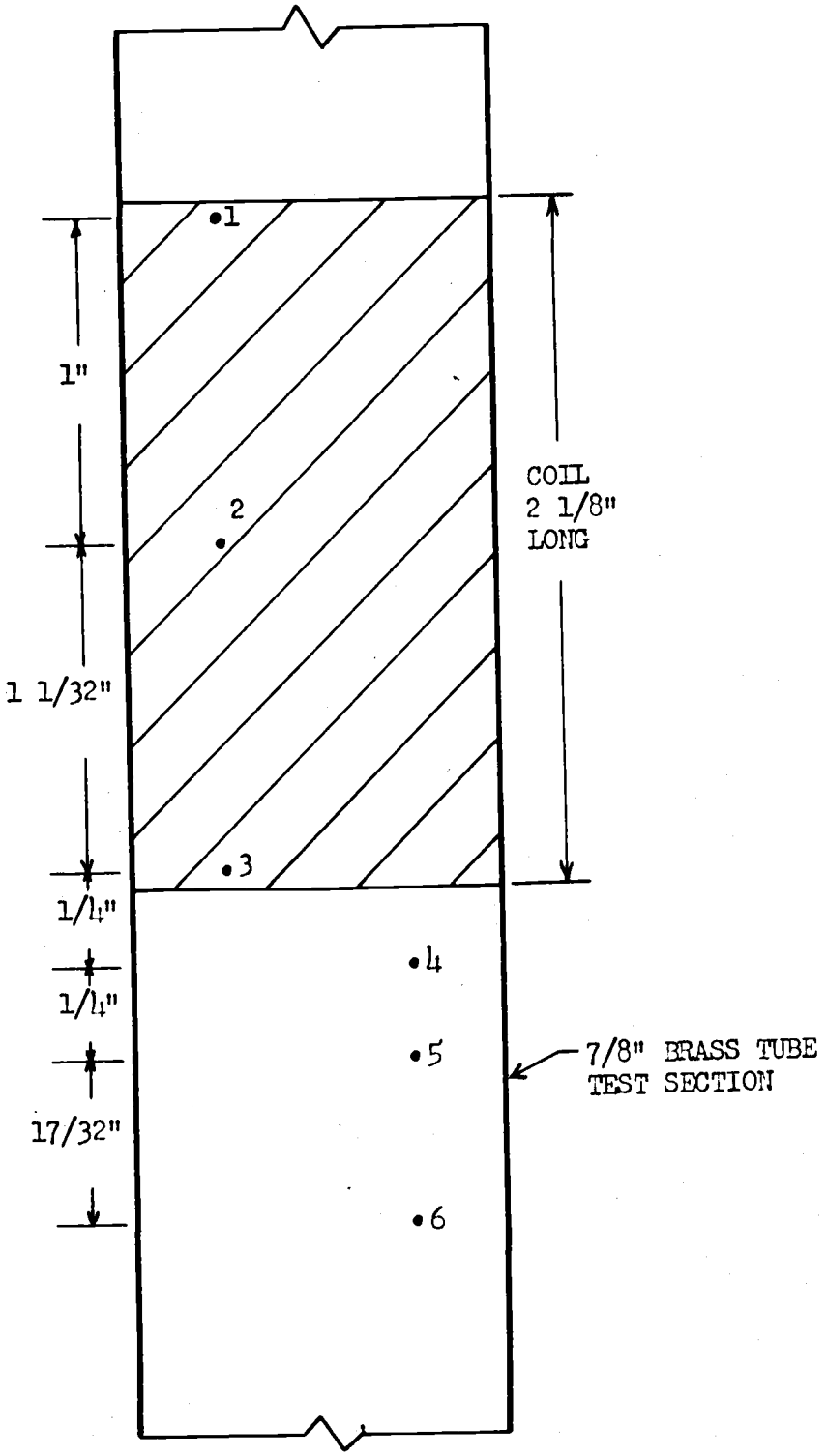

FIGURE 6
RELATIVE LOCATIONS OF HEATER COIL AND THERMOCOUPLES

mounted in the drain plug at the bottom of the pipe loop (see Figure 2). This temperature well consisted of a 5-inch length of 1/2-inch diameter copper tubing closed at one end. The thermocouple junction was soldered to the inside of the closed end of the tube. The temperature well was approximately centered in the flow stream to indicate the temperature of the fluid entering the test section. Each of the seven thermocouples was connected, through a multi-position selector switch, to a cold junction thermocouple and thence to a potentiometer. The cold junction thermocouple was inserted in a thin glass tube filled with oil and the glass tube was immersed in a bath of crushed ice to insure a constant reference junction temperature of 32°F. Thermocouple voltages were measured with a Leeds and Northrup Type K-2 portable precision potentiometer. This instrument permits readings to be made to $\pm$ 0.001 millivolt. A thermocouple wiring diagram is shown in Figure 7. This arrangement of thermocouples and selector switch made it possible to read the seven temperatures in any desired order without making or breaking connections at the potentiometer.

After installation of the thermocouples in the tube wall it was necessary to insulate a 2-inch length of the test section before winding the bare heater wire coil. A coat of clear "Krylon" was sprayed on the tube and a double layer of "Saran Wrap" was applied. This was

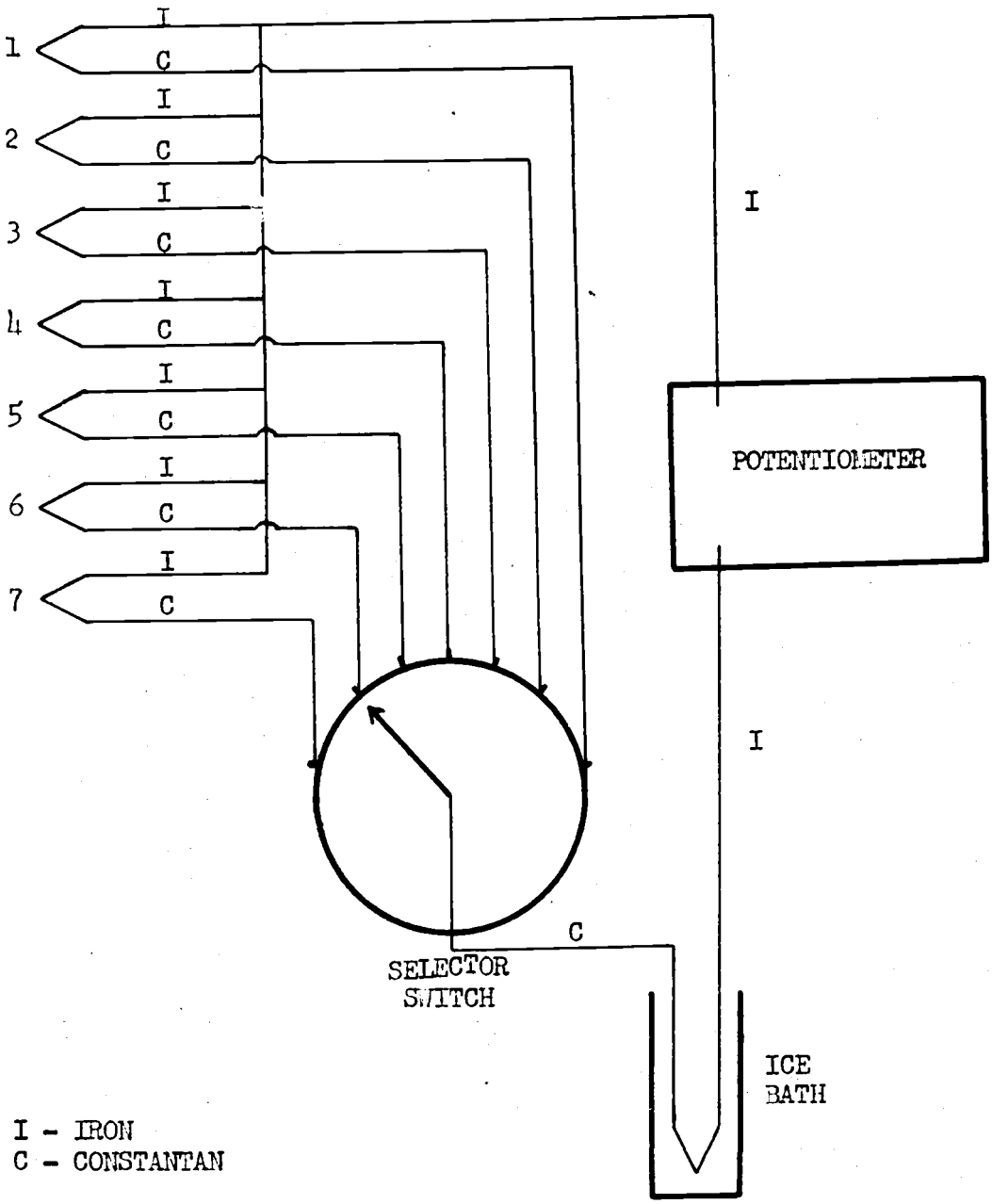

FIGURE 7
THERMOCOUPLE WIRING DIAGRAM

followed by another coat of "Krylon" and an additional single layer of "Saran Wrap". This procedure was found to be satisfactory in producing a thin insulating layer which would not tear when the coil was wound.

The heater wire used was number 18 B & S gauge bare nichrome wire with a resistance of 0.4 ohm per foot. Approximately 10 feet of wire were used giving a total coil resistance of about 4 ohms. Power was supplied by a selenium rectifier battery charger with 115 volt a.c. input and a rated d.c. output of 12.0 volts at 35 amperes. A Raytheon voltage stabilizer was used to reduce fluctuations in the line voltage and thus assure a constant input to the rectifier. A "Powerstat" variable transformer was also installed to permit control of the voltage to the heater coil. Connections between the rectifier and the heater coil were made with number 10 copper wire to provide negligible resistance. With this arrangement the maximum d.c. voltage across the heater coil was found to be about 13 volts. This voltage remained constant within $\pm$0.5 per cent for periods as long as a week. A d.c. ammeter was installed in the circuit to give continuous current readings, and connections were available at the heater coil to permit periodic voltage measurements.

The heater coil and a portion of the test section above and below it were covered with 85 per cent magnesia pipe insulation in order to reduce heat losses to the

room. This insulation was approximately one inch thick and 26 inches long, extending for a distance of one foot above and below the heater coil. Figure 8 shows the heating section with half of the insulation removed to expose the coil.

Manometer System

The pressure differences across the orifice and the test section were measured with double-liquid U-tube manometers. Identical pairs of manometers were provided for the orifice and the test section. Figure 9 shows the manometer board arrangement. One manometer of each pair used water over carbon tetrachloride as the measuring fluid and the other used water over mercury. These combinations give effective specific gravities for the manometer fluids of 0.6 and 12.6 respectively, thus permitting a rather wide range of pressure measurements to be made. The carbon tetrachloride was colored with a small amount of iodine to increase contrast and thus make these manometers easier to use.

The manometers were made of heavy-wall "Pyrex" glass tubing and were 3 feet in length. Connections to the brass seal pots were made with short lengths of rubber tubing secured with wire clamps. Shellac was used as a sealant for these joints. Individual meter sticks were fastened securely to the board to serve as length scales for each

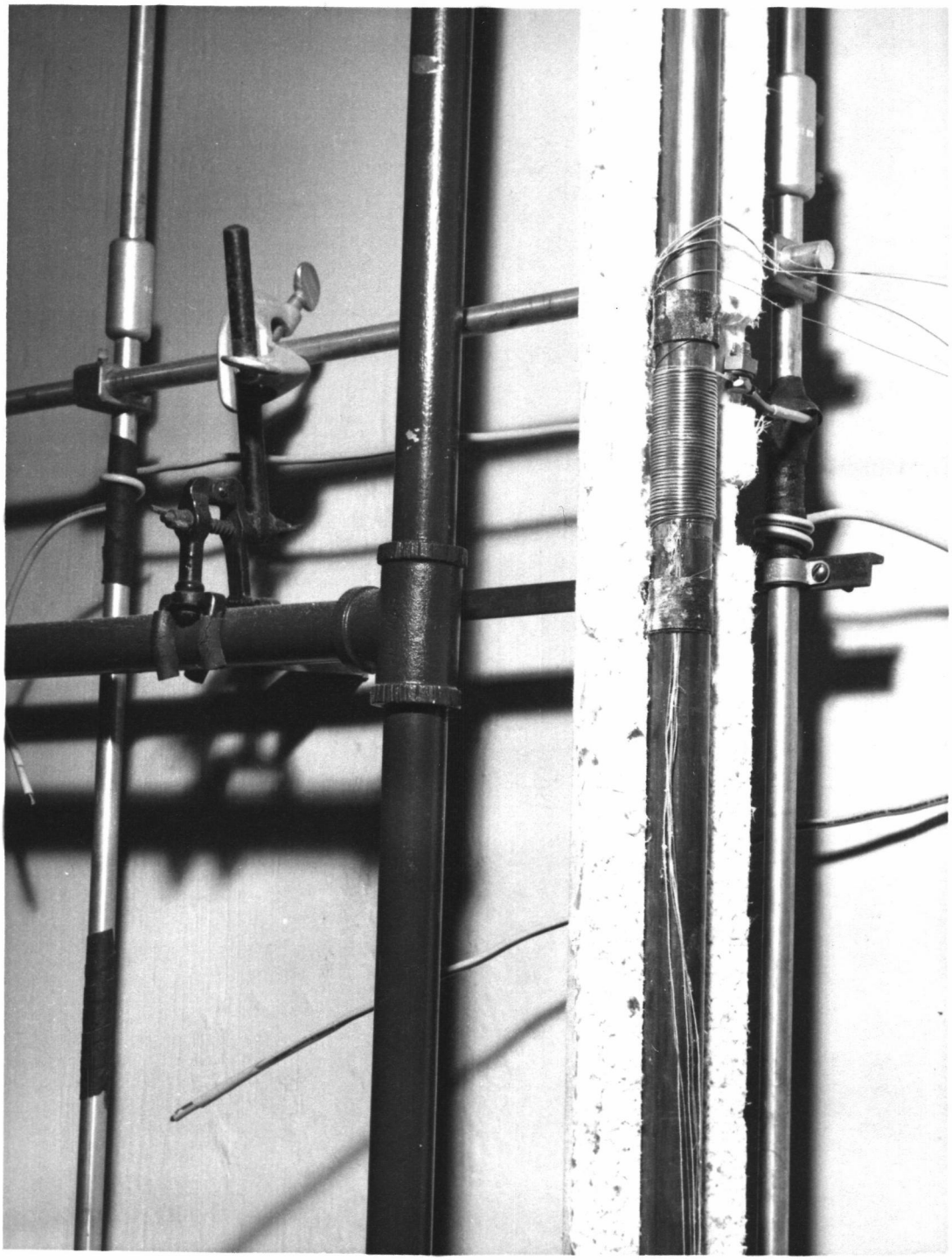

FIGURE 8
HEATING SECTION

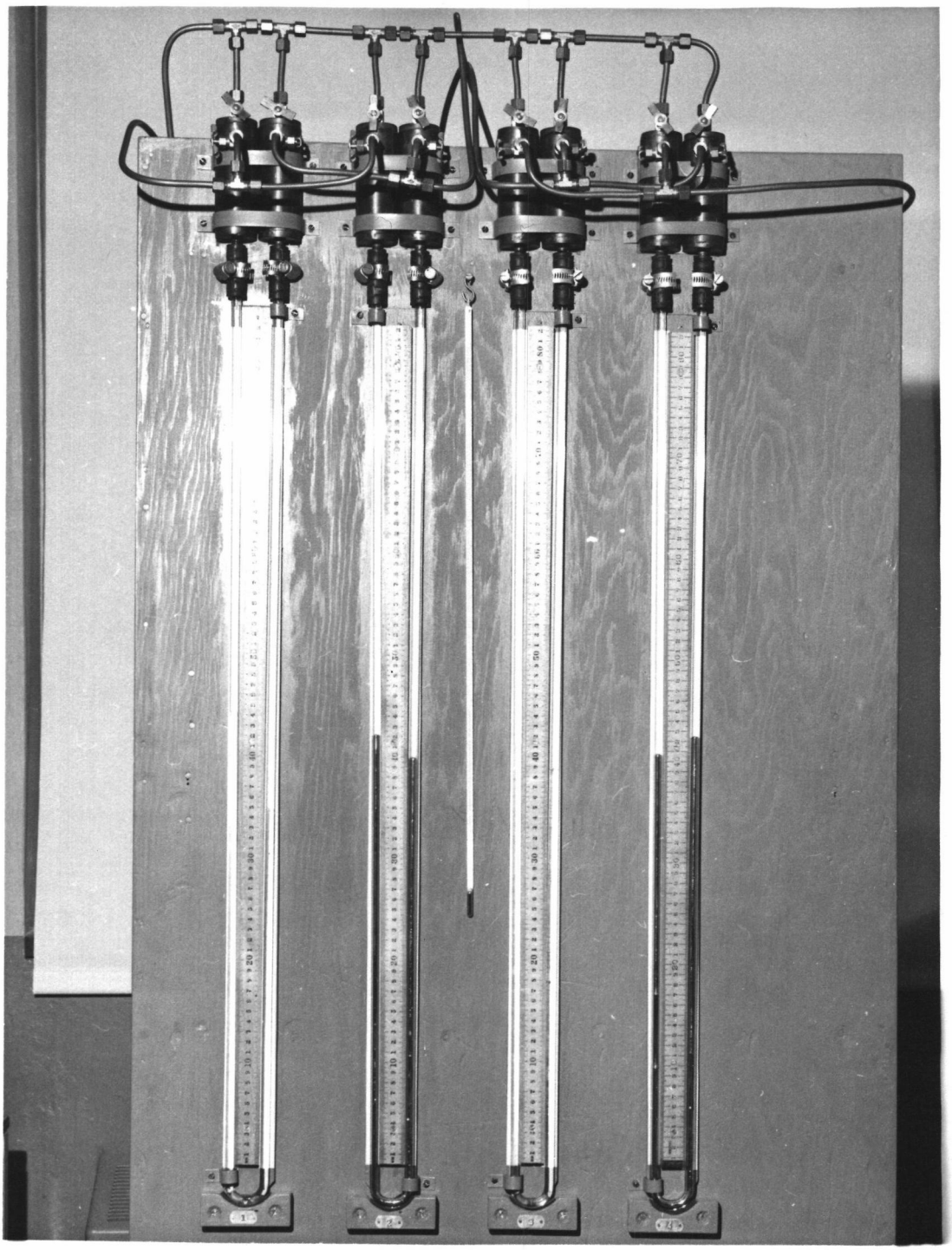

FIGURE 9
MANOMETER BOARD ARRANGEMENT

manometer. A thermometer was also located at the board to indicate the temperature of the manometer fluids.

The lines connecting the pressure taps to the manometers were made of 1/4-inch copper tubing. These lines were filled with water as the pressure transmission medium. Considerable care was taken to avoid leaks since a small amount of air could cause serious errors in the pressure measurements. The lines were run horizontally for a distance of about two feet from each pressure tap before being bent for vertical travel to the manometer board. This was done to prevent transfer of two-phase material from the flow system to the vertical portions of the lines due to movement of the manometer columns. Before operation and between runs the manometer lines were flushed with water to remove traces of air and any two-phase fluid which might have migrated into the vertical lines leading to the manometers. This flushing was accomplished with the aid of a series of 1/4-inch brass needle valves indicated in Figures 2 and 9. This valving was arranged so the manometer legs could be flushed individually or in pairs as desired.

A summary of important equipment dimensions is given below in Table 3.

Table 3

Equipment Dimensions

Orifice diameter, inches	0.695
Pipe diameter, inches	1.366
Orifice-to-pipe diameter ratio	0.5088
Orifice cross section, square feet	0.002634
Vertical distance between orifice pressure taps, feet	0.2370
Length of test section, feet	6.003
Inside diameter of test section, feet	0.05838
Length-to-diameter ratio	102.8
Inside cross section, square feet	0.002676
Outside diameter of test section, feet	0.07292

CHAPTER 4

EXPERIMENTAL PROCEDURE

Scope of Investigation

The liquids used in this investigation were water and "Shellsolv 360", a petroleum solvent manufactured by the Shell Oil Company. Initial tests indicated that mixtures of these liquids separated rapidly into two layers upon cessation of mixing. There appeared to be no tendency toward stable emulsion formation. The purpose of this work was to study the properties of unstable liquid dispersions, and stable emulsions were deliberately avoided.

It was necessary to measure some of the physical properties of the solvent since the manufacturer's specifications did not include them. The properties of water were taken from the literature. Appendix B gives the individual properties for water and solvent, and the properties of mixtures are considered in Chapter 6.

It was initially planned to cover the complete range of compositions, i.e., from 100 per cent water to 100 per cent solvent. However, the instability of the dispersions limited the composition range which could be investigated in the present equipment. Ten series of experimental runs were attempted and these are listed below with the nominal mixture composition of each series:

1. Pure water
2. 50 % solvent in water
3. 20 % solvent in water
4. Pure water
5. 25 % solvent in water
6. (75 % solvent in water)
7. 65 % solvent in water
8. Pure solvent
9. (20 % water in solvent)
10. 10 % water in solvent

The nominal compositions listed above were based on the relative amounts of solvent and water charged to the supply tank. Actual measured compositions deviated slightly from these values. The phrase "solvent in water" indicates that water was the continuous phase (solvent dispersed in water) while "water in solvent" indicates that solvent was the continuous phase.

Series 6 and 9 were unsuccessful. In the case of the nominal 75 per cent solvent in water mixture a single run was made at a measured composition of 75 per cent. After the following run the measured composition was about 61 per cent. This mixture was evidently too unstable to last through a series of runs. When water was added to pure solvent in an attempt to create a 20 per cent water in solvent mixture, no such mixture was obtained even after mixing for about 8 hours.

In each successful series of runs the flow rate was varied from the minimum to the maximum attainable values. In the case of pure water this range was from approximately 1 gpm to 30 gpm. At each flow rate measurements were made of pressure drop across the test section, heat transfer, and orifice pressure drop.

Before any data were collected, pure water was charged to the supply tank and pumped through the piping to check the integrity of the system and the operability of the manometers. Several leaks were detected in this way and repaired. Following this procedure the apparatus was drained and pure solvent was pumped through the piping as a further check on leaks and to assure a clean system free from oil and grease.

Preparation and Analysis of Mixtures

The preparation for a series of runs consisted of charging the required amounts of water and solvent to the supply tank and then mixing the liquids to obtain a uniform dispersion. Mixing was carried out by using the agitator in the supply tank and by pumping the mixture around the loop. Both of these mixing actions appeared to be required to obtain a uniform composition in a reasonable length of time. Mixing times from 2 to 5 hours were required, the longer times corresponding to the higher concentrations. In all but the single series of water

in solvent runs, the mixture was prepared by adding the solvent to the water during mixing. Uniformity of composition was indicated by steady manometer readings, by constant thermocouple readings, and by visual observation. During mixing the appearance of the material in the tank changed gradually from clear liquid to the typical creamy white emulsion color.

Mixture compositions were measured volumetrically. Samples were collected in 500 milliliter graduates. The graduates were covered with watch glasses and set aside to permit separation of the two liquid phases.

Meissner and Chertow [47, p. 857-859] have studied settling and coalescence of unstable emulsions. These writers recognized two distinct periods in the complete phase separation process which they have labeled "primary break" and "secondary break". Primary break occurs rapidly and results in two separate layers, a clear dispersed-phase layer and a cloudy continuous-phase layer. Secondary break was found to occur about 10 times slower than primary break and resulted in a clear continuous-phase layer.

These phenomena were clearly evident in the present work with solvent-water mixtures. While accurate measurements were not made, it was noted that primary break occurred in 1 or 2 hours while secondary break required 10 to 15 hours. The samples were always allowed to stand

overnight before volume measurements were made. Even after settling was complete, large drops of dispersed-phase liquid were observed clinging to the wall of the graduate in the continuous-phase layer. It was necessary to dislodge these drops by gentle stirring with a glass rod before accurate volume measurements could be made. In aggregate these drops represented as much as 2 per cent of the dispersed-phase volume.

As mentioned previously, cooling water was supplied to the double-walled supply tank to keep the temperature of the mixtures below ambient. Periodic adjustments of the cooling water flow rate were made to keep the tank temperature at about 60°F. The volumetric analyses of the samples were actually made at room temperature since the samples were allowed to stand overnight. A temperature correction was therefore applied to the volume compositions, based on the known temperature-density relationship for each of the liquids. These corrections were always small but were made in every case.

After mixing of the nominal 50 per cent dispersion for about 4 hours, samples were taken from various locations throughout the system to determine uniformity of composition. The results are shown in Table 4.

Table 4

Compositions of Samples from Various Locations

Location	Composition, % solvent by volume
Test Section	49.1
Bypass Line	49.4
Return Line	49.5
Supply Tank	49.3

Since these compositions were so nearly equal it was decided that sampling from the return line would be sufficient to indicate the composition of the mixture passing through the piping system. All further sampling was done from the return line to the supply tank.

At the end of a series of runs the mixture in the supply tank was allowed to settle into two layers. In spite of the care taken to maintain a clean system, a small amount of contamination was noted at the interface between the liquid layers. The solvent, which was always clear, was decanted and saved for future runs. The water, together with a small amount of solvent at the interface, was discarded and replaced with fresh water which was used in making a new mixture. Initial runs were made with distilled water, but it was found that the use of city water had no apparent effect on settling times or the amount of contamination at the interface. Therefore, after the 50 per cent runs, city water was used for the balance of the work.

Friction Loss and Orifice Measurements

After preparation of a two-phase mixture as described above, all manometer lines were flushed with water before data were taken. Following this the valve at the end of the return line was closed and no-flow manometer readings were taken (all flow through bypass line). Because both test section and orifice installation were vertical, these readings were zero only for the case of the pure water runs.

The valve at the end of the discharge line was then partially opened to establish flow through the system, and pressure drop measurements were taken across orifice and test section. The carbon tetrachloride manometers were used for low flow rates and the mercury manometers for high flow rates. At intermediate flow rates both manometers were often read to permit intercomparison between them. Pressure measurements covered the range from about 1 centimeter of carbon tetrachloride to 60 centimeters of mercury.

Some fluctuation in the height of the manometer columns was observed. In most cases these fluctuations were reduced by closing down on the needle valves at the pressure taps and at the manometer seal pots until these valves were open about 1/2 turn from the fully closed position. It was observed that movement of the liquid

columns occurred about an equilibrium position and no difficulty was encountered in obtaining satisfactory readings. At low flow rates, however, the fluctuations were generally more serious. In these cases several readings were taken and averaged. In addition to the manometer readings the temperature indicated by the thermometer mounted at the manometer board was read and recorded.

Heat Transfer Measurements

The measurements associated with the heating section were the seven thermocouple voltages and the power supplied to the heating coil. Normally thermocouple voltages were read at intervals of a few minutes until successive readings differed by no more than 0.002 millivolts. It was then presumed that steady state conditions had been attained. As in the case of the pressure drop measurements, there were cases of erratic behavior where steady voltages were not attained.

In each run measurements of current in the heating coil and voltage drop across the coil were taken to establish the power input. For a given setting of the "Powerstat" variable transformer, the power input was steady, varying by about 1 per cent throughout an entire series of runs.

The application of the general energy equation in Chapter 2 was restricted to isothermal flow conditions.

Since the liquid mixtures were actually heated in passing through the test section, this assumption is not strictly valid. Practically, however, the temperature rise was so small that the assumption of isothermal flow was applicable. The maximum attainable power input was about 44 watts giving a maximum heat flux of 4,800 $\frac{\text{Btu}}{(\text{hr})(\text{ft}^2)}$. In most cases the temperature rise due to the heating coil was less than 0.1°F. In the extreme case of pure solvent at the lowest flow rate encountered, the temperature rise was 0.65°F. As a consequence of the low power input, temperature differences between tube wall and flowing fluid were usually less than 10°F, limiting the accuracy attainable in the heat transfer measurements.

Measurement of Flow Rate

The mass flow rate was determined for each run by diverting the flow stream from the supply tank to the weigh tank and timing the collection of a predetermined amount of fluid with a stopwatch. This measurement was performed by starting and stopping the stopwatch as the weight of the tank plus sample passed through two predetermined values. In this way momentary flow irregularities caused by movement of the flexible line were not included in the sample collection period. In most cases 50 pounds of liquid were collected in the weigh tank.

At low flow rates 10 to 20 pounds were collected in order to keep collection times below 120 seconds. At high flow rates collection times were as low as 13 seconds. Successive measurements at a given flow rate generally agreed within 1 per cent.

The total volume of liquid charged to the supply tank was about 50 gallons, which provided a suction head on the pump of about 3 feet. During collection of a sample in the weigh tank this suction head changed by less than 10 per cent. Changes of about 0.5 millimeter in manometer levels often occurred during the sample collection period. These changes were noted and recorded.

Summary of Experimental Procedure

At each flow rate of each series of runs the following data collection procedure was used:

(a) Flush manometer lines with water.

(b) Take and record no-flow manometer readings.

(c) Establish a flow rate through system by adjusting valves 2 and 4 (Figure 2, Chapter 3).

(d) Record valve settings and pump discharge pressure.

(e) Read and record manometer levels for orifice and test section.

(f) Read and record temperature at manometer board.

(g) Read and record seven thermocouple voltages.

(h) Read and record current and voltage through heater coil.

(i) Measure mass flow rate, recording mass of fluid collected and collection time.

(j) Recheck manometer readings during collection in weigh tank.

(k) Read and record temperature of liquid in supply tank.

(l) Withdraw sample from return line for measurement of volume composition.

When the data had been recorded, the flow rate was changed and the above procedure was repeated. Steady state conditions at the new flow rate were apparently achieved very rapidly. A period of 10 to 15 minutes was always allowed before data were taken.

CHAPTER 5

EQUATIONS FOR EVALUATING FRICTION FACTOR, ORIFICE COEFFICIENT AND HEAT TRANSFER COEFFICIENT

Fanning Friction Factor

The expression for the pressure difference between two points in a vertical circular tube carrying a single-phase liquid was derived in Chapter 2 as equation (8). This equation may be written for a two-phase liquid mixture as

$$-\Delta P_f = -\Delta P - \frac{g}{g_c}\rho_m \Delta Z, \tag{30}$$

where ρ_m is the density of the two-phase fluid and the other symbols have the same meaning as given previously.

It is now necessary to consider what the manometer actually indicates. Figure 10 is a sketch of a manometer connected between points 1 and 2 in a vertical conduit. A reference level is indicated in the sketch, at which the pressure is P_r. This reference level pressure may be expressed in terms of either P_1 or P_2:

$$P_1 + \frac{g}{g_c}(c+b)\rho_w = P_r \tag{31}$$

or

$$P_2 + \frac{g}{g_c} a \rho_w + \frac{g}{g_c} b \rho_b = P_r. \tag{32}$$

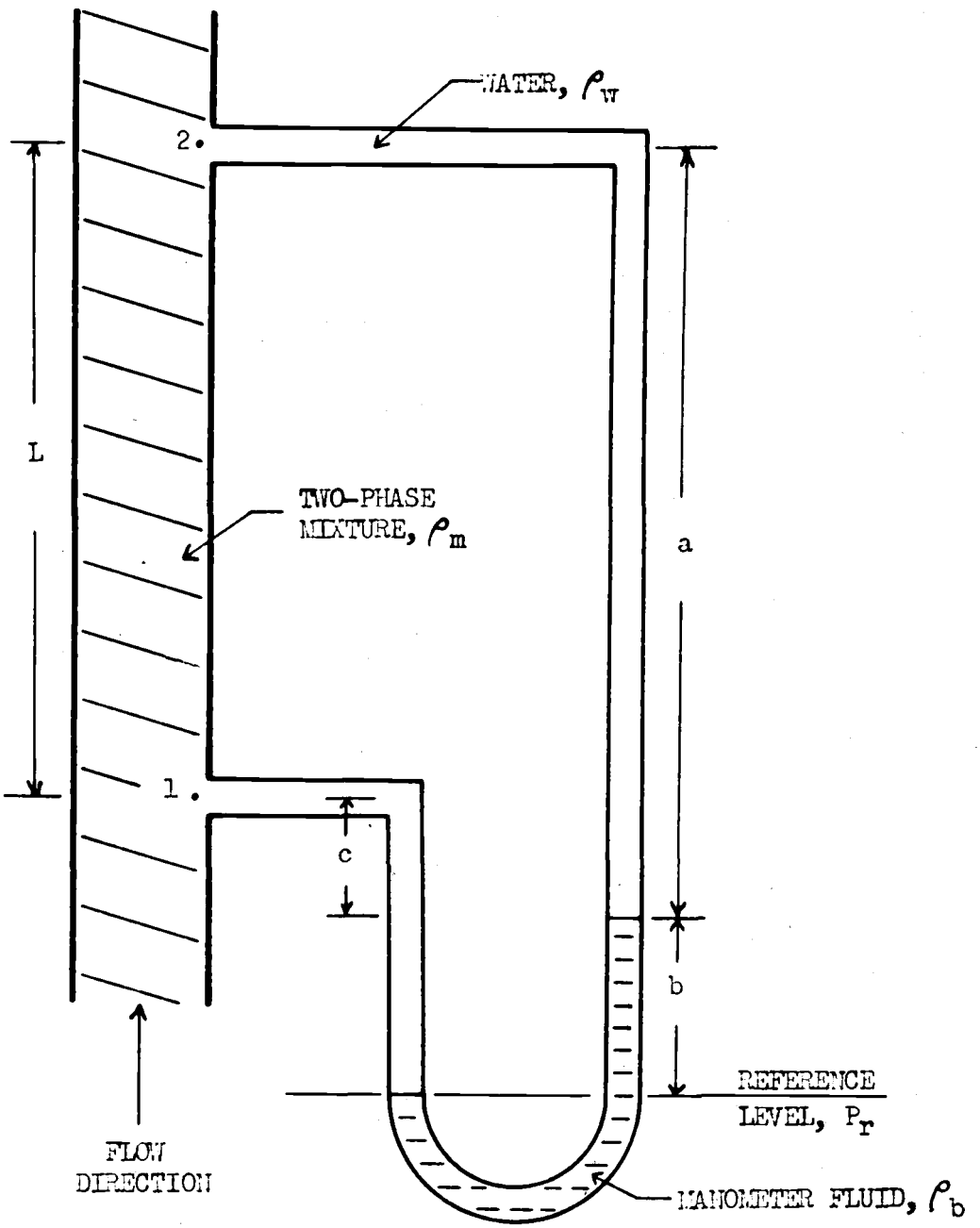

FIGURE 10
MANOMETER CONNECTED ACROSS VERTICAL TEST SECTION

Equating these expressions and solving for the pressure difference between points 1 and 2,

$$(33) \quad P_1 - P_2 = -\Delta P = \frac{g}{g_c}(a-c)\rho_w + \frac{g}{g_c}b(\rho_b - \rho_w).$$

But (a-c) is equal to the length L of the vertical section and $(\rho_b - \rho_w)$ is the effective density ρ_e for the two-fluid manometer. The sign convention which has been adopted is that a manometer reading as indicated in Figure 10 is to be considered positive, i.e.

b = (right leg reading) - (left leg reading).

If equation (33) is solved for the pressure equivalent of the manometer reading, equation (34) is obtained:

$$(34) \quad \frac{g}{g_c} b \rho_e = -\Delta P - \frac{g}{g_c} L \rho_w.$$

Comparison of equations (34) and (30) shows that the manometer does not give the friction pressure drop directly, except when the fluid flowing through the system is pure water. For other cases the quantity $\frac{g}{g_c} L(\rho_w - \rho_m)$ must be added to the manometer reading to give

$$(35) \quad \frac{g}{g_c}b\rho_e + \frac{g}{g_c}L(\rho_w - \rho_m) = -\Delta P - \frac{g}{g_c}L\rho_m = -\Delta P_f.$$

This added term (or rather its negative) is what the manometer indicates under no-flow conditions. Thus the difference between the manometer readings under flow and no-flow conditions is required for evaluation of the friction pressure drop.

After the friction pressure loss has been evaluated, it may be used to compute the friction factor from the Fanning relationship,

$$f = \frac{g_c D \rho_m (-\Delta P_f)}{2LG^2} \tag{36}$$

where

$G = \rho_m V$ is the mass velocity in $\frac{lb_m}{(sec)(ft^2)}$.

Orifice Coefficient

In Chapter 2 the orifice equation was derived as equation (23). This may be written for the two-phase liquid mixture as

$$W = C_D A_O \left[\frac{2g_c \rho_m \left(-\Delta P - \frac{g}{g_c} \rho_m \Delta Z \right)}{1 - \left(\frac{D_O}{D_1} \right)^4} \right]^{\frac{1}{2}}. \tag{37}$$

The pressure difference expression required in the numerator of equation (37) is obtained in exactly the same manner as described above. Again the difference between the flow and no-flow manometer readings is required, and equation (35) becomes

$$\frac{g}{g_c} b \rho_e + \frac{g}{g_c} L' (\rho_w - \rho_m) = -\Delta P - \frac{g}{g_c} L' \rho_m, \tag{38}$$

where L' is the vertical distance between the orifice

pressure taps. Once again when the flowing liquid is water, the manometer reading under flow conditions gives the desired quantity directly.

Substituting (38) into (37) yields the expression for the orifice coefficient in terms of the measured quantities:

$$(39) \qquad C_D = \frac{W}{A_O \left[\frac{2 g_c \rho_m \left[\frac{g}{g_c} b \rho_e + \frac{g}{g_c} L' (\rho_w - \rho_m) \right]}{1 - \left(\frac{D_O}{D_1} \right)^4} \right]^{\frac{1}{2}}} .$$

Heat Transfer Coefficient

Figure 11 shows a portion of the brass tube test section in the vicinity of the heating coil. Heat is supplied by the coil and this heat is partially transferred to the liquid flowing beneath the coil and partially conducted along the tube wall away from the coil. The following assumptions are made:

(a) The power input is small so the liquid flowing through the tube remains at an essentially constant temperature t_a,

(b) The tube material (brass) has a high thermal conductivity so the radial temperature gradient in the wall is negligible,

(c) The thermal conductivity of the brass is independent of temperature,

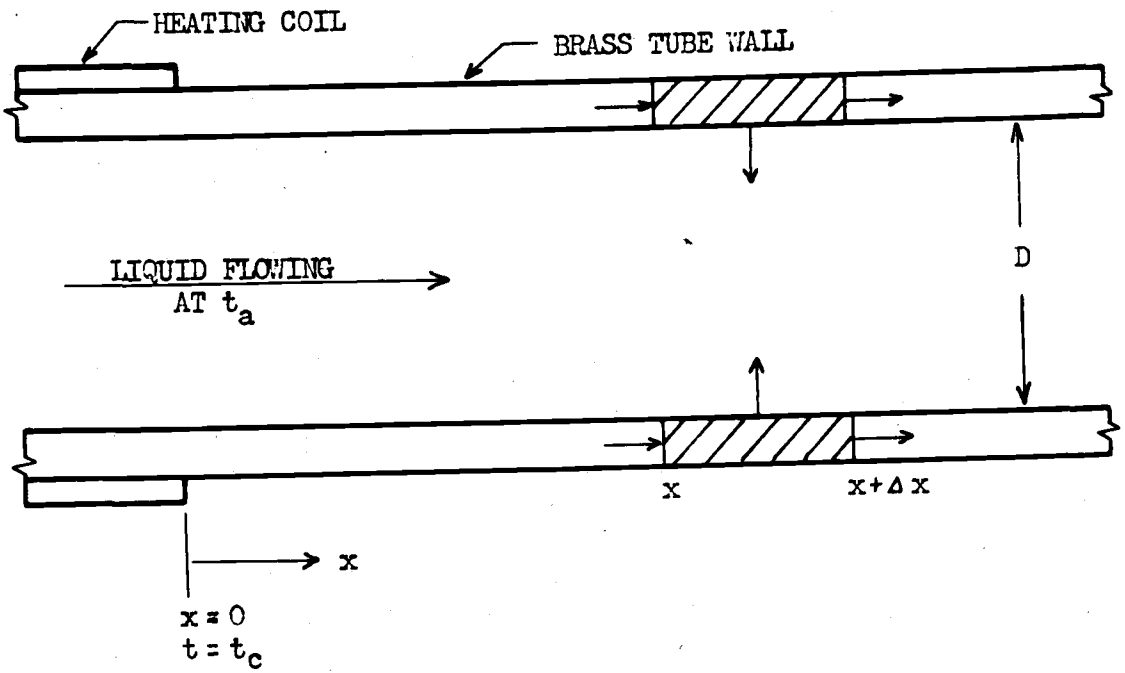

FIGURE 11
SKETCH OF TEST SECTION FOR HEAT BALANCE

(d) There is no heat loss radially outward from the tube (the tube was insulated as described previously),

(e) The tube wall directly under the heating coil is at a uniform temperature t_c,

(f) The cross-sectional area of the tube material, A_{cs}, is uniform along the length of the tube,

(g) Steady state conditions prevail.

With these assumptions a heat balance is made for a short section of tubing of length Δx. The input to the section is by conduction and the output consists of conduction along the tube wall and convection to the fluid flowing in the tube:

$$-kA_{cs}\left.\frac{dt}{dx}\right|_x = -kA_{cs}\left.\frac{dt}{dx}\right|_{x+\Delta x} + h\pi D\,\Delta x(t-t_a) \tag{40}$$

where

x is the distance along the tube measured from the end of the heater coil,

t is the temperature of the tube wall at any value of x,

h is the film heat transfer coefficient.

Applying the mean value theorem,

$$-kA_{cs}\left.\frac{dt}{dx}\right|_x = -kA_{cs}\left[\left.\frac{dt}{dx}\right|_x + \Delta x\left.\frac{d^2t}{dx^2}\right|_{x+\theta\,\Delta x}\right] + h\pi D\,\Delta x(t-t_a) \tag{41}$$

$$0 < \theta < 1$$

or

$$kA_{cs}\,\Delta x\left.\frac{d^2t}{dx^2}\right|_{x+\theta\,\Delta x} = h\pi D\,\Delta x(t-t_a). \tag{42}$$

Dividing equation (42) through by Δx and letting Δx approach zero, the following differential equation is obtained:

$$\frac{d^2t}{dx^2} = \beta^2(t-t_a) \tag{43}$$

where $\beta^2 = \frac{h\pi D}{kA_{cs}}$.

The complete solution of this equation is

$$t = c_1e^{\beta x} + c_2e^{-\beta x} + t_a \tag{44}$$

and the boundary conditions are

$$t(0) = t_c \text{ and } t(\infty) = t_a.$$

Applying the boundary conditions,

$$t - t_a = (t_c - t_a)e^{-\beta x}, \tag{45}$$

and thus the tube wall temperature falls off exponentially on either side of the heater coil.

The total heat transfer rate by condution along the tube wall (in both directions) away from the coil will be given by

$$2\int_0^\infty h\pi D(t-t_a)dx = 2h\pi D(t_c-t_a)\int_0^\infty e^{-\beta x}dx,$$

on the assumption that h is constant along the length of the tube. The total heat output by conduction from the

heating section will thus be

$$\frac{2h\pi D(t_c-t_a)}{\beta} .$$

A heat balance may now be made on the heating section of length l:

$$Q = h\pi Dl(t_c-t_a) + \frac{2h\pi D(t_c-t_a)}{\beta}$$

or

$$Q = h\pi D(t_c - t_a)(1 + \frac{2}{\beta}), \tag{46}$$

where Q is the power input to the coil in $\frac{Btu}{hr}$.

Solving for the heat transfer coefficient,

$$h = \frac{Q}{\pi D\left(1+2\sqrt{\frac{kA_{cs}}{h\pi D}}\right)(t_c-t_a)} . \tag{47}$$

It should be noted that no fluid properties are involved in the determination of the heat transfer coefficient by equation (47).

Most of the assumptions involved in the derivation of the above equation were approximately valid in practice. However, the tube wall temperature under the actual coil was not uniform, and it was necessary to use an "average" temperature in place of t_c in equation (47). This temperature was determined by calibrating the coil with a pure liquid of known properties. The results of this calibration will be presented in Chapter 7.

CHAPTER 6

PHYSICAL PROPERTIES OF MIXTURES OF IMMISCIBLE LIQUIDS

Character of the Mixtures

The milky-white appearance of the mixtures used in this investigation has been noted previously. The creamy color and opacity of the mixture is a result of differing refractive indices and optical dispersive powers of the two phases [10, p. 229]. The dispersed-phase droplet sizes encountered with these mixtures are not accurately known. It is possible however to establish rough limits on the size distribution from qualitative considerations. Individual droplets were not visible to the naked eye, which places the upper limit at about 50 microns [75, p. 15]. Also the milky-white appearance suggests that the droplets were larger than one micron [4, p. 52]. Thus the probable range of droplet sizes was from 1 to 50 microns.

Sutheim [75, p. 2] states that three constituents are necessary to form an emulsion. These are the two immiscible liquids and a stabilizing or emulsifying agent. Most commercial emulsions do involve a third constituent to promote stability. On the other hand, Becher [4, p. 52] and Treybal [78, p. 273-276] refer to liquid extraction systems, in which stabilizing agents are studiously

avoided, as unstable emulsions. In order to emphasize the unstable nature of the mixtures used in this work, the terms suspension or dispersion are probably to be preferred.

The physical properties of importance in the study of fluid friction and forced convection heat transfer are the density, viscosity, specific heat, and thermal conductivity. Various methods of estimating these properties for dispersions of immiscible liquids are considered below.

Density, Specific Heat, and Thermal Conductivity

In the case of immiscible liquids, density and specific heat are additive quantities and the calculation of effective mixture properties offers no difficulty. Thus the mixture density, ρ_m, may be computed from

$$\rho_m = N_w \rho_w + N_s \rho_s, \tag{48}$$

where

N_w is the volume fraction of water in the mixture

and

$N_s = 1 - N_w$ = the volume fraction of solvent.

In a similar manner the specific heat of the mixture may be calculated from

$$C_{p_m} = N'_w C_{p_w} + N'_s C_{p_s}, \tag{49}$$

where N'_w and N'_s are the mass fractions of water and solvent respectively [21, p. 246].

Wang [83, p. 28-49] has measured the thermal conductivities of several stabilized emulsions. One of his systems consisted of water and a petroleum solvent practically identical to that used in the present investigation. Several equations for predicting thermal conductivities of mixtures were tested. For the solvent-water system the best agreement with experimental results was obtained using equation (50):

$$k_m = N_w k_w + N_s k_s, \tag{50}$$

where k_m, k_w, and k_s are the thermal conductivities of mixture, pure water, and pure solvent respectively. This equation was found to reproduce the data within 10 per cent over the temperature range from 65 to 80°F. Wang found that the thermal conductivity was independent of the phase distribution of the emulsion, i.e. oil-in-water or water-in-oil. It was also found that the presence of the small amounts of emulsifying agents used had negligible effect on the thermal conductivity.

Viscosity

The viscosity of dispersions cannot be successfully predicted using the simple "mixture laws" discussed above. The situation appears to be quite complex, and a vast body

of literature on this subject exists.

One of the earliest viscosity equations was that due to Einstein [14, p. 300; 15, p. 592]:

$$\mu_m = \mu_c(1 + 2.5\phi), \tag{51}$$

where

μ_m is the effective viscosity of the dispersion,

μ_c is the viscosity of the continuous phase, and

ϕ is the volume fraction of the dispersed phase.

This equation was derived on the assumption of uniform rigid spheres dispersed in a liquid and separated by distances large compared to the particle diameter. It is actually a limiting equation, and is not considered applicable for values of ϕ greater than about 0.02 [4, p. 59].

Hatschek [28, p. 80] presented an equation identical in form to equation (51) with a constant of 4.5 replacing the value of 2.5 in the Einstein equation. Later, Hatschek [29, p. 164] deduced an equation applicable at higher dispersed-phase concentrations,

$$\mu_m = \mu_c\left(\frac{1}{1-\phi^{1/3}}\right). \tag{52}$$

This equation successfully predicted the viscosities of suspensions of red blood corpuscles. Sibree [72, p. 35], working with stabilized paraffin-in-water emulsions, found it necessary to modify Hatschek's equation by the

introduction of a "volume factor" multiplying ϕ in the denominator of equation (52).

Several attempts have been made to modify the Einstein equation by the introduction of a polynomial in ϕ, in order to make the equation applicable at higher concentrations. These equations have the form

$$\mu_m = \mu_c(1 + 2.5\phi + \alpha\phi^2 + \beta\phi^3 + \ldots), \tag{53}$$

where α and β are constants. The writer has found values of the "constant", α, in the literature ranging from 4.9 to 14.1 [4, p. 60; 58, p. 397; 80, p. 299]. Other viscosity equations have been given by Robinson [67, p. 1044], Broughton and Squires [7, p. 259], and Kunitz [40, p. 716].

It is of interest to note that the viscosity of the dispersed phase does not appear in any of the above equations even though many of them have been used in describing liquid-liquid dispersions. Several equations which incorporate this factor have been proposed. Taylor [76, p. 46] theoretically extended the Einstein equation to apply to a fluid dispersed phase at low concentrations. Vermeulen, Williams, and Langlois [81, p. 91F] presented equation (54):

$$\mu_m = \frac{\mu_c}{1-\phi}\left(1 + \phi\,\frac{1.5\,\mu_d}{\mu_c+\mu_d}\right), \tag{54}$$

where μ_d is the viscosity of the dispersed phase. Miller and Mann [53, p. 719] and Olney and Carlson [59, p. 475]

succeeded in correlating mixing data for immiscible liquids using a logarithmic mixture equation:

$$\mu_m = \mu_d^{\phi} \cdot \mu_c^{1-\phi} . \tag{55}$$

Another complicating factor is that some emulsions, particularly at high concentrations, exhibit non-Newtonian behavior, i.e. they do not obey the Newton law of viscosity [48, p. 81]. Still another factor, neglected in the equations considered above, is the possible effect of particle size and size distribution. Several workers have studied model emulsions consisting of suspensions of solid spheres of varying size distribution. Roscoe [69, p. 268] suggests two viscosity equations, one for very diverse sizes and one for high concentrations of uniform spheres. Further work with suspensions of solid spheres has been carried out by Ting and Luebbers [77, p. 111-116] and Ward and Whitmore [85, p. 286-290]. These writers reached the conclusion that viscosity was independent of absolute sphere size but dependent on size distribution, decreasing with increasing size range.

Richardson [65, p. 412-413; 66, p. 368-373] found that for real emulsions both the absolute particle size and the size distribution affected the viscosity. Working with stabilized oil-in-water emulsions, he concluded that the apparent viscosity of emulsions having the same concentration and the same size distribution about a

mean globule diameter was inversely proportional to this mean globule diameter. Increased viscosity with decreasing particle size was also noted by Hatschek [28, p. 82]. Becher [4, p. 215] describes some work in which highly concentrated emulsions were homogenized by forcing them through capillary tubes under pressure. In one experiment particles with size in excess of 10 microns disappeared and the number of particles of about 1 micron in size increased. After 12 passages through the tube, the viscosity of the emulsion had increased by a factor of 2.5. Sibree's work [10, p. 215-216] also indicated that fine emulsions were more viscous than course emulsions at equivalent values of ϕ, the difference increasing as ϕ was increased. A common example of this phenomenon is the increased viscosity of milk caused by homogenization [75, p. 149].

All of the liquid-liquid work described above has been performed with stabilized emulsions. For such systems, it appears that the viscosity may depend on (a) the viscosity of the continuous phase, (b) the volume fraction of the dispersed phase, (c) the viscosity of the dispersed phase, (d) the rate of shear, (e) the size distribution of the droplets of dispersed-phase liquid, (f) the absolute size of the droplets of dispersed phase. In addition, the nature and concentration of the emulsifying agent has been shown to affect the viscosity, but

this effect would not be involved in the unstable dispersions considered in this investigation.

CHAPTER 7

SUMMARY AND ANALYSIS OF RESULTS

General Discussion

A study has been made of the flow and heat transfer properties of various mixtures of petroleum solvent and water. These liquids form an immiscible system producing highly unstable dispersions upon agitation. The limitations on achievable mixture compositions imposed by this instability have been mentioned previously (Chapter 4). This problem will be considered further in the following discussion.

The ranges of observed data encountered in this investigation are presented in Table 5 for each of the nominal mixture compositions. The table is inserted here to provide a quick look at the overall investigation. The detailed results are described below.

Friction Losses

The von Kármán friction factor equation for turbulent flow in smooth tubes has been given previously as

$$\frac{1}{\sqrt{f}} = 4.0 \log(Re \sqrt{f}) - 0.40. \qquad (10)$$

The curve in Figure 12 represents this equation over the range of Reynolds numbers from 3,000 to 125,000. The

Table 5

Ranges of Observed Data

Nominal Composition	Measured Compositions, % Solvent by Volume	Flow Rate, $\frac{lb_m}{sec}$	Temperature, $^{o}F.$	Average Linear Velocity, $\frac{ft}{sec}$
Pure Water	———	0.079-4.2 (Re: 2,200-125,000)	58-67	0.47-25
20% solvent in water	20.2 - 20.7	0.10-4.0	57-60	0.64-25
25% solvent in water	24.4 - 24.9	0.13-3.9	62-64	0.80-25
50% solvent in water	48.7 - 49.5	0.21-3.7	62-64	1.4-25
65% solvent in water	60.0 - 63.3	0.11-3.6	65-70	0.77-25
10% water in solvent	90.7 - 96.6	0.083-3.4	62-66	0.63-25
Pure solvent	100	0.11-3.3 (Re: 3,700-104,000	63-69	0.84-25

FIGURE 12
FRICTION FACTOR VERSUS REYNOLDS NUMBER

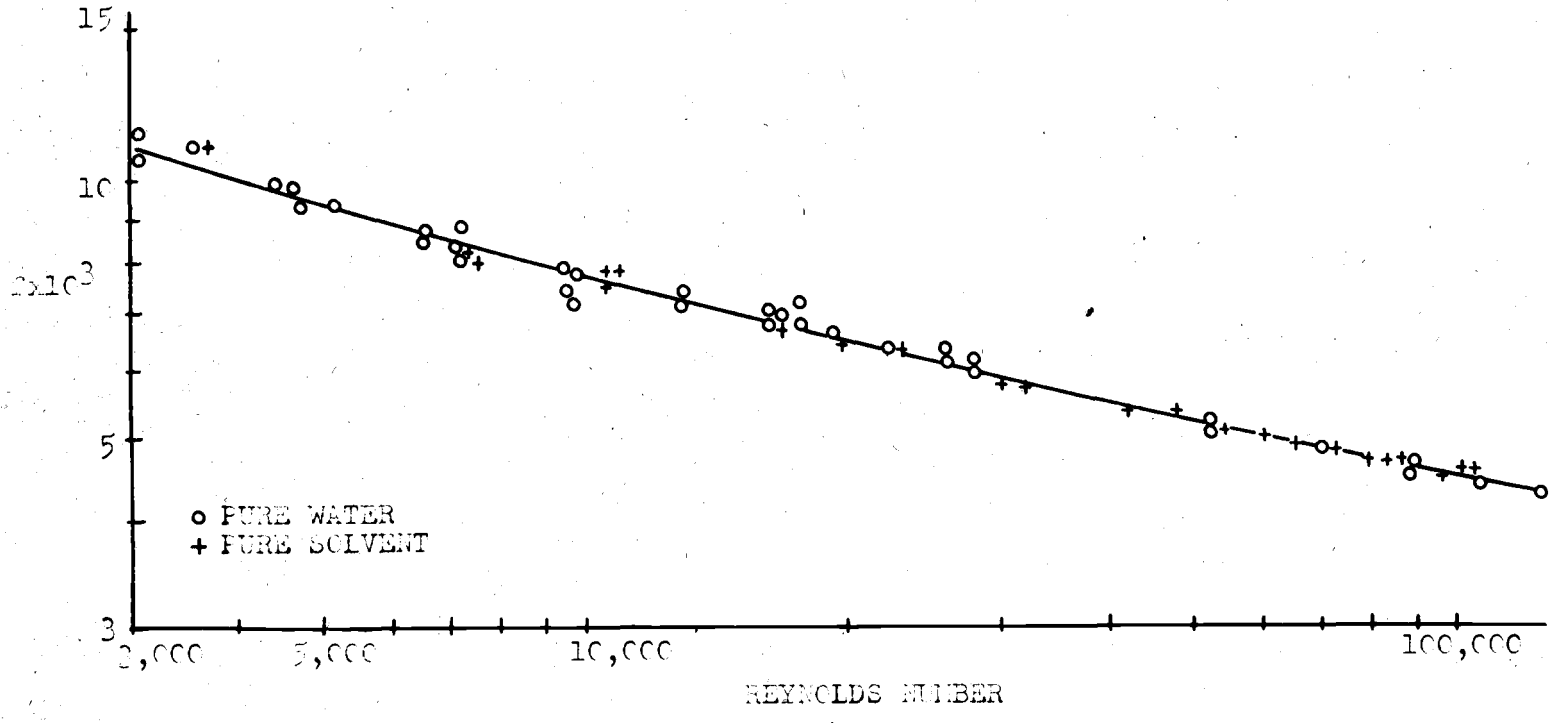

experimentally determined friction factors for pure water and pure solvent are shown as points in the figure. Approximately 65 per cent of these points fall within ±2 per cent of the curve. In this range of Reynolds numbers, 84 per cent of Nikuradse's data [57, p. 30-31] and 62 per cent of the extensive data of Stanton and Pannell [74, p. 217-224] fall within ±2 per cent of the curve. It will be recalled that the constants in equation (10) were determined using Nikuradse's data. For the present data maximum deviations from the curve occur for Reynolds numbers below 20,000, and this is also true for the data of Nikuradse and of Stanton and Pannell. At low flow rates the experimental error is greatest, particularly in the pressure measurements, and this accounts for the larger spread of the data at low Reynolds numbers.

The results for pure water and pure solvent were taken as an indication that the apparatus was functioning properly and that the test section tubing could indeed be considered smooth.

It has been pointed out in the previous chapter that prediction of the viscosity of suspensions is difficult, as indicated by the large number of viscosity equations appearing in the literature. Since the viscosity appears in the Reynolds number, it is important to be able to estimate this quantity in order to calculate friction factors. Further, it would be convenient in estimating

friction losses to be able to use existing relationships between the friction factor and the Reynolds number. It was therefore decided to evaluate "effective" or "apparent" viscosities which when used in the Reynolds number would satisfy the von Kármán equation. It should be noted here that attempts to measure the dispersion viscosity with an Ostwald viscometer failed. Mixture samples were withdrawn into the viscometer as rapidly as possible from the agitated tank. Coalescence was so rapid that large droplets of dispersed-phase liquid were observed blocking the capillary tube of the viscometer, and meaningful determinations could not be made.

For each run the Fanning friction factor was evaluated from the experimental data by equation (36) of Chapter 5 and the corresponding Reynolds number was determined from the curve of Figure 12 (actually the von Kármán equation was plotted on a greatly expanded scale and this curve was used to determine the Reynolds number corresponding to each value of the friction factor). From this Reynolds number and the measured flow rate, the apparent viscosity of the mixture was calculated from

$$\mu_m = \frac{DG}{Re} . \tag{56}$$

Viscosities evaluated in this manner have been used in the study of suspensions of solids in liquids by Salamone and Newman [71, p. 286], Ward and Dalla Valle [84, p. 10],

and others, and are often called "turbulent viscosities" [5, p. A-105].

The mixture viscosities determined from equation (56) have been plotted in Figure 13 as functions of the mass flow rate for each mixture composition. A single line has been drawn through the data points representing the nominal 20 per cent and 25 per cent solvent-in-water mixtures. On a larger scale a slight separation was noted. To account for the small temperature differences among the various runs, a correction was applied to each viscosity value before plotting. The base temperature to which all of the viscosities were corrected was 63°F, which represented roughly the average temperature for all of the runs. These corrections were based on the viscosity of the continuous-phase liquid and generally amounted to less than 3 per cent. Several features of Figure 13 require discussion.

The procedure described above for evaluating apparent viscosities was applied to the pure solvent runs to obtain an indication of the magnitude of experimental errors inherent in this procedure. The points are shown grouped around the horizontal line representing the known viscosity of pure solvent. Errors as large as 23 per cent occurred at the lowest flow rates investigated (about 0.1 $\frac{lb_m}{sec}$) and the errors decreased with increasing flow rate as expected. Above a flow rate of 0.4 $\frac{lb_m}{sec}$ the average

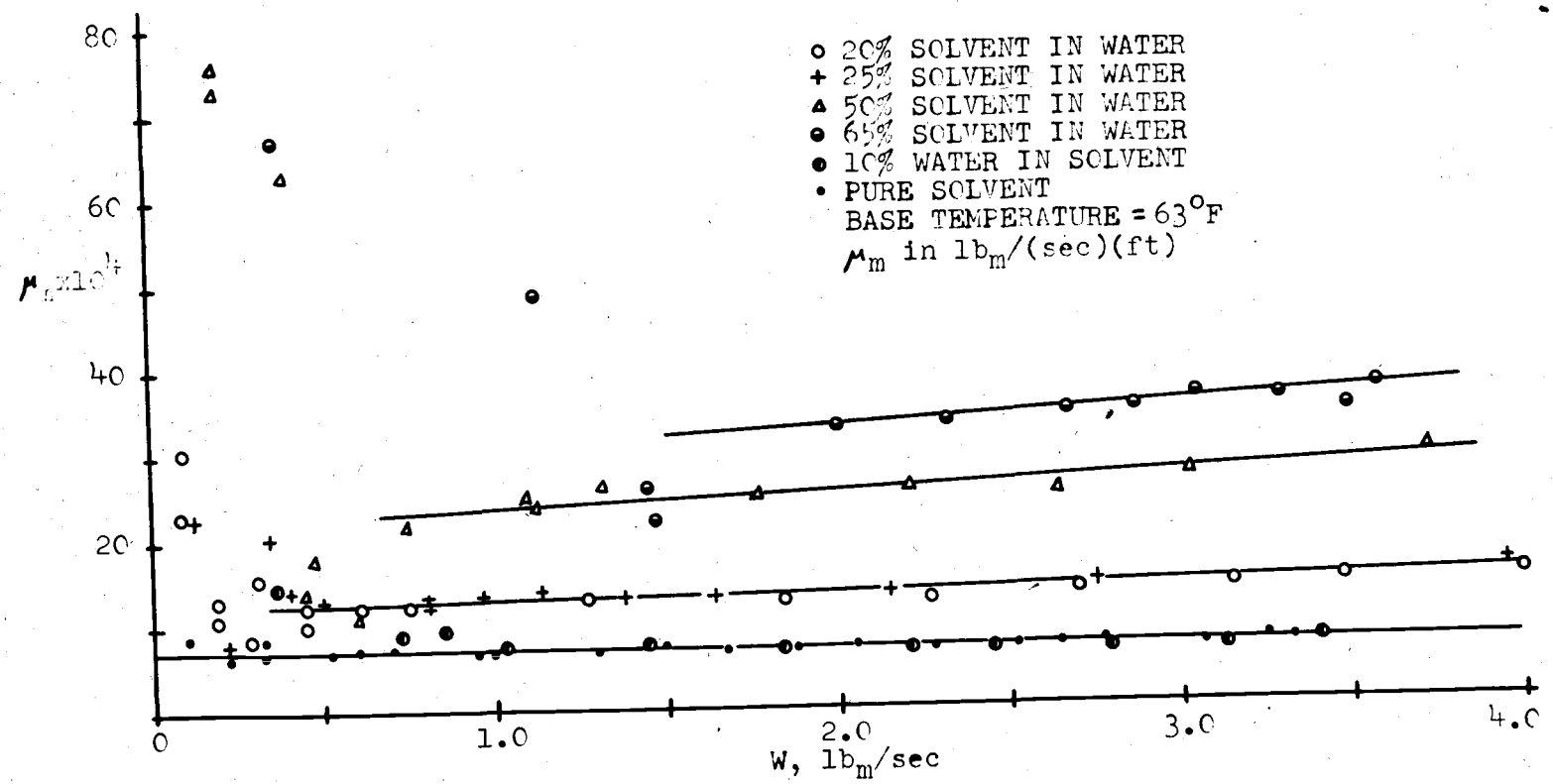

FIGURE 13
APPARENT VISCOSITY VERSUS MASS FLOW RATE

observed error was approximately ±4 per cent. The large errors at low flow rates were attributable principally to errors in the pressure drop measurements, since the net friction pressure drop was obtained by taking the difference between pressure readings under flow and no-flow conditions. This involves the well known difficulty in taking the difference between two nearly equal numbers.

Deviations as large as 400 per cent from the lines drawn in Figure 13 were noted for the high concentration dispersions. It is evident that measurement errors alone cannot explain the very great scatter of the data for mixtures at low flow rates. These large deviations are believed to be due to mixture instability manifesting itself as unpredictable concentration changes during flow through the apparatus. It was noted that the higher the concentration of dispersed phase, the greater were the deviations from the lines in Figure 13, and the longer they persisted as flow rates were increased. Both unpredictable manometer fluctuations and erratic thermocouple readings were sometimes noted in the mixture runs at low flow rates. Table 6 shows some measured mixture compositions as observed after runs at various flow rates for several nominal compositions.

Table 6

Measured Mixture Compositions at Various Flow Rates

Nominal % solvent	Measured % solvent	Mass flow rate, $\frac{lb_m}{sec}$
65	60.0	0.11
65	62.8	0.37
65	63.1	0.81
65	63.2	1.48
65	63.3	2.67
65	63.2	3.05
25	24.4	0.13
25	24.9	0.34
25	24.8	0.50
25	24.7	0.96
25	24.9	1.37
25	24.7	2.16
25	24.8	3.94
90	96.6	0.083
90	95.4	0.38
90	92.6	0.86
90	90.6	1.04
90	90.2	1.84
90	91.0	2.44
90	91.1	3.13

These values provide an indication of the instability at low flow rates. It should also be noted that because of the practical impossibility of obtaining flow rate, pressure drop, and composition data simultaneously, further changes of unpredictable magnitude could have gone undetected.

In many of the low flow-rate runs, large friction factor values beyond the range of Figure 12 were obtained. For these cases it was necessary to assume that the laminar

flow relation, $f = \frac{16}{Re}$, was applicable. The use of this equation resulted in indicated Reynolds numbers as low as 100, and thus in high values of the apparent viscosity by equation (56). Some of the highest of these apparent viscosities were beyond the range of Figure 13.

It has been noted previously that water-in-solvent mixtures with dispersed-phase concentrations greater than about 10 per cent could not be prepared in the present equipment. When the attempt was made to prepare a 20 per cent water-in-solvent dispersion, the system acted as though the relatively small quantity of water was attempting to become the continuous phase surrounding the large amount of solvent which was present. A uniform mixture was never attained in this case. Even the nominal 10 per cent water-in-solvent dispersion which was successfully prepared showed instability at low flow rates as indicated by Table 6 and Figure 13. At higher rates of flow, beyond the instability range, this mixture behaved approximately as pure solvent as indicated in Figure 13. The compositions indicated in Figure 13 are nominal values. For flow rates beyond the instability range, mixture compositions were quite uniform as indicated in Table 6. Average values for the stable flow range are given in Table 7 below.

Table 7

Average Measured Compositions
for Mixtures in Stable Flow Range

Nominal Composition, % by Volume	Average Measured Composition, % Solvent
20 % Solvent in Water	20.6 %
25 % Solvent in Water	24.8 %
50 % Solvent in Water	49.2 %
65 % Solvent in Water	63.1 %
10 % Water in Solvent	90.7 %

It should also be noted from Figure 13 that the viscosity lines drawn through the experimental points for the solvent-in-water dispersions are not horizontal, but show increasing apparent viscosities with increasing flow rates. This positive slope is characteristic of non-Newtonian fluids of the dilatant type.

There are several factors other than dilatancy which could possibly explain the positive slopes notes in Figure 13. One of these of course is experimental error. However, at high flow rates the measurements of pressure differences, flow rates, and mixture compositions were all accurate to about 1 per cent. Maximum deviations from the viscosity lines for the concentrated mixtures at high flow rates (in the stable flow region) were of the order of 6 per cent. Experimental errors of 30 to 50 per cent would

be required to explain the slopes noted. This factor may therefore be dismissed.

Several workers [10, p. 216; 67, p. 1045] have noted that entrained air may increase the apparent viscosity of emulsions. In the present work agitation was carried out in an open tank, and the liquids in the supply tank were certainly aerated. The absence of any apparent effect in the runs with pure liquids, plus the fact that there is little reason to expect increased air entrainment with increased flow rate, leads to the conclusion that air entrainment cannot account for the observed results.

A third item which deserves consideration is the possible effect of both dispersed particle size and size distribution on the apparent viscosity. Some of the evidence indicating increased viscosity with homogenization and reduction of droplet size has been cited in the preceding chapter. Roy and Rushton [70, p. 33-36] have studied the effect of turbulent pipe flow on drop size for a 2 per cent oil-in-water dispersion. The oil was injected into a turbulent water stream at one end of a smooth plastic pipe and measurements of drop sizes were made at a point 100 pipe diameters downstream from the point of injection. Care was taken to obtain break-up of the dispersed phase by the exclusive action of the shear stresses involved in pipe flow turbulence. It was concluded that the average drop size was independent of

the Reynolds number over the range from 30,000 to 100,000. In the work of Clay, as described by Becher [4, p. 218], emulsions were "refined" (i.e. the mean droplet size decreased) by pumping in turbulent flow through a closed pipe loop, a situation more nearly analogous to that of the present work. Clay found a definite improvement in the fineness of the emulsions on increasing the flow rate. He was able to produce a mean diameter of 10 microns from an emulsion containing droplets approximately 10 times this size.

In all of the emulsion work known to the writer, including some with systems chemically and physically similar to the solvent-water system considered here, the non-Newtonian behavior observed was of the pseudo-plastic type. For this type of fluid, the viscosity decreases with shear rate (or flow rate in a given apparatus). Becher [4, p. 56], in his extensive treatment of emulsion technology, states that dilatancy is apparently quite rare in emulsion systems.

While the situation is not perfectly clear, it appears that the viscosity of a liquid dispersion may be increased markedly by homogenization and reduction of average droplet size, and that such homogenization may be brought about by pumping the dispersion in turbulent flow through a pipe line. Based on the evidence cited above the writer hypothesizes that the apparent dilatancy

evident in Figure 13 is due to refinement of particle sizes, resulting in increased viscosity, with increasing flow rates. In the present work it was not possible to separate the effects of non-Newtonian behavior (if present) and particle size refinement. These effects may well have acted in opposing directions with the net result showing up in the plots of Figure 13. It would appear that further work, along the lines of separating these effects, would be highly desirable.

From Figure 13, values of apparent viscosity for each composition were taken at flow rates of 1.5 and 3.5 $\frac{lb_m}{sec}$, and these viscosity values are plotted versus the volume fraction of solvent in Figure 14. Several of the viscosity equations discussed in Chapter 6 are also indicated as dotted lines on the graph. It is evident that none of these equations fit the observed data. The data at a given flow rate are reasonably well fitted by a second degree polynomial in ϕ, in which the coefficient of the ϕ term is taken to be 2.5, the same coefficient that appears in the Einstein equation. This equation thus reduces to the Einstein equation at small values of ϕ. In this sense any polynomial in ϕ, in which the coefficient of the first degree term is 2.5, is a modified Einstein equation.

The coefficient of the ϕ^2 term is a function of the flow rate. At 1.5 $\frac{lb_m}{sec}$ the apparent viscosities are

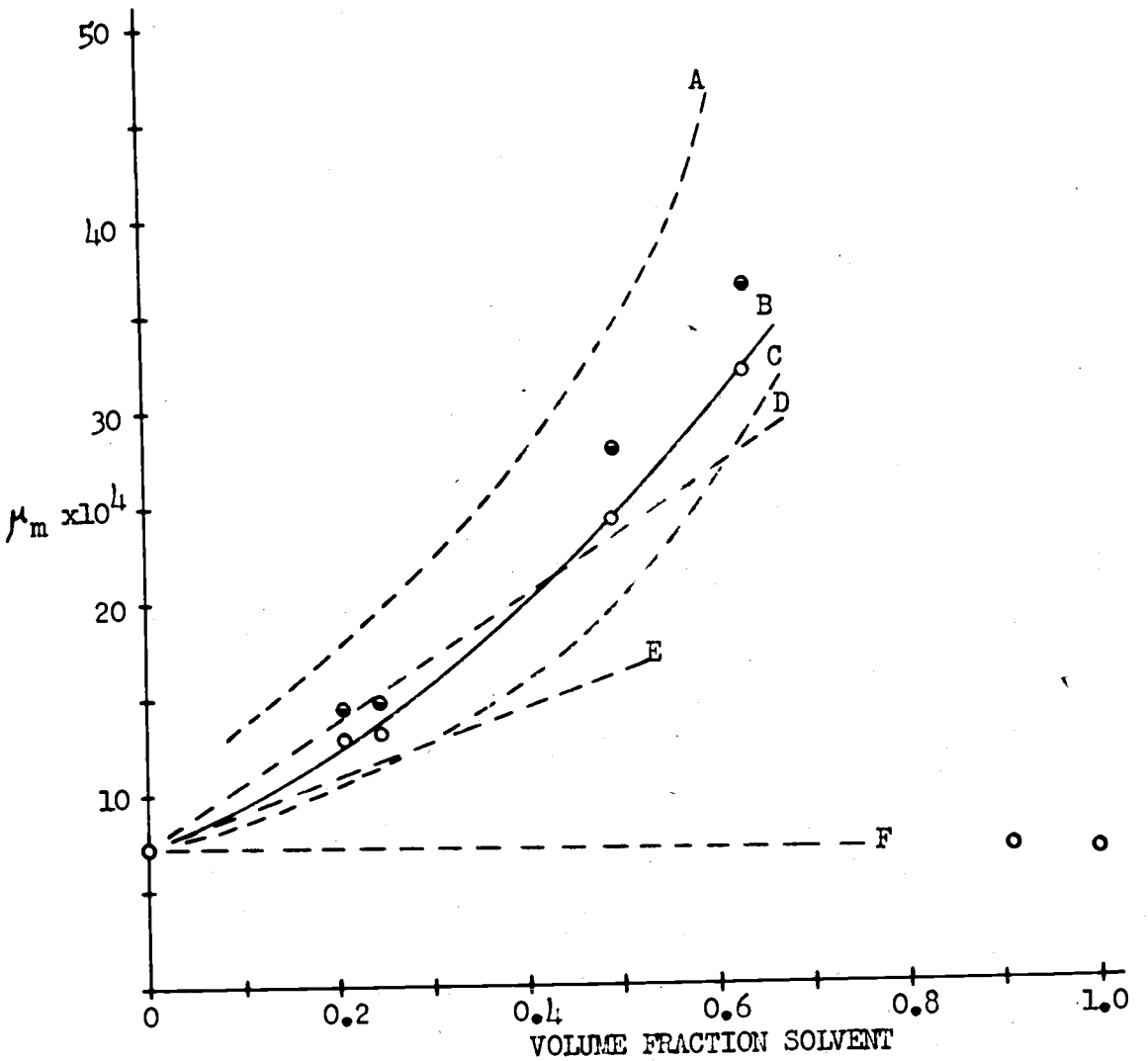

A - HATSCHEK EQUATION
B - $\mu_m = \mu_c(1+2.5\phi + 4.6\phi^2)$
C - VERMEULEN EQUATION
D - HATSCHEK MODIFICATION OF EINSTEIN EQUATION
E - EINSTEIN EQUATION
F - MILLER AND MANN - OLNEY AND CARLSON

o W 1.5 lb_m/sec
• W 3.5 lb_m/sec

FIGURE 14
APPARENT VISCOSITY VERSUS VOLUME FRACTION SOLVENT

represented within ±4 per cent by the relation

$$\mu_m = \mu_c(1 + 2.5\phi + 4.6\phi^2), \tag{57}$$

which is plotted as the solid line in Figure 14. The lower limit of 1.5 $\frac{lb_m}{sec}$ was selected since above this flow rate all apparent viscosity values fall close to the lines of Figure 13 for all dispersion concentrations. At a flow rate of 0.4 $\frac{lb_m}{sec}$ the coefficient of the ϕ^2 term was found to be 3.4 and at 4.0 $\frac{lb_m}{sec}$ it was 7.3. From this information the effect of flow rate could be taken into account. All of the viscosity data in the stable flow region may be represented by the equation

$$\mu_m = \mu_c[1 + 2.5\phi + (3.0 + 1.06W)\phi^2] \tag{58}$$

where W must be expressed as $\frac{lb_m}{sec}$. This equation is tested with several sets of viscosity data in Figure 15. This equation is limited to the prediction of viscosities for the system and apparatus used in this investigation. It will suitably predict viscosities of dispersions containing 63 per cent solvent at flow rates above 1.5 $\frac{lb_m}{sec}$. For dispersions containing less than 50 per cent solvent the equation will predict viscosities at flow rates as low as 0.4 $\frac{lb_m}{sec}$. With these restrictions on flow rates, equation (58) showed an average deviation from the experimental values of apparent viscosity of about 4 per cent. Using this equation together with the friction factor plot of

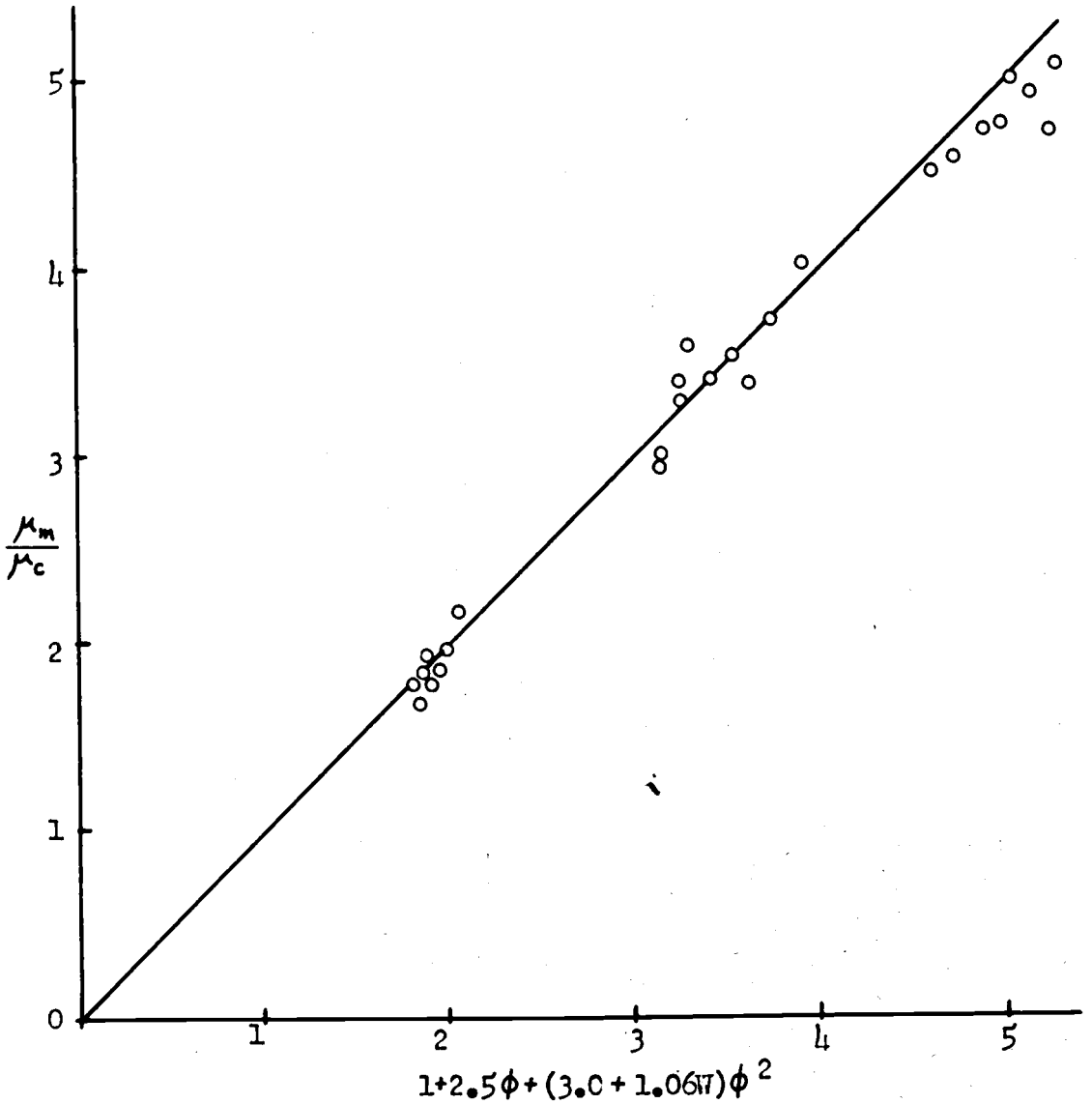

FIGURE 15
TEST OF EQUATION (58)

Figure 12, the experimentally determined friction pressure losses in the smooth tube may be reproduced within about 2 per cent.

It would be desirable to have a relation which did not involve the flow rate. Between the values of 1.5 and 3.5 $\frac{lb_m}{sec}$ the following equation suitably represents the average viscosity over this flow rate range:

$$\mu_m = \mu_c(1 + 2.5\phi + 5.6\phi^2). \tag{59}$$

This equation reproduces the viscosity data within $\pm$9 per cent. If this equation were used to evaluate Reynolds numbers for the prediction of friction pressure losses, the Reynolds numbers would be in error by at most $\pm$9 per cent, assuming that the curves of Figure 13 accurately represent the apparent viscosities of the mixtures. Using these Reynolds numbers to evaluate friction factors for flow in smooth tubes from the friction factor plot, leads to pressure losses in error by about $\pm$3 per cent over this flow range. By extrapolating the viscosity lines of Figure 13 to lower flow rates, other sets of points could be obtained as in Figure 14 and equations similar to (57) could be written for them.

The above viscosity equations do not contain the viscosity of the dispersed phase. In the temperature range involved in this investigation, the viscosities of solvent

and water differed only slightly. At 63°F for example, the viscosity of pure solvent was found to be about 3 per cent lower than that of water. The study of immiscible systems involving liquids of widely differing viscosities would be most interesting in the light of the results of the present work and the discussion in Chapter 6.

It is concluded that for solvent-water dispersions in the stable flow range, friction pressure losses in smooth tubes may be estimated within ±5 per cent using apparent viscosities calculated from equation (59) and the conventional relationship between the Fanning friction factor and the Reynolds number.

Orifice Coefficients

Figure 16 is an orifice calibration curve in which the mass flow rate is plotted against the pressure difference across the orifice meter on a log-log scale. According to the orifice equation, such a plot should yield a straight line with a slope of 0.5 as long as the discharge coefficient is constant. Previous experimental work with single-phase fluids has shown that the discharge coefficient is approximately constant for orifice Reynolds numbers greater than about 30,000, regardless of the nature of the fluid or the value of the orifice-to-pipe diameter ratio [8, p. 158]. Orifice Reynolds numbers

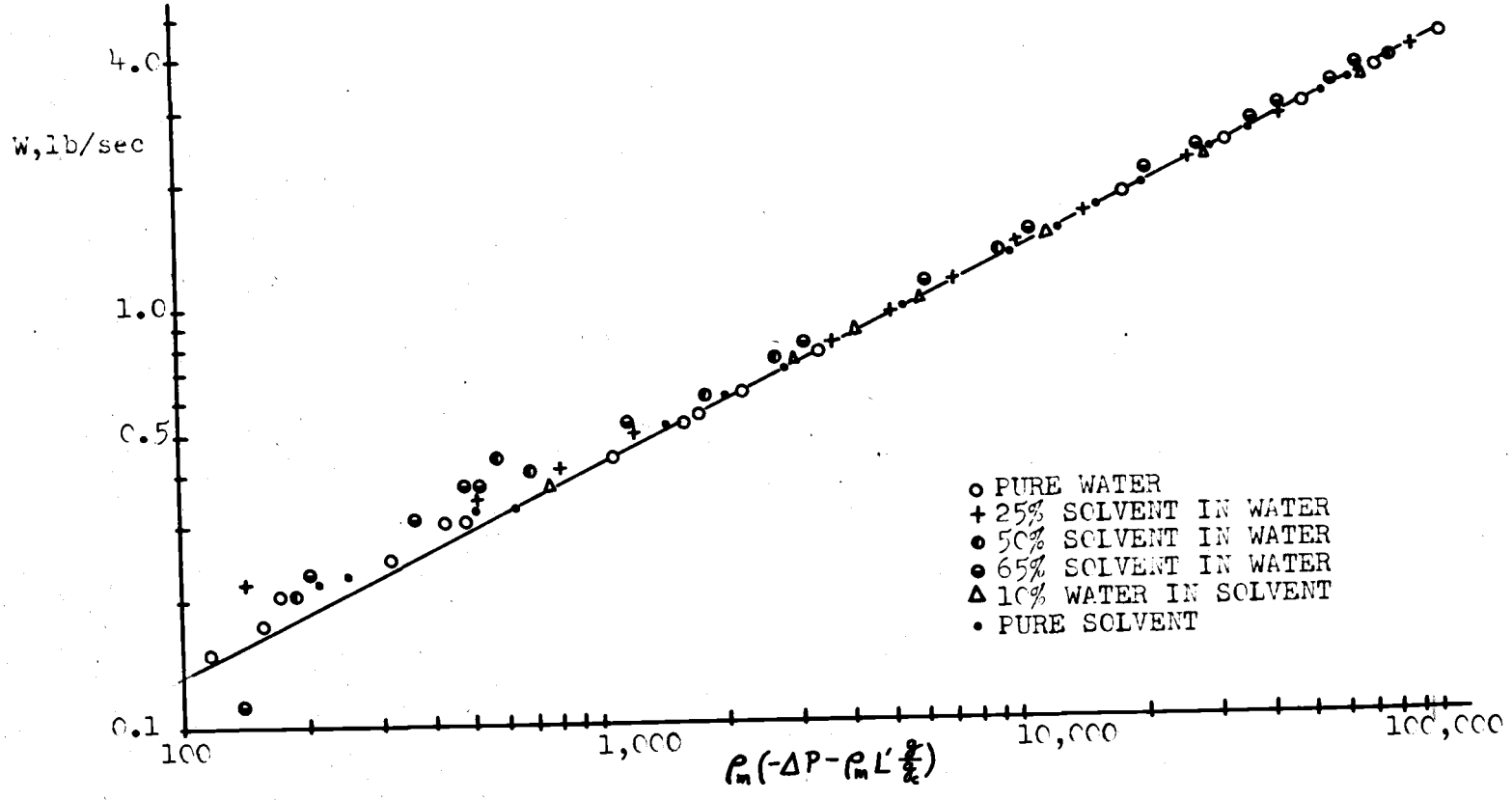

FIGURE 16 - ORIFICE CALIBRATION CURVE

are computed using the diameter of the hole in the orifice plate instead of the pipe diameter. In the present work, the orifice diameter was slightly smaller than that of the test-section tubing. The orifice Reynolds numbers were about 1 per cent larger than the values given in Table 5 for the test section.

The quantity actually plotted as the abscissa of Figure 16 was $\rho_m(-\Delta P - \rho_m L' \frac{g}{g_c})$. This was done to eliminate the effect of the different densities of the various mixtures. It is evident from inspection of the figure that all of the points for pure liquids and for mixtures fall close to the same straight line for high flow rates. The line was drawn with a slope of 0.5. At low flow rates most of the experimental points are seen to fall above the line indicating increasing values of the discharge coefficient with decreasing orifice Reynolds numbers. This is in agreement with the previous experimental work with single-phase fluids [8, p. 158]. Flow rates greater than about 1 $\frac{lb_m}{sec}$ correspond to Reynolds numbers greater than 30,000 for both pure water and pure solvent.

For each run with pure liquids and with mixtures, an orifice discharge coefficient was evaluated from equation (39) of Chapter 5. It was found that approximate constancy of the discharge coefficient occurred for orifice

Reynolds numbers greater than about 20,000. Table 8 shows the average value of the experimentally determined orifice coefficients (for orifice Reynolds numbers above 20,000) for each nominal mixture composition.

Table 8

Average Orifice Discharge Coefficients for Various Mixtures

(Re_o > 20,000)

Nominal Composition	Average Value of C_D
Pure Water	0.613
20 % Solvent in Water	0.600
25 % Solvent in Water	0.613
50 % Solvent in Water	0.612
65 % Solvent in Water	0.634
10 % Water in Solvent	0.609
Pure Solvent	0.611

It is evident that these values differ but little with mixture composition. A discharge coefficient of 0.61 could be applied to any of the mixtures (as well as either pure liquid) with a maximum error of about 4 per cent.

At low flow rates, the experimental discharge coefficients were usually larger than 0.61 as expected. Occasional very large and very small values were obtained in the unstable flow region and some of these are indicated by the widely scattered points in Figure 16. In the application of orifice meters, the orifice-to-pipe diameter

ratio is chosen to ensure orifice Reynolds numbers greater than 30,000, in order to take advantage of the constancy of the discharge coefficient.

It is concluded that the sharp-edged orifice meter should be quite suitable for metering the flow of two-phase liquid dispersions of solvent and water. The generally accepted value of 0.61 for orifice discharge coefficients may be applied in designing such meters for orifice-to-pipe diameter ratios near 0.5.

Film Heat Transfer Coefficients

Heat transfer coefficients were computed from equation (47) of Chapter 5:

$$h = \frac{Q}{\pi D\left(1 + 2\sqrt{\frac{kA_{cs}}{h\pi D}}\right)(t_c - t_a)}. \qquad (47)$$

As mentioned previously the tube-wall temperature beneath the heating coil was not uniform so it was necessary to calibrate the coil in order that it could be used to determine heat transfer coefficients. The first step in this procedure was to compute heat transfer coefficients for the pure solvent runs from the Dittus-Boelter equation,

$$Nu = 0.023(Re)^{0.8}(Pr)^{0.4}. \qquad (28)$$

These values were then compared with coefficients calculated from equation (47) using various measured temperature

differences in place of the quantity (t_c-t_a).

The measured tube-wall temperatures for one of the solvent runs at a Reynolds number of 10,600 have been plotted in Figure 17. It was found empirically that the use of (t_1-t_7) gave heat transfer coefficients in good agreement with the Dittus-Boelter equation over the range of flow rates investigated. The pure solvent data were chosen for this calibration since the lower heat capacity of the solvent compared to water led to the highest observed temperature differences between the tube wall and the flowing liquid. The temperature distribution along the tube wall was derived mathematically in Chapter 5 as

$$t - t_a = (t_c - t_a)e^{-\beta x}. \tag{45}$$

This distribution, using (t_1-t_7) in place of (t_c-t_a), is shown by the dotted line in Figure 17, while the actual measured temperatures are indicated as points. This measured temperature distribution was typical of those observed at relatively low values of the Reynolds number. At higher flow rates the measured temperature distributions under the coil were flatter than that indicated in Figure 17. Several values of $(t-t_a)$ as computed from equation (45) for various distances from the edge of the heating coil are presented below in Table 9.

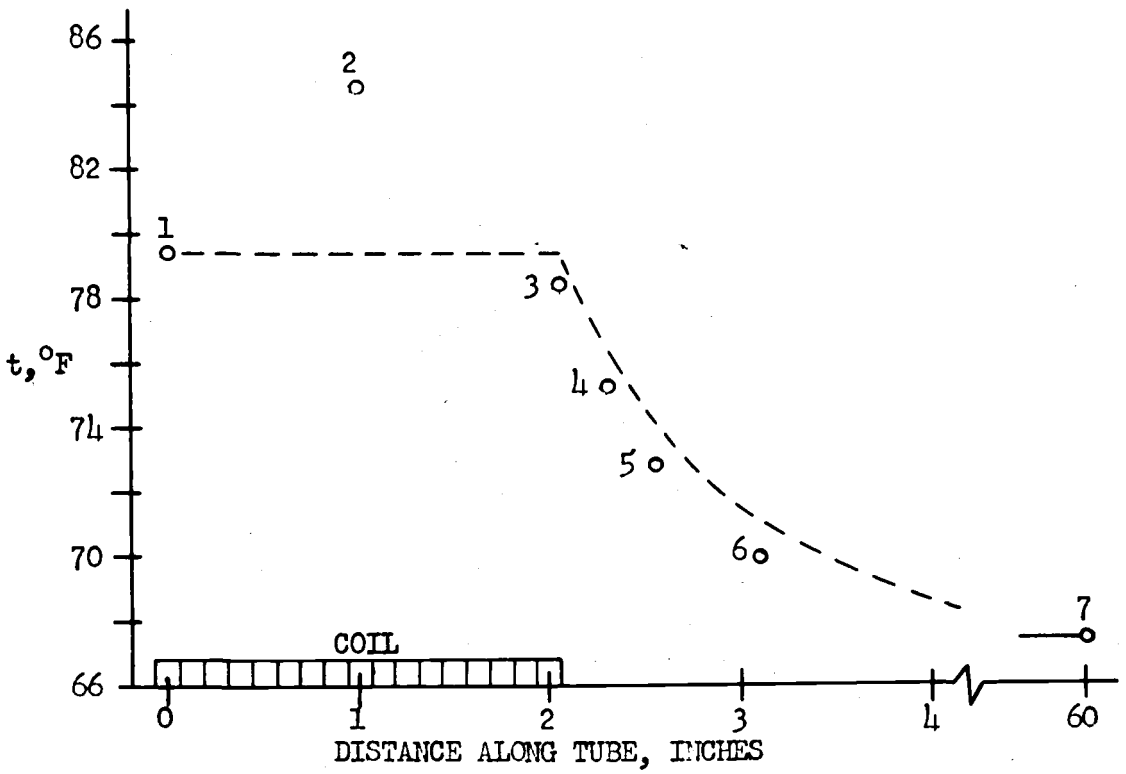

Re = 10,600
h = 170

FIGURE 17
TUBE-WALL TEMPERATURE DISTRIBUTION

Table 9

Calculated Tube-Wall Temperature Distribution

(Pure solvent run; Re = 10,600; $t_1-t_7 = 12.0^{\circ}F$)

Distance from edge of coil, inches	$(t-t_a)$, $^{\circ}F$
1/8	10.4
1/4	9.0
1/2	6.7
1	3.8
6	0.01
12	10^{-5}

It was mentioned previously that the test section tubing was insulated for a distance of 1 foot beyond each end of the heating coil. It is evident from the data in Table 9 that this length of insulation was sufficient to ensure the practical equivalence of wall temperature and fluid temperature within the insulated section.

Following the calibration of the heating coil with pure solvent as described above, a check was made using the pure water data. Heat transfer coefficients calculated from equation (47), again using t_1-t_7 as the temperature difference, were compared with coefficients evaluated from the Dittus-Boelter equation. These results agreed within about 10 per cent, which is considered satisfactory in view of the low temperature differences involved in the water runs and the approximate nature

of the Dittus-Boelter equation [46, p. 219].

The film heat transfer coefficients for the various mixtures are plotted in Figure 18 as a function of the mass flow rate. The expected higher value of the heat transfer coefficient for water as compared to pure solvent or the mixtures is evident. It is also apparent that for solvent-in-water dispersions with solvent concentrations up to 50 per cent, the mixtures behave more nearly like water than like solvent. In the case of the nominal 65 per cent solvent dispersion the reverse appears to be true. Apparently the solvent influence was predominant at this concentration. The crossing of the curves for pure solvent and 65 per cent solvent is difficult to understand. It should be noted that the accuracy of the heat transfer data was limited at both ends of the flow rate range. At low flow rates the instability effects mentioned previously may cause large errors. At high flow rates the temperature differences between tube wall and fluid were small, leading to experimental errors of the order of 20 to 30 per cent. Thus for the high concentration mixtures the data must be considered of doubtful validity at both low and high flow rates. The deviation of the experimental values of the heat transfer coefficients from the curves drawn in Figure 18 was approximately $\pm$10 per cent. It should also be noted from Figure 18 that the nominal 10 per cent water-in-solvent dispersion behaved substantially

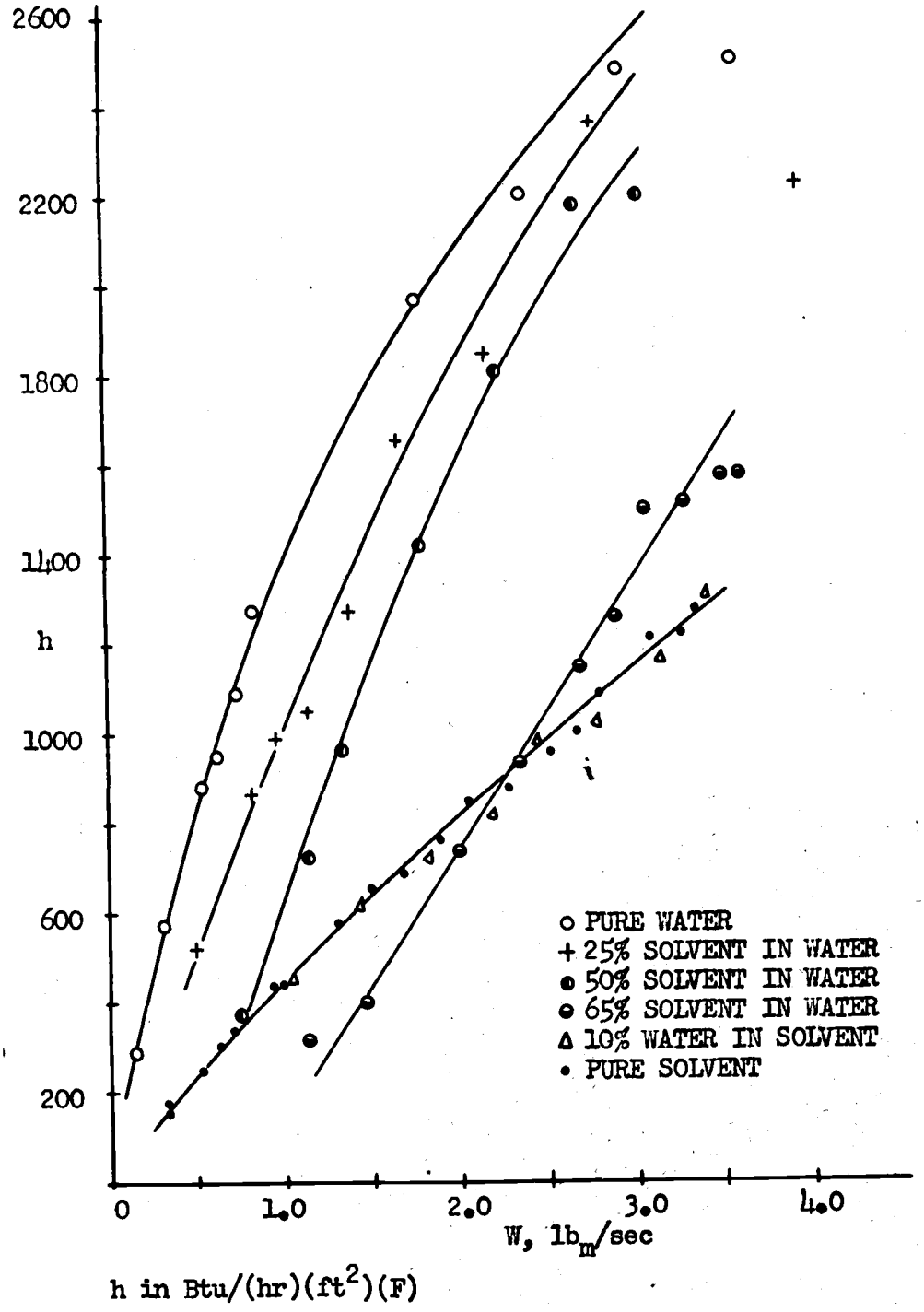

FIGURE 18
HEAT TRANSFER COEFFICIENT VERSUS MASS FLOW RATE

FIGURE 19
HEAT TRANSFER CORRELATION

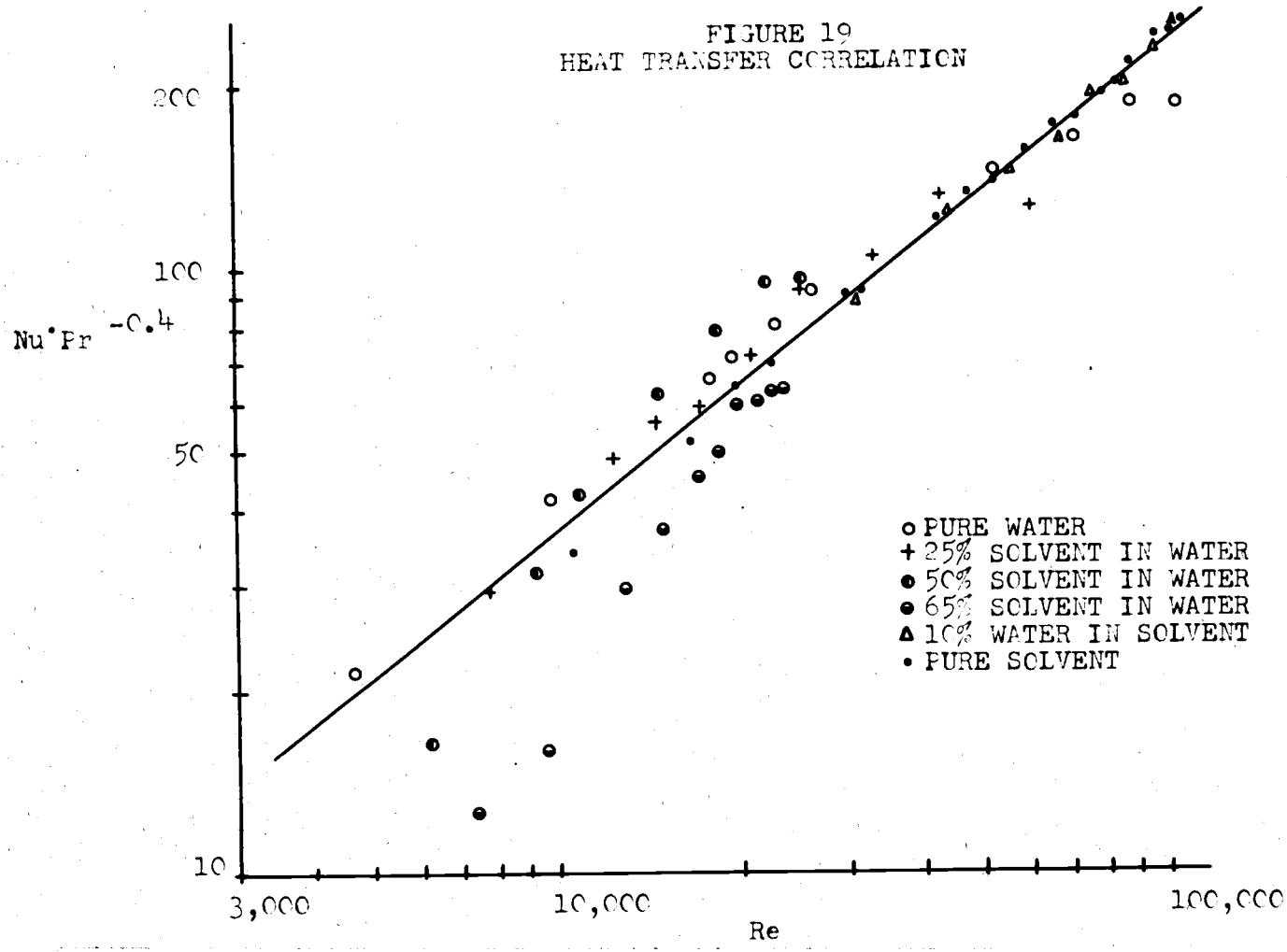

maximum deviation of ±40 per cent. The use of the specific heat and thermal conductivity of pure water together with mixture viscosities in computing the dimensionless groups is not satisfying from the theoretical point of view, but is justified pragmatically in the present study.

The ranges of fluid properties and the dimensionless Nusselt and Prandtl groups encountered in this investigation are summarized in Table 10 below.

Table 10

Ranges of Physical Properties and Dimensionless Groups

Quantity	Range of Values	
Density	48.9 - 62.4	$\frac{lb_m}{ft^3}$
Specific Heat	0.46 - 1.0	$\frac{Btu}{(lb_m)(^oF)}$
Thermal Conductivity	0.11 - 0.36	$\frac{Btu}{(hr)(ft)(^oF)}$
Apparent Viscosity	$6.6 - 37 \times 10^{-4}$	$\frac{lb_m}{(sec)(ft)}$
Nusselt Number	48 - 640	
Prandtl Number	6.9 - 42	

It is concluded that the heating-coil method employed in this investigation for the determination of film heat transfer coefficients is a promising one. Further investigation of this technique would appear to be highly worthwhile.

For the solvent-water system considered here, it has been found that heat transfer coefficients for dispersions may be predicted within about ±35 per cent by the following equation:

$$\frac{h_m D}{k_c} = 0.023 \left[\frac{DG}{\mu_m}\right]^{0.8} \left[\frac{(C_p)_c \mu_m}{k_c}\right]^{0.4}, \tag{60}$$

where the subscripts c and m refer to the continuous phase and the mixture respectively.

The calculated data on which this discussion has been based are tabulated in Appendix C, and the original data are on file in the Chemical Engineering Department.

CHAPTER 8

CONCLUSIONS

The conclusions of this investigation may be summarized as follows:

(1) In the absence of emulsifying agents, the solvent-water dispersions utilized in this work were highly unstable, the instability increasing with increasing dispersed-phase concentration. This instability was evident in measurements of friction factors, orifice discharge coefficients, and film heat transfer coefficients, and made the measurements extremely unreliable at low flow rates.

(2) Friction pressure losses in smooth tubes may be estimated for highly turbulent flow of solvent-in-water dispersions with solvent concentrations up to 63 volume per cent by using the existing relationship between the friction factor and the Reynolds number. The dynamic viscosity to be used in the Reynolds number is an apparent viscosity evaluated from a modified Einstein equation,

$$\mu_m = \mu_c(1 + 2.5\phi + 5.6\phi^2). \tag{59}$$

Pressure losses evaluated in this manner reproduced the experimental values within ± 5 per cent.

(3) Apparent viscosity values for solvent-water dispersions may be as much as 500 per cent larger than

the viscosities of the pure liquids. To a first approximation, these apparent viscosities are dependent only on the viscosity of the continuous-phase liquid and the volume fraction of the dispersed phase. Secondary effects caused by particle size refinement and/or non-Newtonian behavior were noted, and these effects should be investigated further.

(4) Water-in-solvent dispersions behave essentially as pure solvent up to a water concentration of about 9 volume per cent. Higher concentrations of water in solvent could not be produced in the present equipment.

(5) The sharp-edged orifice meter should be a highly suitable instrument for metering the flow of two-phase liquid mixtures. For the dispersions investigated, orifice discharge coefficients were found to be substantially constant above an orifice Reynolds number of 20,000. The use of 0.61 as the orifice coefficient in design calculations involving any of the mixtures investigated here would involve a maximum error of about 4 per cent.

(6) The heating-coil method employed in this investigation for evaluation of film heat transfer coefficients shows definite promise and should be investigated further.

(7) Film heat transfer coefficients for solvent-in-water dispersions are intermediate between those for pure water and pure solvent. Coefficients may be evaluated within about ± 35 per cent, for Reynolds numbers greater

than 10,000, by the use of a Dittus-Boelter type equation,

$$\frac{h_m D}{k_c} = 0.023 \left[\frac{DG}{\mu_m}\right]^{0.8} \left[\frac{(c_p)_c \mu_m}{k_c}\right]^{0.4} . \qquad (60)$$

In applying this equation, the use of the specific heat and thermal conductivity of pure water (continuous phase) gives better results than the mixture laws. As with the pressure loss determinations, water-in-solvent dispersions up to 9 volume per cent water behave essentially as pure solvent. It would be desirable to determine heat transfer coefficients of dispersions by another method in order to check both the heater-coil technique and the results indicated by equation (60).

CHAPTER 9

RECOMMENDATIONS FOR FURTHER WORK

The investigation which has been described in this thesis must be considered a preliminary survey of the subjects of friction pressure losses and forced convection heat transfer for mixtures of immiscible liquids flowing in circular tubes. Many avenues for further investigation appear to be open. Some specific recommendations, based on the results of the present study, are given below:

(1) It would be most desirable to investigate other liquid-liquid dispersions. The use of a pair of immiscible liquids having widely differing viscosities should provide an interesting test of the conclusion of this investigation that the mixture viscosity is independent of the dispersed-phase viscosity. The stability situation might be improved by matching the densities of the two liquids closely, perhaps permitting accurate measurements at low flow rates.

(2) The use of a horizontal test section, perhaps in conjunction with the existing vertical test section, should be investigated with the aim of reducing the pressure measurement errors at low flow rates.

(3) A study should be directed toward separating the effects of droplet size refinement and non-Newtonian

behavior in order to obtain a better understanding of factors affecting the viscosity of liquid-liquid dispersions in turbulent flow. Light transmittance or photographic techniques as described by Trice and Rodger [79, p. 205-210], Vermeulen, Williams, and Langlois [81, p. 85F-94F], and Rodger, Trice, and Rushton [68, p. 515-520] might be applied to the study of droplet sizes and size distributions. The rheological properties of liquid-liquid dispersions should be determined in a capillary tube viscometer of the flow type, along the lines of the work done for suspensions of solids in liquids by Metzner and Reed [49, p. 434-440] and Dodge [12].

(4) Evaluation of film heat transfer coefficients with the coil technique described herein should be investigated further. Improvements in the design of the heating coil might result in flatter tube-wall temperature distributions, making the mathematical treatment more closely applicable.

(5) Other test section tube diameters and increased pumping capacity should be utilized to extend the range of Reynolds numbers achievable with high viscosity liquid-liquid dispersions.

(6) A fundamental investigation of the fluid mechanics of turbulent flow of dispersions should include the measurement of velocity profiles. It should be

interesting to compare turbulent profiles for dispersions with those obtained for the pure liquids.

CHAPTER 10

BIBLIOGRAPHY

1. Alves, George E. Cocurrent liquid-gas flow in a pipe-line contactor. Chemical Engineering Progress 50:449-456. 1954.

2. _____. Flow of non-Newtonian suspensions. Chemical Engineering 56:107-109. May, 1949.

3. Alves, George E., D. F. Boucher, and R. L. Pigford. Pipe-line design for non-Newtonian solutions and suspensions. Chemical Engineering Progress 48:385-393. 1952.

4. Becher, Paul. Emulsions: theory and practice. New York, Reinhold, 1957. 382 p.

5. Binder, R. C. and J. E. Busher. A study of flow of plastics through pipes. American Society of Mechanical Engineers Transactions 68:A101-A105. 1946.

6. Bonilla, Charles F. et al. Heat transfer to slurries in pipe: chalk and water in turbulent flow. In: Chemical Engineering Progress Symposium Series no. 5, vol. 49. New York, American Institute of Chemical Engineers, 1953. p. 127-135.

7. Broughton, Geoffrey and Lombard Squires. The viscosity of oil-water emulsions. Journal of Physical Chemistry 42:253-263. 1938.

8. Brown, George Granger, et al. Unit operations. New York, Wiley, 1950. 611 p.

9. Chenoweth, J. M. and M. W. Martin. Turbulent two-phase flow. Petroleum Refiner 34:151-155. October, 1955.

10. Clayton, William. The theory of emulsions and their technical treatment. 5th ed. New York, Blakiston, 1954. 669 p.

11. Coulson, J. M. and J. F. Richardson. Chemical engineering. New York, McGraw-Hill, 1954. 2 vols.

12. Dodge, Donald W. Turbulent flow of non-Newtonian fluids in smooth round tubes. Ph.D. thesis. Newark, University of Delaware, 1957. 287 numb. leaves.

13. Drew, T. B., E. C. Koo, and W. H. McAdams. The friction factor for clean round pipes. American Institute of Chemical Engineers Transactions 28:56-72. 1932.

14. Einstein, Albert. Eine neue Bestimmung der Moleküldimensionen. Annalen der Physik 19:289-306. 1906.

15. _____. Berichtigung zu meiner Arbeit: Eine neue Bestimmung der Moleküldimensionen. Annalen der Physik 34:591-592. 1911.

16. Farbar, Leonard. Flow characteristics of solids-gas mixtures in horizontal and vertical conduit. Industrial and Engineering Chemistry 41:1184-1191. 1949.

17. Fisher Scientific Company. Fisher/Tag manual for inspectors of petroleum. 28th ed. Chicago, 1954. 218 p.

18. Fried, Lawrence. Pressure drop and heat transfer for two-phase, two-component flow. In: Chemical Engineering Progress Symposium Series no. 9, vol. 50. New York, American Institute of Chemical Engineers, 1954. p. 47-51.

19. Galegar, W. C., W. B. Stovall, and R. L. Huntington. Report on two-phase vertical flow. Pipeline Industry 4:38-42. February, 1956.

20. Gambill, Wallace R. Predict thermal conductivity. Chemical Engineering 64:271-276. March, 1957.

21. _____. You can predict heat capacities. Chemical Engineering 64:243-248. June, 1957.

22. _____. Predict liquid heat capacities. Chemical Engineering 64:263-268. July, 1957.

23. _____. Equations give liquid heat capacities. Chemical Engineering 64:257-258. August, 1957.

24. Glasstone, Samuel. Textbook of physical chemistry. 2d ed. New York, Van Nostrand, 1946. 1320 p.

25. Grover, Shamsher Singh. Heat transfer between immiscible liquids for concurrent flow. Master's thesis. Corvallis, Oregon State College, 1952. 123 numb. leaves.

26. Happel, John and B. J. Byrne. Motion of a sphere and fluid in a cylindrical tube. Industrial and Engineering Chemistry 46:1181-1186. 1954.

27. Hariu, O. H. and M. C. Molstad. Pressure drop in vertical tubes in transport of solids by gases. Industrial and Engineering Chemistry 41:1148-1160. 1949.

28. Hatschek, Emil. The general theory of viscosity of two-phase systems. Faraday Society Transactions 9:80-92. 1913.

29. _____. Die Viskosität von Blutkörperchen-Suspensionen. Kolloid-Zeitschrift 27:163-165. 1920.

30. _____. The viscosity of liquids. London, G. Bell and Sons, 1928. 239 p.

31. Hinze, J. O. Fundamentals of the hydrodynamic mechanism of splitting in dispersion processes. American Institute of Chemical Engineers Journal 1:289-295. 1955.

32. Hoopes, John W. Jr. Flow of steam-water mixtures in a heated annulus and through orifices. American Institute of Chemical Engineers Journal 3:268-275. 1957.

33. Hougen, Olaf A. and Kenneth M. Watson. Chemical process principles. Vol. 1. New York, Wiley, 1943. 452 p.

34. Jakob, Max. Heat transfer. Vol. 1. New York, Wiley, 1949. 758 p.

35. Johnson, H. A. Heat transfer and pressure drop for viscous-turbulent flow of oil-air mixtures in a horizontal pipe. American Society of Mechanical Engineers Transactions 77:1257-1264. 1955.

36. von Kármán, T. Mechanische Ähnlichkeit und Turbulenz. Nachrichten von der Gesellschaft der Wissenschaften zu Göttingen 1:58-76. 1930.

37. Keulegan, Garbis H. Interfacial instability and mixing in stratified flows. Journal of Research of the National Bureau of Standards 43:487-500. 1949.

38. Kidder, Ray E. Flow of immiscible fluids in porous media: exact solution of a free boundary problem. Journal of Applied Physics 27:866-869. 1956.

39. Knudsen, James G. and Donald L. Katz. Fluid dynamics and heat transfer. Ann Arbor, 1953. 243 p. (Michigan. University. Engineering Research Bulletin no. 37).

40. Kunitz, M. An empirical formula for the relation between viscosity of solution and volume of solute. Journal of General Physiology 9:715-725. 1926.

41. Lange, Norbert Adolph (ed.). Handbook of chemistry. 6th ed. Sandusky, Ohio, Handbook Publishers, 1946. 1767 p.

42. Leeds and Northrup Company. Standard conversion tables for Leeds and Northrup thermocouples. Philadelphia, n.d. 43 p.

43. Levenspiel, Octave and J. S. Walton. Bed-wall heat transfer in fluidized systems. In: Chemical Engineering Progress Symposium Series no. 9, vol. 50. New York, American Institute of Chemical Engineers, 1954. p. 1-13.

44. Lockhart, R. W. and R. C. Martinelli. Proposed correlation of data for isothermal two-phase, two-component flow in pipes. Chemical Engineering Progress 45:39-48. 1949.

45. Lucas, Howard J. Organic chemistry. New York, American Book Company, 1935. 686 p.

46. McAdams, William H. Heat transmission. 3d ed. New York, McGraw-Hill, 1954. 532 p.

47. Meissner, H. P. and B. Chertow. Accelerated breaking of unstable emulsions. Industrial and Engineering Chemistry 38:856-859. 1946.

48. Metzner, A. B. Non-Newtonian technology: fluid mechanics, mixing and heat transfer. In: Drew, Thomas B. and John W. Hoopes, Jr. (eds.). Advances in chemical engineering. Vol. 1. New York, Academic Press, 1956. p. 77-153.

49. Metzner, A. B. and J. C. Reed. Flow of non-Newtonian fluids---correlation of the laminar, transition, and turbulent flow regions. American Institute of Chemical Engineers Journal 1:434-440. 1955.

50. Meyer, H. I. and A. O. Garder. Mechanics of two immiscible fluids in porous media. Journal of Applied Physics 25:1400-1406. 1954.

51. Mickley, H. S. and D. F. Fairbanks. Mechanism of heat transfer to fluidized beds. American Institute of Chemical Engineers Journal 1:374-384. 1955.

52. Miller, Benjamin. Equation gives friction factor. Chemical Engineering 64:253-254. December, 1957.

53. Miller, Shelby A. and Charles A. Mann. Agitation of two-phase systems of immiscible liquids. American Institute of Chemical Engineers Transactions 40:709-745. 1944.

54. Millikan, Clark B. A critical discussion of turbulent flows in channels and circular tubes. In: Den Hartog, J. P. and H. Peters (eds.). Proceedings of the Fifth International Congress for Applied Mechanics. New York, Wiley, 1939. p. 386-392.

55. Moody, Lewis F. Friction factors for pipe flow. American Society of Mechanical Engineers Transactions 66:671-684. 1944.

56. Nelson, W. L. Petroleum refinery engineering. 3d ed. New York, McGraw-Hill, 1949. 830 p.

57. Nikuradse, J. Gesetzmässigkeiten der turbulenten Strömung in glatten Röhren. Verein deutscher Ingenieure Forschungsheft no. 356, 1932. Beilage zu Forschung auf dem Gebiete des Ingenieurwesens, Ausgabe B.

58. Oliver, D. R. and Stacey G. Ward. Relationship between relative viscosity and volume concentration of stable suspensions of spherical particles. Nature 171:396-397. 1953.

59. Olney, Richard B. and George J. Carlson. Power absorption in mixers: correlation with equipment dimensions and fluid properties. Chemical Engineering Progress 43:473-480. 1947.

60. Orr, Clyde, Jr. and J. M. Dalla Valle. Heat transfer properties of liquid-solid suspensions. In: Chemical Engineering Progress Symposium Series no. 9, vol. 50. New York, American Institute of Chemical Engineers, 1954. p. 29-45.

61. Perry, John H. (ed.). Chemical engineers' handbook. 3d ed. New York, McGraw-Hill, 1950. 1942 p.

62. Prandtl, L. Neuere Ergebnisse der Turbulenzforschung. Zeitschrift des Vereines deutscher Ingenieure 77:104-114. 1933.

63. Reid, R. C. et al. Two-phase pressure drops in large diameter pipes. American Institute of Chemical Engineers Journal 3:321-324. 1957.

64. Rhodes, Thomas J. Industrial instruments for measurement and control. New York, McGraw-Hill, 1941. 573 p.

65. Richardson, E. G. The formation and flow of emulsion. Journal of Colloid Science 5:404-413. 1950.

66. _____. The flow of emulsions. II. Journal of Colloid Science 8:367-373. 1953.

67. Robinson, James V. The viscosity of suspensions of spheres. Journal of Physical and Colloid Chemistry 53:1042-1055. 1949.

68. Rodger, W. A., V. G. Trice, Jr. and J. H. Rushton. Effect of fluid motion on interfacial area of dispersions. Chemical Engineering Progress 52:515-520. 1956.

69. Roscoe, R. The viscosity of suspensions of rigid spheres. British Journal of Applied Physics 3:267-269. 1952.

70. Roy, P. H. and J. H. Rushton. Effect of turbulence on drop size for an oil-water dispersion. Paper read before the 48th annual meeting of American Institute of Chemical Engineers, Detroit, Michigan, November 30, 1955.

71. Salamone, Jerome J. and Morris Newman. Heat transfer design characteristics: water suspensions of solids. Industrial and Engineering Chemistry 47:283-288. 1955.

72. Sibree, J. O. The viscosity of emulsions. Faraday Society Transactions 26:26-36. 1930.

73. Sieder, E. N. and G. E. Tate. Heat transfer and pressure drop of liquids in tubes. Industrial and Engineering Chemistry 28:1429-1435. 1936.

74. Stanton, T. E. and J. R. Panell. Similarity of motion in relation to the surface friction of fluids. Philosophical Transactions of the Royal Society (London) 214A:199-224. 1914.

75. Sutheim, George M. Introduction to emulsions. Brooklyn, Chemical Publishing Company, 1947. 260 p.

76. Taylor, G. I. The viscosity of a fluid containing small drops of another fluid. Royal Society of London Proceedings 138A:41-48. 1932.

77. Ting, Andrew Pusheng and Ralph H. Luebbers. Viscosity of spherical and other isodimensional particles in liquids. American Institute of Chemical Engineers Journal 3:11-116. 1957.

78. Treybal, Robert E. Liquid extraction. New York, McGraw-Hill, 1951. 422 p.

79. Trice, Virgil G. and Walton A. Rodger. Light transmittance as a measure of interfacial area in liquid-liquid dispersions. American Institute of Chemical Engineers Journal 2:205-210. 1956.

80. Vand, Vladimir. Viscosity of solutions and suspensions. Journal of Physical and Colloid Chemistry 52:277-314. 1948.

81. Verneulen, Theodore, Gael M. Williams, and Gordon E. Langlois. Interfacial area in liquid-liquid and gas-liquid agitation. Chemical Engineering Progress 51: 85F-94F. 1955.

82. Walker, William H. et al. Principles of chemical engineering. 3d ed. New York, McGraw-Hill, 1937. 749 p.

83. Wang, Ruey-Hsi. Thermal conductivity of emulsions made up of two immiscible liquids. Master's thesis. Corvallis, Oregon State College, 1957. 78 numb. leaves.

84. Ward, Henderson C. and J. M. Dalla Valle. Cocurrent turbulent-turbulent flow of air and water-clay suspensions in horizontal pipes. In: Chemical Engineering Progress Symposium Series no. 10, vol. 50. New York, American Institute of Chemical Engineers, 1954. p. 1-14.

85. Ward, S. G. and R. L. Whitmore. Studies of the viscosity and sedimentation of suspensions, part I the viscosity of suspensions of spherical particles. British Journal of Applied Physics 1:286-290. 1950.

APPENDICES

APPENDIX A

NOMENCLATURE

Many of the equations in this paper involve dimensionless ratios, and any consistent system of units might be used. The units given below are merely those chosen by the writer for this work.

Latin Letter Symbols

Symbol	Meaning	Units
A	Cross sectional area of flow channel	ft^2
A'	Surface area of wall of flow channel	ft^2
A_{cs}	Cross sectional area of tube material	ft^2
a	Height of water column in manometer line (Chapter 5)	ft
a	Constant in forced convection heat transfer equation (Chapter 2)	
B	Constant in Prandtl-Kármán equation	
b	Manometer reading	ft
b	Constant in forced convection heat transfer equation (Chapter 2)	
C	Coefficient in orifice equation	
C_D	Orifice discharge coefficient	
c	Height of water column in manometer line (Chapter 5)	ft
c	Constant in forced convection heat transfer equation (Chapter 2)	

Symbol	Meaning	Units
c_p	Specific heat at constant pressure	$\frac{Btu}{(lb_m)(^oF)}$
D	Inside diameter of tube	ft
D_o	Outside diameter of tube	ft
d	Constant in forced convection heat transfer equation (Chapter 2)	
E	Constant in Prandtl-Kármán equation	
e	Base of natural logarithms	
e	Pipe roughness, average height of projections on pipe wall	ft
F	Frictional resistance force at wall of conduit	lb_f
f	Fanning friction factor	
G	Mass velocity	$\frac{lb_m}{(sec)(ft^2)}$
g	Gravitational acceleration	$\frac{ft}{sec^2}$
g_c	Conversion constant = 32.174	$\frac{(lb_m)(ft)}{(lb_f)(sec^2)}$
h	Film heat transfer coefficient	$\frac{Btu}{(hr)(ft^2)(^oF)}$
K	UOP characterization factor for petroleum fractions	$(^oR)^{1/3}$
k	Thermal conductivity	$\frac{Btu}{(hr)(ft)(^oF)}$
L	Length of conduit	ft
L'	Vertical distance between orifice pressure taps	ft
l	Length of heater coil	ft

Symbol	Meaning	Units
N	Volume fraction in a mixture	
N'	Mass fraction in a mixture	
P	Static pressure	$\frac{lb_f}{ft^2}$
Q	Power input to heater coil	$\frac{Btu}{hr}$
q	Steady state heat transfer rate	$\frac{Btu}{hr}$
S	Specific gravity at 60°F	
T_B	Average boiling point of petroleum fraction	°R
t	Temperature	°F
t_a	Temperature of flowing fluid	°F
t_c	Temperature of tube wall under heating coil	°F
V	Average linear velocity of fluid	$\frac{ft}{sec}$
W	Mass flow rate	$\frac{lb_m}{sec}$
$\overline{w}$	Work done by a flowing fluid	$\frac{(ft)(lb_f)}{lb_m}$
x	Length coordinate in the direction of flow	ft
x	Distance along test section tubing measured from end of heating coil	ft
z	Elevation above an arbitrary datum plane	ft

Greek Letter Symbols

Symbol	Meaning	Units
α	Correction factor in expression for kinetic energy of fluid	
Δ	Finite difference	
Θ	Time of efflux through capillary tube of viscometer	sec
μ	Dynamic viscosity	$\frac{lb_m}{(sec)(ft)}$
μ_c	Viscosity of continuous phase	$\frac{lb_m}{(sec)(ft)}$
μ_d	Viscosity of dispersed phase	$\frac{lb_m}{(sec)(ft)}$
μ_m	Apparent viscosity of mixture	$\frac{lb_m}{(sec)(ft)}$
π	Dimensionless product in Buckingham Pi Theorem	
ρ	Density	$\frac{lb_m}{ft^3}$
ϕ	Volume fraction of dispersed phase	
ψ	Function of undetermined form in expression for heat transfer coefficient	
ψ'	Function of undetermined form in expression for heat transfer coefficient	

Composite Symbols

API	Specific gravity scale adopted by the American Petroleum Institute	
B & S	Brown and Sharpe wire gauge	
gpm	U. S. gallons per minute	$\frac{gal}{min}$

Symbol	Meaning	Units
log	Common logarithm (base 10)	
$\overline{lw}$	Lost work due to friction in a flowing fluid	$\frac{(ft)(lb_f)}{lb_m}$
$Nu=\frac{hD}{k}$	Nusselt number	
$Pr=\frac{c_p\mu}{k}$	Prandtl number	
$Re=\frac{DG}{\mu}$	Reynolds number	
Re_O	Reynolds number based on orifice diameter	
ΔP	Pressure difference between two points in a flowing fluid	$\frac{lb_f}{ft^2}$
ΔP_f	Pressure difference due to fluid friction	$\frac{lb_f}{ft^2}$

Subscripts

a	Flowing fluid
b	Manometer fluid
c	Continuous phase, or tube wall under heater coil
D	Discharge
d	Dispersed phase
e	Effective
f	Force (as in lb_f), or friction (as in ΔP_f)
m	Mass (as in lb_m), or mixture
O	Orifice
r	Reference level

Symbol	Meaning
s	Solvent, or surface of conduit
w	Water
1,2	Refer to positions in a flow system

APPENDIX B

PROPERTIES OF PURE LIQUIDS

Characterization of the Petroleum Solvent

The solvent used as the organic component of the immiscible liquid pair in this investigation was a commercial cleaning solvent manufactured by the Shell Oil Company under the name "Shellsolv 360". This material is clean and colorless, and is readily available in 55 gallon drum quantities at reasonable cost. The properties of this solvent, as given by the Shell Oil Company Specifications, are presented in Table 11.

The solvent is a mixture of hydrocarbons whose exact composition is not known. The data of Table 11 do however permit some rough deductions to be made regarding the character of the mixture. Petroleum fractions may be characterized through the use of the Universal Oil Products Company (UOP) characterization factor K, which is defined as [33, p. 330]

$$K = \frac{T_B^{1/3}}{S}, \tag{61}$$

where T_B is the average boiling point in degrees Rankine and S is the specific gravity at 60°F. The API gravity is a special specific gravity scale adopted by the American Petroleum Institute for use with petroleum

products [33, p. 20]. It is related to the specific gravity as follows:

$$\text{Degrees API} = \frac{141.5}{S} - 131.5. \tag{62}$$

Table 11

Properties of "Shellsolv 360"
(Data from Company Specifications)

Gravity, API, 60°F	49.1
Specific Gravity, 60/60°F	0.7835
Color, Saybolt	26+
Flash Tag, O.C., °F	110
Flash Tag, C.C., °F	103
Aromatics, Stoddard, % v	2
A.S.T.M. Distillation, °F:	
Initial Boiling Point	304
Final Boiling Point	362
10 % Recovered	317
50 % Recovered	323
90 % Recovered	342
% Recovered	98.5

Using the 50 per cent point of the distillation as the average boiling point together with the specific gravity from Table 11 leads to a K value of 11.8. Table 11 indicates that the solvent is low in aromatic hydrocarbon content, and the relatively high value of the

characterization factor indicates a high paraffinic content [33, p. 330]. Based on the boiling points of normal paraffin hydrocarbons [45, p. 50], the composition would appear to be in the nonane-decane range. The characterization factor has been related to various properties of petroleum through empirical correlations [33, p. 331-334]. Utilizing one of these correlations [33, p. 331], the average molecular weight may be estimated from the K value and the API gravity. The result is an estimated average molecular weight of 134, and this value is also consistent with compositions in the nonane-decane range.

The solubilities of hydrocarbons in water, and vice versa, are quite low. For example, Lange [41, p. 418, 586] lists both nonane and decane as insoluble in water, and Nelson [56, p. 171] indicates a water solubility in petroleum fractions of the order of 0.05 mole per cent at 70°F. It is seen that the solvent-water system used in this investigation represents a practically immiscible pair of liquids.

As pointed out previously, the physical properties of interest in the study of friction pressure losses and forced convection heat transfer are the density, specific heat, thermal conductivity, and viscosity. The measurements and sources of data used in evaluating these properties for solvent and water are discussed below.

Density

In order to determine the density of the solvent as a function of temperature, a constant temperature bath was utilized. This bath was controllable within ±0.1°F at a preselected temperature. A glass cylinder filled with solvent was immersed in the bath and determinations were made after the solvent had reached bath temperature. Densities (or rather specific gravities) were determined with precision hydrometers according to the procedure recommended for testing petroleum products [17, p. 8-9]. Successive determinations were reproducible within ±0.06 per cent. At a temperature of 60°F, the measured specific gravity was found to be about 0.4 per cent higher than that given in the specifications. The density of water was taken from the literature [41, p. 1360]. The densities of solvent and water are plotted versus temperature in Figure 20.

The effective densities of the manometer fluids were required in order to evaluate pressure differences from manometer readings. In the present equipment the manometer lines were filled with water so the effective density was given by the difference between the density of the manometer liquid (mercury or carbon tetrachloride) and the density of water. Densities of mercury and carbon tetrachloride were taken from the literature [41, p. 1358;

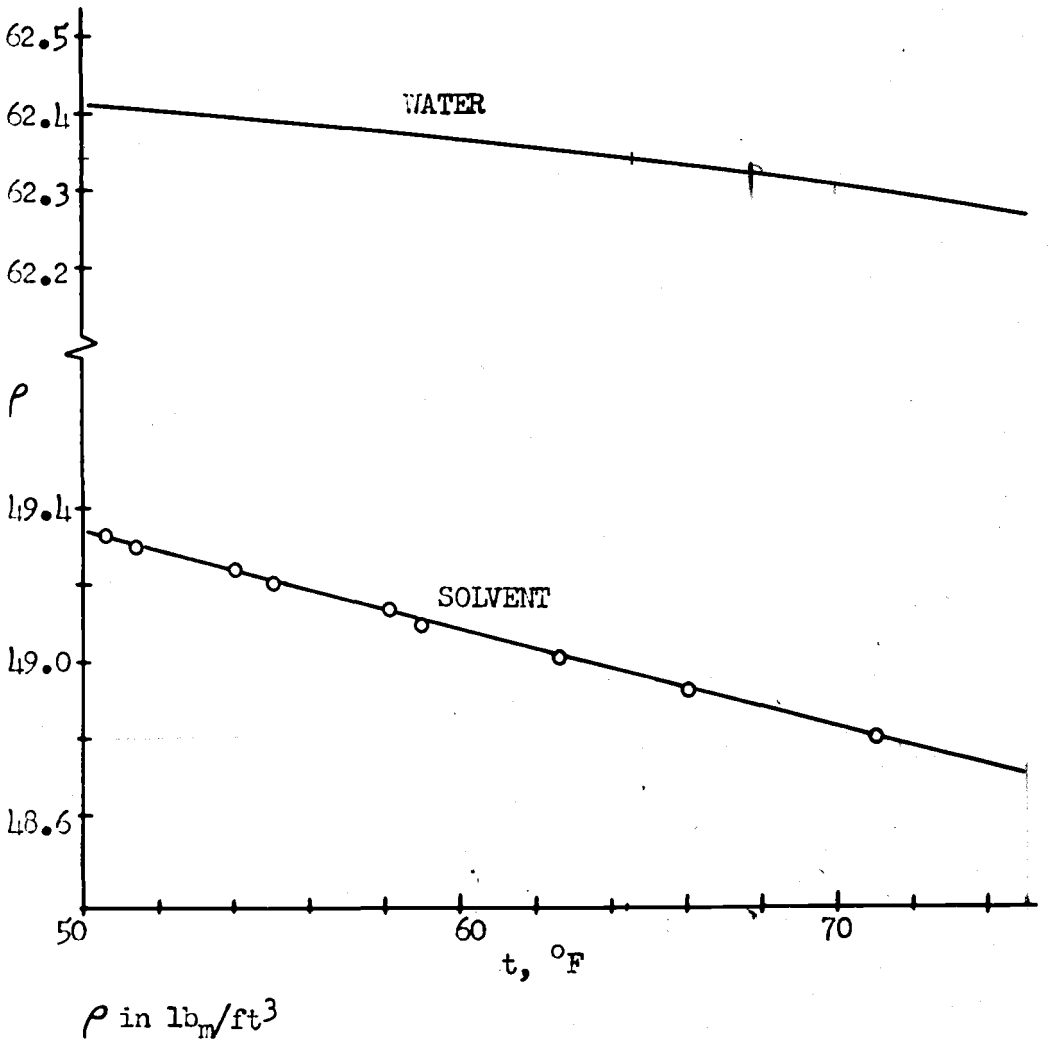

FIGURE 20
DENSITY OF WATER AND SOLVENT VERSUS TEMPERATURE

8, p. 585], and the effective densities have been plotted against temperature in Figure 21.

Specific Heat

Specific heats of petroleum oils have been correlated empirically with the characterization factor and API gravity and convenient plots for estimating the specific heat as a function of temperature are available. Hougen and Watson [33, p. 334] present a family of curves of specific heat versus temperature with API gravity as a parameter. Correction factors are also given to account for variations in characterization factor. Over the narrow temperature range involved in the present work these curves are practically straight, parallel lines. The specific heat versus temperature relationship was estimated using the measured specific gravity and the characterization factor computed from equation (61). As a check on the accuracy of this procedure the heat capacity of the solvent was measured at an average temperature of 79°F. Mr. F. D. Stevenson made this determination using a calorimeter which was calibrated with benzene and checked with water previous to the solvent measurements. The temperature rise produced in a known amount of liquid by a measured electrical power input was used to evaluate the specific heat at constant pressure. A value of 0.472 $\frac{\text{Btu}}{(\text{lb}_m)(^\circ\text{F})}$

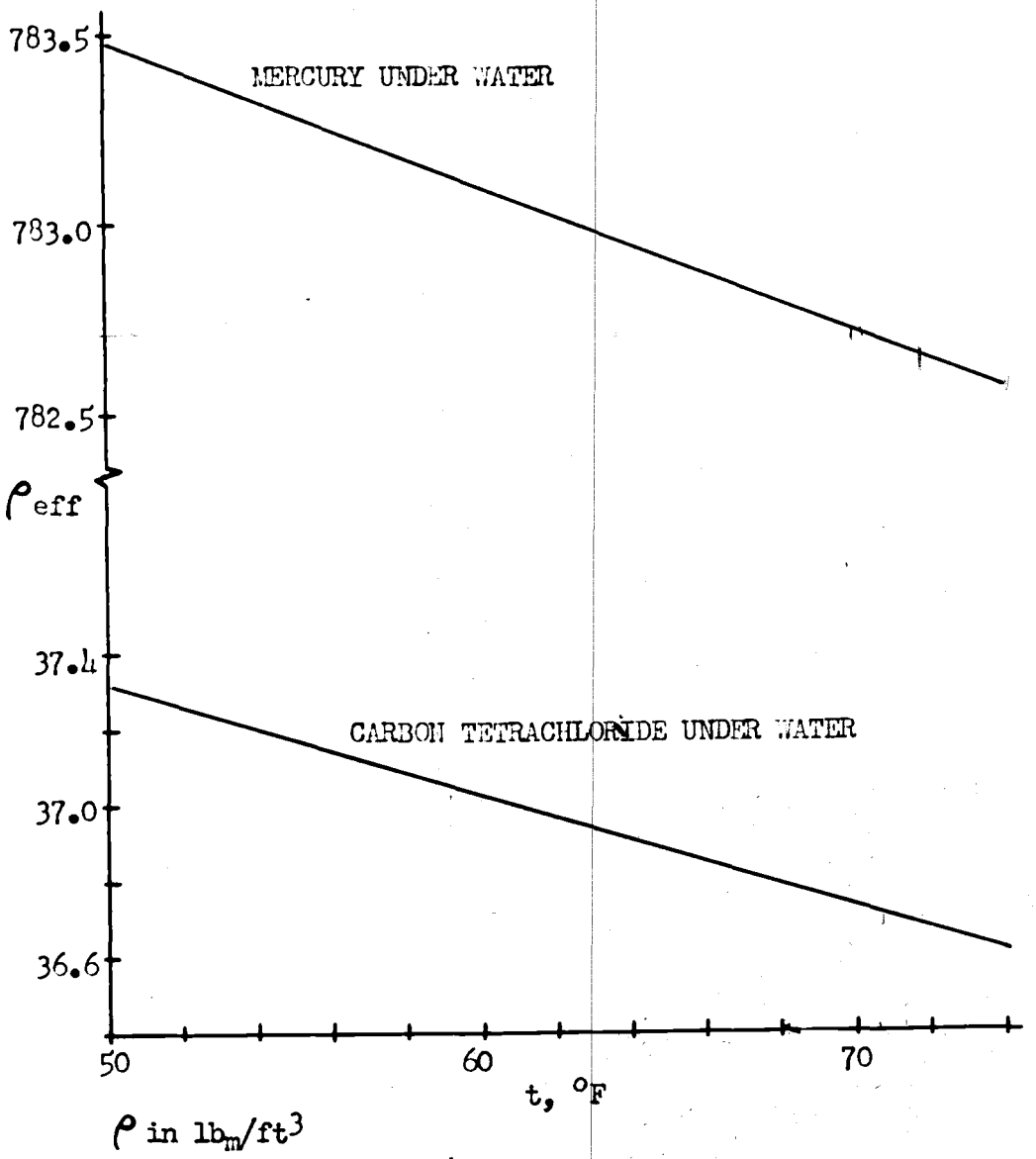

FIGURE 21
EFFECTIVE DENSITIES OF MANOMETER FLUIDS VERSUS TEMPERATURE

was obtained with an estimated accuracy of ±1 per cent. The experimental value was approximately 2 per cent higher than that estimated using the characterization factor and the API gravity. A line drawn through the measured value and parallel to the line estimated by the procedure described above was used to represent the variation of specific heat with temperature. This relationship is indicated in Figure 22. Over the temperature range from 50 to 80°F the specific heat of water has a value of 1.0 $\frac{Btu}{(lb_m)(^oF)}$ within ±0.1 per cent [61, p. 225], and this value was used throughout the course of the present work. A review of methods for estimating the specific heat of liquids has been given in a series of articles by Gambill [21, 22, 23].

Mr. Stevenson was also kind enough to measure the thermal conductivity of the brass tubing used in the test section. This quantity was required in the evaluation of the film heat transfer coefficient by equation (47) of Chapter 5. The method used was based on a comparison with the known thermal conductivity of a length of pure copper tubing, and this method has been described in detail by Jakob [34, p. 211-217]. The value obtained was 107 $\frac{Btu}{(hr)(ft)(^oF)}$, and this value was used in computing the heat transfer coefficients by equation (47).

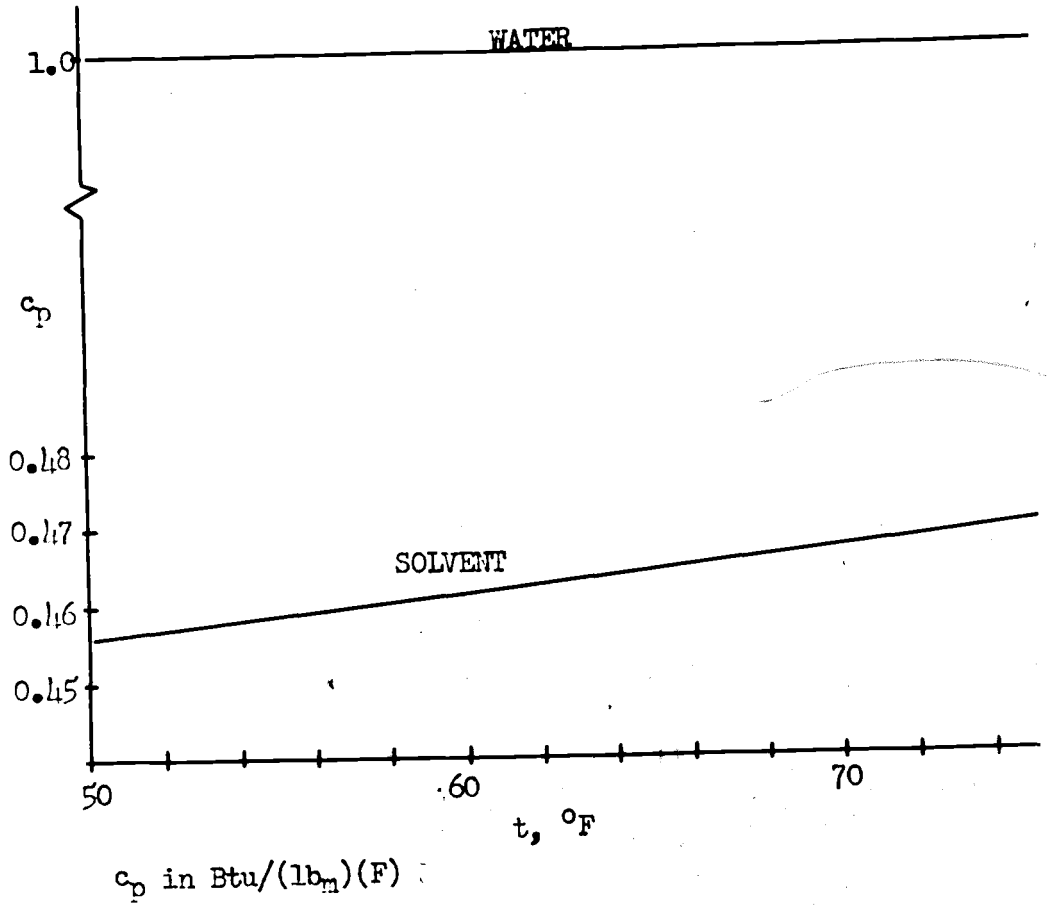

FIGURE 22
SPECIFIC HEAT OF WATER AND SOLVENT VERSUS TEMPERATURE

Thermal Conductivity

Wang [83, p. 36] has measured the thermal conductivity of a petroleum solvent with properties practically identical to those of the solvent used in this investigation. His values are in good agreement with those given by Nelson [56, p. 473] for petroleum oils with similar specific gravity. Nelson's data also indicate that thermal conductivities of hydrocarbon mixtures change slowly with changes in composition at a given temperature. On the basis of these facts Wang's data were applied in the present work and his curve of thermal conductivity of solvent versus temperature has been reproduced in Figure 23.

All of Wang's data were referred to the thermal conductivity of water calculated from the following equation [83, p. 7]:

$$(63)\quad k_w = 1.41 \times 10^{-3} + 3.28 \times 10^{-6} t - 1.02 \times 10^{-8} t^2.$$

As written above, this equation gives the thermal conductivity of water in $\frac{\text{cal}}{(\text{sec})(\text{cm})(^{\circ}\text{C})}$ for temperature in degrees Centigrade. Equation (63) was based on recent measurements of the conductivity of water, and it has been plotted in Figure 23 along with the solvent data. Over the temperature range covered by the figure this curve gives thermal conductivities 3 to 5 per cent higher than the

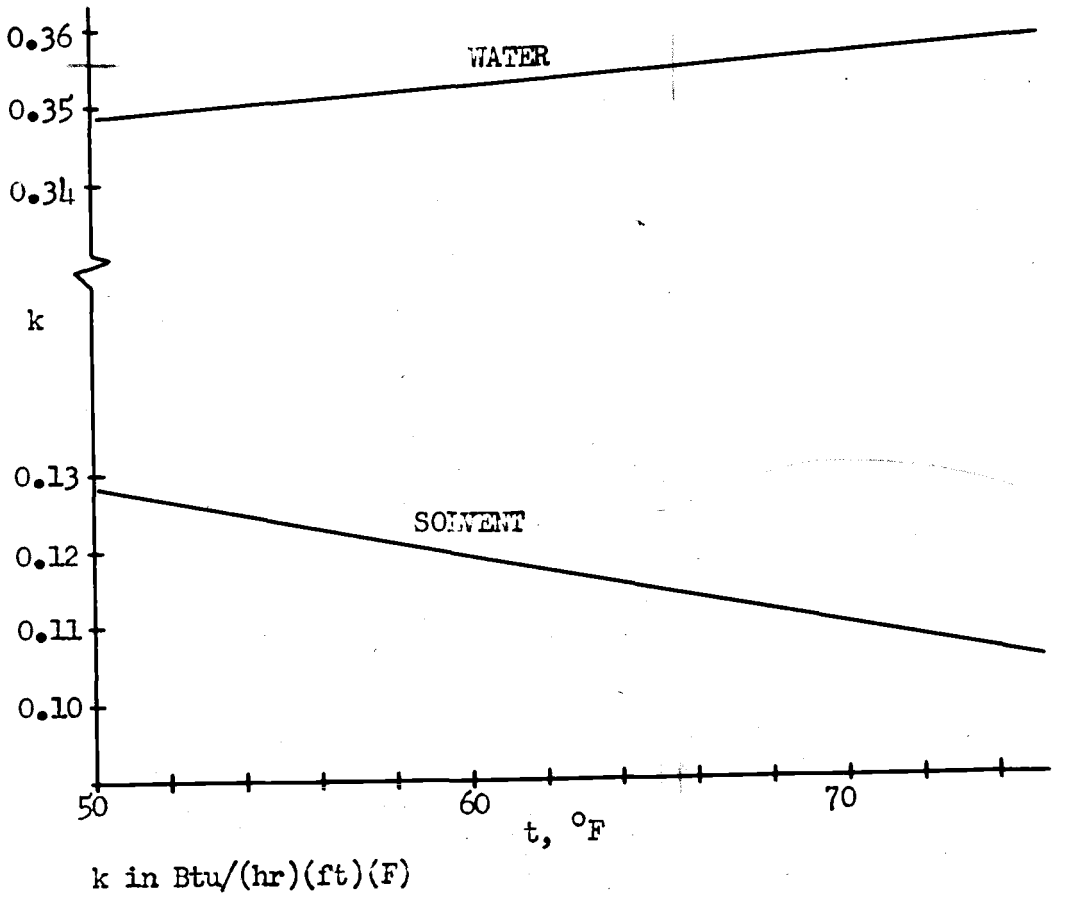

FIGURE 23
THERMAL CONDUCTIVITY OF WATER AND SOLVENT VERSUS TEMPERATURE

values presented by McAdams [46, p. 456]. A survey of available methods for estimating liquid thermal conductivities has recently been given by Gambill [20, p. 271-276].

Viscosity

No data were available on the dynamic viscosity of the petroleum solvent, so it was necessary to measure this property as a function of temperature. The measurements were made relative to distilled water with a viscometer of the Ostwald type. In this instrument the flow of a definite amount of liquid through a capillary tube is timed and this time of efflux is compared with the time for the same amount of reference liquid (water). As shown by Glasstone [24, p. 498] the viscosities of the two liquids are related by

$$\frac{\mu_s}{\mu_w} = \frac{\rho_s \theta_s}{\rho_w \theta_w}, \tag{64}$$

where μ is the dynamic viscosity, ρ is the density, θ is the time of efflux through the capillary, and s and w refer to solvent and water respectively. The measurements were made in the constant temperature bath described previously and flows were timed with a stopwatch. Whenever the liquid in the viscometer was changed, the instrument was thoroughly rinsed with acetone and dried by drawing filtered laboratory air through the capillary tube. At each

temperature, four determinations each were made on water and solvent. Successive times of efflux were reproducible to ±0.1 per cent. Using the measured efflux times and the previously determined densities, the solvent viscosity was evaluated from equation (64). The results are indicated in Figure 24 along with data for water taken from Lange [41, p. 1582]. A very complete discussion of the Ostwald viscometer and the errors involved in its use has been given by Hatschek [30, p. 17-58].

It has been mentioned previously that the solvent was recovered after a series of mixture runs and used again to prepare the next mixture. In order to determine whether or not such recovery and reuse had any effect on the solvent viscosity, a sample of solvent twice recovered was taken for viscosity measurements. Determinations made at several temperatures indicated that the used solvent viscosity differed from that of the fresh solvent by less than 0.2 per cent.

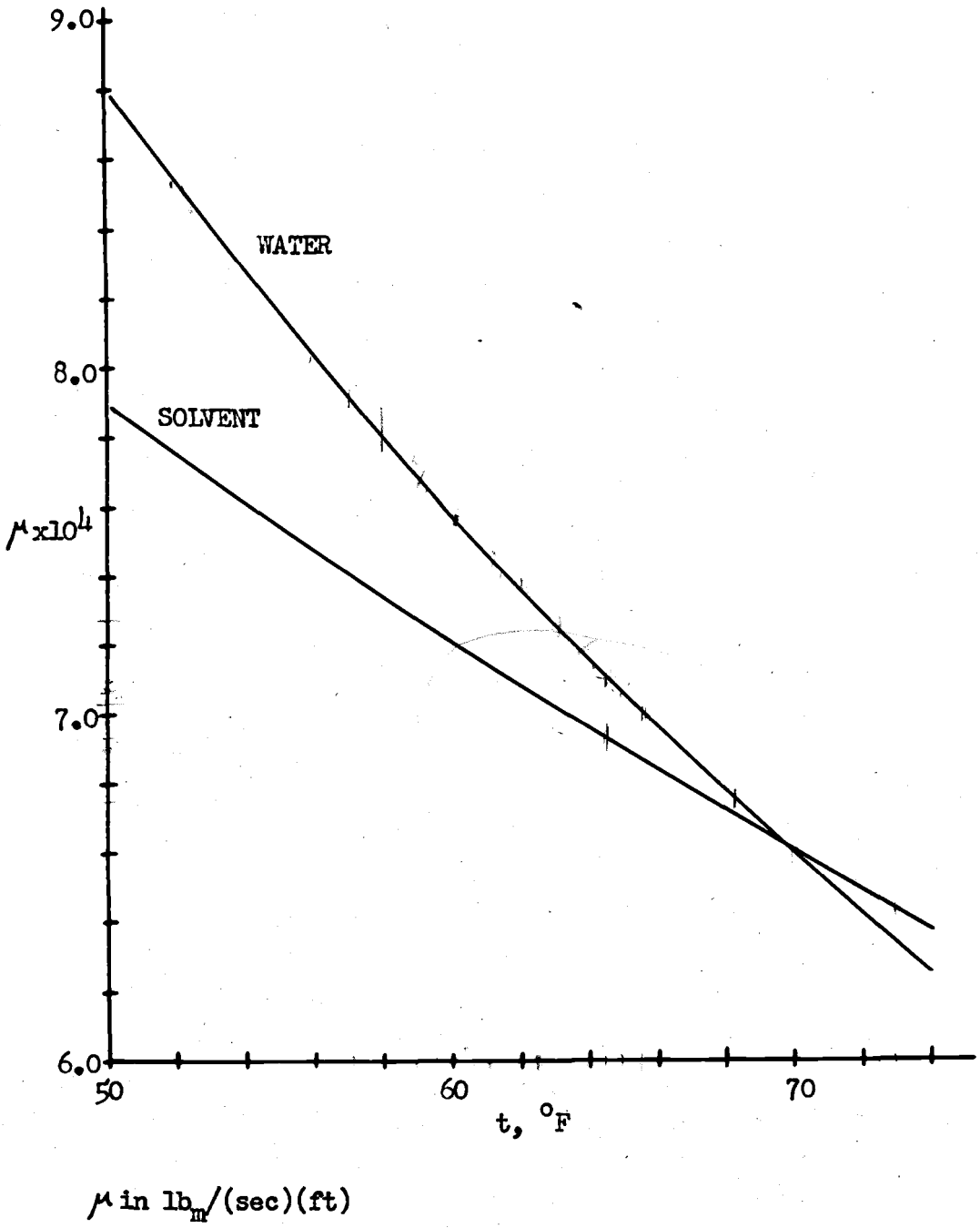

FIGURE 24
VISCOSITY OF WATER AND SOLVENT VERSUS TEMPERATURE

APPENDIX C

TABULATED DATA

Table 12

Observed Data

(1)* Run No.	(2) Orifice Manometer, mm	(3) Test Section Manometer, mm	(4) Mass of Fluid, lb_m	(5) Time, sec
W-1	10.0(CCl_4)	28.0	10.0	68.9
2	12.0 "	"	"	67.1
3	21.0 "	47.0	"	50.9
4	23.0 "	"	"	48.1
5	24.0 "	50.0	"	47.0
6	24.0 "	"	"	47.4
7	57.0 "	91.0	"	32.8
8	3.5(Hg)	4.0	"	"
9	59.0(CCl_4)	93.0	"	32.2
10	3.0(Hg)	4.0	"	"
11	537.0(CCl_4)	538.0	20.0	24.0
12	25.5(Hg)	25.0	"	"
13	505.0(CCl_4)	510.0	50.0	60.1
14	215.0 "	250.0	20.0	37.1
15	10.5(Hg)	11.5	"	"
16	207.0(CCl_4)	242.0	50.0	93.2
17	236.0 "	269.0	20.0	35.7
18	11.5(Hg)	13.0	"	"
19	228.0(CCl_4)	260.0	50.0	89.0
20	293.0 "	326.0	20.0	31.6
21	14.5(Hg)	15.0	"	"
22	288.0(CCl_4)	318.0	50.0	79.2
23	407.0 "	430.0	20.0	26.9
24	19.5(Hg)	20.0	"	"
25	397.0(CCl_4)	420.0	50.0	67.5
26	689.0 "	678.0	20.0	21.0
27	33.0(Hg)	31.5	"	"
28	677.0(CCl_4)	666.0	50.0	51.8
29	112.5(Hg)	92.0	20.0	11.3
30	111.5(Hg)	91.0	50.0	28.1
31	198 "	151.5	"	21.1
32	197 "	150.5	"	21.3
33	304 "	223	"	17.0
34	303 "	222	100.0	34.4
35	305.5 "	221.5	"	"

* The run number code is as follows: the first number (or symbol) represents the nominal composition and the second number represents the run number within the series. Thus, W-1 is the first water run, 50-2 is the second run with 50 per cent solvent in water, etc.

Table 12 - Continued

Observed Data

(1)* Run No.	(6) t_7, Flow Temp., °F	(7) t_1, Coil Temp., °F	(8) Coil Current, Amps.	(9) Coil Voltage, Volts
W-1	66.3	74.2	3.00	11.85
2	"	"	"	11.80
3	67.1	73.2	"	11.85
4	"	"	"	"
5	64.4	70.7	"	11.77
6	"	"	"	11.76
7	65.6	71.0	3.31	12.95
8	"	"	3.32	"
9	"	"		
10	"	"		
11	"	68.3	3.30	12.95
12	"	"	3.31	12.97
13	"	"		
14	65.1	68.9	3.33	13.02
15	"	"	3.32	13.03
16	"	"		
17	66.3	69.8	3.32	13.03
18	"	"	"	13.04
19	"	"		
20	64.3	67.8	3.31	13.00
21	"	"	3.30	"
22	"	"		
23	63.5	66.6	3.30	13.00
24	"	"	3.32	"
25	"	"		
26	60.4	63.0	3.32	13.02
27	"	"	"	13.06
28	"	"		
29	61.5	63.4	3.36	13.05
30	"	"	3.38	13.08
31	62.9	64.6	3.35	13.06
32	"	"	3.32	13.03
33	63.1	64.6	3.30	12.98
34	"	"	3.31	13.00
35				

(1)*	(2)	(3)	(4)	(5)
W-36	449 (Hg)	313.5	70.0	19.6
37	448 "	312.5	"	"
38	644.5 "	435	"	16.5
39	643.5 "	434	"	"
50-1	13.0(CCl_4)	-175.0	10.0	48.6
2	15.0 "	- 8.0(Hg)	"	"
3	88.0 "	- 73.0	20.0	49.2
4	74.0 "	- 55.0	"	42.2
5	72.0 "	-105.0	"	45.5
6	4.0(Hg)	- 5.0	"	"
7	253.0(CCl_4)	46.0	"	32.5
8	13.0(Hg)	2.5	"	"
9	376.0(CCl_4)	295.0	"	26.8
10	18.0(Hg)	14.0	"	"
11	45.0 "	45.5	"	17.8
12	49.0 "	"	"	17.9
13	64.5 "	67.0	35.0	26.5
14	118.5 "	121.0	50.0	28.1
15	189.0 "	186.0	"	22.6
16	272.0 "	267.5	"	18.9
17	357.5 "	347.5	"	16.5
18	542.0 "	513.5	"	13.4
20-1	(CCl_4)	-103.0	10.0	97.6
2	(Hg)	- 4.5	"	"
3	53.0(CCl_4)	- 34.0	"	34.3
4	66.0 "	- 3.0	20.0	63.1
5	149.0 "	89.0	"	43.9
6	138.0 "	84.0	"	43.0
7	28.5 "	- 65.0	"	101.7
8	19.0 "	- 78.0	10.0	51.7
9	(Hg)	- 3.5	"	51.1
10	274.0(CCl_4)	237.0	20.0	32.5
11	13.5(Hg)	11.0	"	"
12	430.0(CCl_4)	394.0	"	26.4
13	21.0(Hg)	18.5	"	"
14	61.5 "	57.0	"	15.7
15	"	"	"	15.6
16	128.5 "	112.5	50.0	27.2
17	130.5 "	"	"	27.0
18	195.5 "	169.5	"	2.0
19	279.5 "	236.0	"	18.4
20	372.5 "	311.0	"	15.8
21	455.0 "	372.0	"	14.4
22	604.0	479.0	"	12.5

(1)*	(6)	(7)	(8)	(9)
W-36	62.4	63.9	3.32	12.96
37	"	"	3.33	13.00
38	61.3	62.8	3.30	12.94
39	"	"	"	12.92
50-1	64.5		3.32	13.0
2	"		3.31	"
3	63.4		3.32	"
4	66.6		"	"
5	64.2		3.35	13.08
6	"		"	"
7	63.2		3.32	13.00
8	"		"	"
9	62.1	70.0	3.32	13.00
10	"	"	"	"
11	61.6	66.1	3.33	13.02
12	"	"	"	"
13	61.5	65.0	"	13.00
14	"	64.0	"	"
15	"	63.5	"	"
16	61.8	"	"	"
17	62.5	64.2	3.35	13.03
18	62.9	64.4	"	13.02
20-1	60.1		3.35	13.08
2	"		"	"
3	58.3		"	13.05
4	58.2		"	13.06
5	57.8		3.33	13.00
6	58.6		"	13.03
7	59.8		"	13.00
8	60.0		3.35	13.05
9	"		"	"
10	58.0		"	13.00
11	"		"	"
12	57.8		"	13.02
13	"		"	"
14	57.5		"	13.00
15	"		"	"
16	57.4		3.33	"
17	58.6		3.32	12.96
18	"		"	12.97
19	"		"	12.96
20	58.8		"	12.97
21	59.2		"	12.95
22	59.6		"	12.94

(1)*	(2)	(3)	(4)	(5)
W-40	(CCl_4)	11.0	10.0	127.0
41	5.0 "	19.5	"	103.8
42	10.0 "	20.0	"	81.4
43	7.0 "	24.0	"	92.0
44	" "	19.5	"	92.6
45	"	21.0	"	"
46	7.0 "	19.5	"	93.2
47	42.0 "	89.5	"	39.5
48	41.5 "	83.0	50.0	199.7
49	15.5 "	26.0	10.0	67.2
50	20.5 "	34.0	"	57.2
51	41.5 "	60.5	"	39.8
52	144.0 "	165.0	50.0	113.9
53	6.5(Hg)	8.0	"	"
54	230.0(CCl_4)	248.0	"	90.6
55	10.5(Hg)	12.0	"	"
56	448.0(CCl_4)	457.5	"	64.1
57	20.5(Hg)	21.5	"	"
25-1	- 4.5(CCl_4)	-134.0	10.0	78.6
2	13.5 "	-106.0	20.0	91.3
3	65.0 "	- 9.0	"	58.3
4	106.5 "	26.0	"	48.6
5	164.0 "	95.5	"	39.9
6	496.0 "	413.0	50.0	61.9
7	23.0(Hg)	20.0	"	"
8	32.5 "	30.0	"	52.0
9	46.0 "	43.0	"	44.1
10	66.0 "	62.0	"	36.4
11	96.5 "	87.5	"	30.5
12	169.5 "	147.5	"	23.2
13	278.0 "	233.5	"	18.2
14	578.0 "	461.0	"	12.7
75-1	104 (Hg)	147	50.0	28.8
2	200 "	227	"	22.6
65-1	22.0(Hg)	39.0	20.0	24.6
2	44.0 "	57.0	50.0	44.2
3	77.5 "	78.0	"	33.8
4	8.5 "	21.0	"	95.0
5	76.5 "	78.0	"	34.5
6	147.0 "	165.0	"	24.9
7	196.5 "	220.0	"	21.5
8	264.0 "	289.0	"	18.7
9	307.0 "	331.0	"	17.4
10	351.0 "	374.0	"	16.4
11	410.0 "	428.0	"	15.2
12	457.0 "	472.5	"	14.3

(1)*	(6)	(7)	(8)	(9)
W-40	58.3			
41	58.8			
42	60.0			
43	58.0			
44	58.7			
45	"			
46	59.0			
47	59.4			
48	59.6			
49	62.2			
50	61.5			
51	60.4			
52	61.6			
53	"			
54	62.2			
55	"			
56	61.0			
57	"			
25-1	63.5		3.00	11.61
2	62.1		3.00	11.62
3	63.1		3.37	13.00
4	63.0		3.38	13.05
5	62.8	68.9	"	13.03
6	63.0	66.9	3.36	13.02
7	"			
8	62.1	65.6	3.37	13.04
9	"	65.4	"	"
10	"	64.9	3.36	13.01
11	62.7	64.9	3.37	13.03
12	"	64.7	"	13.02
13	"	64.3	"	"
14	62.5	64.2	"	13.4
75-1	67.3		3.37	13.10
2	66.5		3.36	13.05
65-1	66.5		3.33	13.00
2	66.3	75.4	3.35	13.03
3	66.2	73.7	"	13.02
4	67.2		3.31	12.90
5	66.2			
6	65.0	69.4	3.32	12.97
7	64.9	68.5	"	12.98
8	65.0	68.0	"	12.97
9	65.1	67.9	3.35	13.03
10	65.2	67.6	3.34	"
11	"	"	3.36	"
12	65.3	"	3.35	13.04

(1)*	(2)	(3)	(4)	(5)
65-13	476.0(Hg)	488.5	50.0	14.0
14	6.0(CCl_4)	-255.0	10.0	89.7
15	16.0 "	- 45.0	"	43.2
16	40.0 "	42.0	20.0	64.7
17	67.0 "	197.0	"	53.4
18	3.5(Hg)	9.5	"	"
S-1	22.0(Hg)	- 8.5	20.0	28.2
2	5.0 "	- 25.0	"	61.0
3	42.5 "	8.5	40.0	40.5
4	75.5 "	34.5	"	30.6
5	99.5 "	53.0	50.0	33.6
6	123.5 "	71.0	"	29.8
7	157.5 "	95.0	"	26.6
8	187.0 "	117.0	"	24.3
9	230.5 "	147.0	"	21.9
10	283.5 "	182.5	"	19.8
11	318.5 "	205.5	"	18.8
12	11.5 "	- 18.0	40.0	76.5
13	38.5 "	5.5	40.0	42.6
14	351.5 "	226.0	50.0	18.0
15	418.5 "	270.0	"	16.3
16	487.5 "	314.0	"	15.4
17	505.5 "	327.0	"	15.0
18	40.0(CCl_4)	-594.0	20.0	87.0
19	2.0(Hg)	- 28.0	"	"
20	8.0(CCl_4)	-647.0	"	182.8
21	36.0 "	-608.0	"	90.2
22	85.0 "	-547.0	"	61.0
23	4.0(Hg)	- 25.0	"	"
24	341.0(CCl_4)	-288.0	"	32.4
25	16.0(Hg)	- 13.5	"	"
90-1	6.0(Hg)	- 22.0	20.0	53.1
2	2.0 "	- 6.5	40.0	55.0
3	45.0 "	12.5	"	38.7
4	90.5 "	48.0	50.0	34.7
5	147.5 "	88.0	"	27.2
6	216.5 "	133.0	"	22.6
7	265.5 "	165.5	"	20.4
8	341.5 "	217.0	"	17.9
9	430.5 "	269.0	"	16.0
10	517.5 "	327.0	"	14.7
11	0.5 "	- 23.0	20.0	241.6
12	31.5 "	2.3	50.0	58.5

(1)*	(6)	(7)	(8)	(9)
65-13	65.3	67.6	3.35	13.03
14	69.9		"	"
15	67.9		"	13.05
16	67.3		3.34	13.00
17	66.9		"	"
18	"			
S-1	67.2	75.7	3.33	13.00
2	68.9	84.2	3.32	"
3	67.0	73.8	"	"
4	66.9	72.3	3.33	"
5	66.3	71.2	3.32	"
6	65.7	70.4	"	"
7	65.3	69.6	"	"
8	64.9	68.8	"	"
9	64.2	68.0	"	12.95
10	63.9	67.4	"	12.97
11	63.8	67.2	"	13.00
12	66.7	77.7	3.35	13.05
13	66.0	72.9	3.36	13.08
14	64.3	67.5	3.35	13.05
15	63.8	66.7	"	13.06
16	63.3	66.2	"	13.07
17	63.1	65.9	3.37	13.08
18	68.9	84.7	3.00	11.70
19	"	"	"	"
20	71.5	99.1	"	"
21	68.5	84.6	"	"
22	67.4	79.4	"	"
23	"	"	"	"
24	66.4	73.8	"	"
25	"	"	"	"
90-1	62.6		3.32	13.00
2	61.9		"	13.02
3	61.5	68.3	"	13.00
4	"	66.6	3.33	"
5	61.3	65.8	3.32	"
6	61.1	65.2	"	"
7	61.7	"	3.35	13.05
8	61.8	"	"	13.04
9	61.9	64.9	3.34	13.01
10	62.2	"	3.33	13.00
11	65.6		3.35	13.05
12	62.9		"	13.04

Table 13

Calculated Data

(1) Run No.	(2) W, $\frac{lb_m}{sec}$	(3) $fx10^3$	(4) $\mu_m x10^4$ $\frac{lb_m}{sec\ ft}$	(5) $Rex10^{-3}$	(6) C_D	(7) h, $\frac{Btu}{(hr)(ft^2)(^oF)}$	(8) $Nu \times Pr^{-.4}$
W-1	0.145	9.79	6.90	4.59	0.765	290	21.8
2	0.149	9.28	"	4.71	0.717	"	"
3	0.196	9.60	6.84	6.26	0.714		
4	0.208	8.57	"	6.63	0.723		
5	0.213	8.58	7.08	6.56	"		
6	0.211	8.73	"	6.50	0.717		
7	0.305	7.93	6.98	9.53	0.673	570	42.8
8	"	7.40	"	"	0.589	"	"
9	0.310	7.82	"	9.70	0.674		
10	"	7.13	"	"	0.648		
11	0.833	6.47	6.99	26.0	0.600	1280	95.5
12	"	6.40	"	"	0.596	"	"
13	0.832	6.15	"	"	0.617		
14	0.539	7.13	7.03	16.7	0.612	880	65.8
15	"	6.97	"	"	0.601	"	"
16	0.536	6.98	"	16.6	0.621		
17	0.560	7.11	6.92	17.7	0.608		
18	"	7.32	"	"	0.597		
19	0.562	6.83	"	"	0.620		
20	0.633	6.75	7.10	19.4	0.616	955	71.3
21	"	6.62	"	"	0.600	"	"
22	0.631	"	"	"	0.620		
23	0.743	6.49	7.18	22.6	0.614	1100	81.6
24	"	6.43	"	"	0.608	"	"
25	0.741	6.39	"	22.5	0.620		
26	0.952	6.27	7.50	27.7	0.604		
27	"	6.18	"	"	0.599		
28	0.965	5.99	"	28.1	0.618		
29	1.770	5.26	7.39	52.2	0.603	1970	145
30	1.779	5.14	"	52.5	0.609	"	"
31	2.370	4.83	7.24	71.4	0.608	2200	163
32	2.347	4.89	"	70.7	0.604	"	"
33	2.941	4.62	"	88.6	0.609	2480	184
34	2.911	4.69	"	87.7	0.604	"	"
35	"	4.68	7.09	89.6	0.602		
36	3.571	4.40	7.30	107	0.609	2500	184
37	3.562	4.41	"	106	0.608	"	"
38	4.242	4.33	7.41	125	0.604		
39	"	4.32	"	"	"		

(1)	(2)	(3)	(4)	(5)	(6)	(7)	(8)
50-1	0.206	25.9	72.8	0.62	0.714		
2	"	26.8	75.4	0.60	0.688		
3	0.406	11.3	62.9	1.41	0.713		
4	0.474	8.94	17.6	5.87	0.896		
5	0.440	8.43	13.2	7.24	0.840		
6	"	8.39	13.0	7.36	0.783		
7	0.615	7.33	11.0	12.2	0.664		
8	"	7.47	11.8	11.4	0.637		
9	0.748	8.33	21.6	7.55	0.667	370	16.4
10	"	8.36	21.9	7.44	0.662	"	"
11	1.124	7.71	24.3	10.1	0.636	727	31.8
12	1.117	7.80	25.2	9.65	0.605	"	"
13	1.321	7.56	26.6	10.8	0.625	970	42.5
14	1.779	6.91	25.2	15.4	0.622	1420	62.3
15	2.212	6.60	26.2	18.4	0.613	1810	79.4
16	2.646	6.26	25.0	23.1	0.612	2180	95.5
17	3.030	6.17	27.1	24.4	0.611	2200	96.5
18	3.731	5.98	29.2	27.9	0.612		
20-1	0.102	17.2	24.0	0.93			
2	"	22.8	31.8	0.70			
3	0.292	8.67	9.71	6.55	0.651		
4	0.317	9.83	16.4	4.22	0.640		
5	0.456	8.34	13.2	7.54	0.624		
6	0.465	7.82	10.6	9.58	0.661		
7	0.197	12.6	33.8	1.27	0.577		
8	0.193	10.2	11.3	3.72	0.671		
9	0.196	10.7	13.6	3.15			
10	0.615	7.73	13.4	10.0	0.627		
11	"	7.66	12.9	10.4	0.613		
12	0.758	7.31	13.3	12.4	0.618		
13	"	7.30	13.2	12.5	0.607		
14	1.274	6.57	14.7	18.8	0.600		
15	1.278	6.53	14.4	19.3			
16	1.838	5.97	"	27.9	0.598		
17	1.852	5.89	13.6	29.6	"		
18	2.273	5.63	13.8	36.0	0.600		
19	2.717	5.48	14.7	40.4	"		
20	3.155	5.36	15.4	44.6	0.604		
21	3.472	5.29	16.0	47.3	0.601		
22	4.000	5.14	16.1	54.2	"		
W-40	0.079	14.9	7.77	2.21			
41	0.096	17.6	7.71	2.73	0.719		
42	0.123	11.1	7.58	3.54	0.648		
43	0.109	12.8	7.80	3.04	0.684		
44	0.108	10.6	7.72	3.05	0.680		
45	"	11.4	"	"			

(1)	(2)	(3)	(4)	(5)	(6)	(7)	(8)
W-46	0.107	10.7	7.69	3.04	0.676		
47	0.253	8.86	7.64	7.21	0.649		
48	0.250	8.37	7.62	7.17	0.647		
49	0.149	9.89	7.35	4.42	0.630		
50	0.175	9.39	7.42	5.14	0.643		
51	0.251	8.12	7.54	7.25	0.648		
52	0.439	7.22	7.41	12.9	0.609		
53	"	7.45	7.41	"	0.622		
54	0.552	6.86	7.35	16.4	0.606		
55	"	7.07	"	"	0.615		
56	0.780	6.33	7.47	22.8	0.614		
57	"	6.34	"	"	0.622		
25-1	0.127	13.1	22.7	1.22	1.624		
2	0.219	8.81	7.74	6.17	0.844		
3	0.343	10.2	20.2	3.70	0.695		
4	0.412	8.76	14.2	6.31	0.663		
5	0.501	8.11	13.1	8.34	0.658	520	29.3
6	0.808	7.01	12.1	14.6	0.617	865	48.9
7	"	7.16	13.2	13.4	0.621		
8	0.962	6.89	13.5	15.6	0.623	990	55.7
9	1.134	6.68	14.0	17.7	0.619	1050	59.1
10	1.374	6.26	13.0	23.0	0.626	1270	71.5
11	1.639	6.01	13.1	27.3	0.618	1660	93.4
12	2.155	5.67	13.5	34.9	0.614	1850	105
13	2.747	5.43	14.2	42.3	0.611	2360	133
14	3.937	5.14	15.9	54.0	0.608	2220	125
75-1	1.733	8.53	54.5	6.94	0.668		
2	2.212	7.83	50.6	9.54	0.605		
65-1	0.813	13.8	152	1.16	0.666		
2	1.130	9.31	48.5	5.08	0.658	315	12.7
3	1.479	6.92	21.0	15.3	0.653	399	16.1
4	0.526	22.8	163	0.70	0.701		
5	1.449	7.21	24.3	13.0	0.644		
6	2.008	7.10	21.7	13.8	0.643	740	29.4
7	2.326	6.87	32.2	15.8	0.645	935	37.1
8	2.674	6.70	33.4	17.5	0.639	1150	45.6
9	2.874	6.58	33.5	18.7	0.637	1260	50.0
10	3.049	6.57	35.2	18.9	0.632	1500	59.5
11	3.290	6.42	34.5	20.8	0.631	1510	60.1
12	3.496	6.24	33.0	23.1	0.635	1580	62.5
13	3.584	6.33	35.5	22.0	0.638	"	"
14	0.111	85.7	130	0.19	0.434		
15	0.231	49.5	156	0.32	0.742		
16	0.309	34.4	145	0.46	0.745		
17	0.374	31.9	163	0.50	0.754		
18	"	32.2	164	"	0.778		

(1)	(2)	(3)	(4)	(5)	(6)	(7)	(8)
S-1	0.709	6.33	6.76	22.8	0.615	340	70.0
2	0.328	7.85	6.66	10.7	0.598	164	34.0
3	0.988	5.70	6.78	31.8	0.618	445	91.3
4	1.309	5.38	"	42.1	0.614	585	120
5	1.488	5.34	6.82	47.6	0.608	655	133
6	1.678	5.10	6.86	53.4	0.616	686	140
7	1.880	5.02	6.88	59.6	0.611	765	156
8	2.058	4.92	6.90	65.0	0.614	850	172
9	2.283	4.81	6.94	71.8	0.613	876	176
10	2.525	4.72	6.96	79.1	0.611	960	192
11	2.660	4.71	6.97	83.2	0.607	1000	200
12	0.523	6.70	6.79	16.8	0.629	250	51.3
13	0.939	5.83	6.84	29.9	0.617	445	90.7
14	2.778	4.70	6.94	87.3	0.604	1090	218
15	3.068	4.51	6.97	96.0	0.611	1215	243
16	3.257	4.59	7.00	102	0.601	1220	244
17	3.333	4.54	7.01	104	0.604	1280	256
18	0.230	8.12	6.66	7.53	0.684		
19	"	7.98	"	"	0.663		
20	0.109	10.9	6.50	3.67	0.710		
21	0.222	8.18	6.68	7.24	0.695		
22	0.328	7.54	6.74	10.6	0.669	170	35.2
23	"	7.85	"	"	"	"	"
24	0.617	6.53	6.81	19.8	0.628	313	63.7
25	"	6.46	"	"	0.629	"	"
90-1	0.377	9.06	14.6	5.61	0.622		
2	0.727	6.64	8.80	18.0	0.624		
3	1.034	5.86	7.44	30.3	0.620	446	87.7
4	1.441	5.49	7.80	40.3	0.609	625	123
5	1.838	5.09	7.11	56.4	"	725	142
6	2.212	4.84	6.85	70.5	0.605	810	159
7	2.445	4.75	6.94	76.9	0.604	985	193
8	2.793	4.60	6.75	90.3	0.608	1020	200
9	3.135	4.41	6.68	110	"	1160	228
10	3.401	4.48	7.25	102	0.601	1300	255
11	0.083	16.1	181	0.10	0.475		
12	0.855	6.47	9.32	20.1	0.616		